CALCULATION OF WAKE ROLL - UP BEHIND A LARGE ASPECT RATIO WING IN STEADY INVISCID FLOW

by

ANIL KUMAR CHAWLA

DEPARTMENT OF AERONAUTICAL ENGINEERING

INDIAN INSTITUTE OF TECHNOLOGY, KANPUR

JULY, 1988

CALCULATION OF WAKE ROLL - UP BEHIND A LARGE ASPECT RATIO WING IN STEADY INVISCID FLOW

A Thesis Submitted
In Partial Fulfilment of the Requirements
for the Degree of

MASTER OF TECHNOLOGY

by

ANIL KUMAR CHAWLA

to the

DEPARTMENT OF AERONAUTICAL ENGINEERING
INDIAN INSTITUTE OF TECHNOLOGY, KANPUR

JULY, 1988

Dedicated
To
My Parents

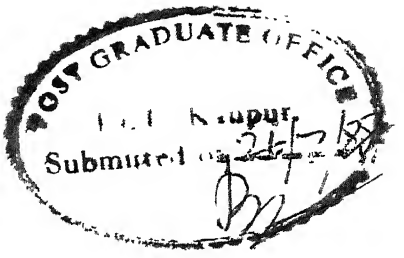

CERTIFICATE

This is to certify that the thesis entitled, "CALCULATION OF WAKE ROLL UP BEHIND A LARGE ASPECT RATIO WING IN STEADY INVISCID FLOW" by Anil Kumar Chawla is a record of work carried out under my supervision and has not been submitted elsewhere for the award of any degree

N L Arora

Dr. N.L. Arora
Professor
Department of Aeronautical Engineering
Indian Institute of Technology, Kanpur

July, 1988

ACKNOWLEDGEMENTS

I express my sincere gratitude to Dr. N.L. Arora for his assiduous guidance, constant encouragement and erudite suggestions throughout this endeavour. I am deeply indebted to him for his keen interest and concientious efforts.

I deeply thank Mr. Rajiv Lochan for his excellent help in dealing with computational and several other problems.

Thanks also to Mr. Sushil Kumar Tiwari for his typing and B.K. Jain for tracing and drawings.

Finally I thank Mr. Phool Chand and Mr. Jatinder Singh for their timely help and others who extended their direct or indirect help to me.

Anil Kumar Chawla

TABLE OF CONTENTS

LIST OF FIGURES

LIST OF SYMBOLS

a_1-a_5	Coefficients of vorticity distribution.
AR	Aspect Ratio
C_p	Pressure coefficients
d	direction cosine
$\underline{e}$	dimensionless velocity vector
$\underline{f}$	Wake surface
l_{13}	Distance between the nodal points 1 and 3
L	Vector dnotes any line
N	Number of point vortices per turn roll-up
NB	Number of bound vortex panels
NW	Number of panels over free vortex sheet in the direction of flow
NX	Number of panels over lifting surface, in the free stream direction
NZ	Number of panels per semi span
n	Normal to the Surface is positive in the positive direction of y-axis.
U	Velocity
v	Induced velocity component per unit of coefficient a's.
$\underline{V}$	Total velocity vector
$\underline{w}$	Vorticity vector
$\hat{e}$	Unit vector
x,y,z	Coordinates of a point in global system of referen

c_r	root chord
$\hat{i},\hat{j},\hat{k}$	Unit vectors in the global axes system
ξ,η,ζ	Coordinates in the local axis system
u,v,w	Components of total induced velocity in x,y and z direction respectively.
TE	Trailing edge
X	Two dimensional vector
α	Angle of attack in degrees
ϕ	Perturbation velocity potential
Φ	Total velocity potential
σ	Surface
Γ	Circulation
θ	Angle at a point vortex between the line joining previous and next vortex in the same row, measured positive in the anticlockwise direction

Subscripts

av	Average value
c	Critical condition
Cp	Control point
i	Refers to i^{th} panel
k	Sender panel
loc	Local axes system
m	Receiver panel
R	Refers to global coordinate system
x,y,z	Used to denote three components of velocity vector
ξ,η,ζ	Three components of a vector in local axes system

Superscripts

n	n^{th} row of panel

ABSTRACT

A higher order panel method has been used to simulate three dimensional wake roll-up for large aspect ratio symmetric wings in steady inviscid incompressible flow.

Two methods have been considered for this purpose. The first method which will be referred to as vorticity distribution method - consists of determination of wake geometry iteratively in three steps. The first step aims at computation of linear vorticity distribution over lifting surface using appropriate boundary conditions. The second step is concerned with determination of induced velocities. This is followed by final step of updating wake geometry. These steps are performed repeatedly to achieve convergence.

This method leads to certain numerical difficulties which have been alleviated in second method here after called circulation distribution method by replacing linear vorticity by quadratic circulation distribution over the lifting surface, other steps remaining unaltered. This has been successfully employed for generation of wake roll-up geometry for rectangular wings in steady flow.

The vorticity distribution method could only be used for obtaining the vorticity distribution on the wing surface and hence the pressure distributions over a flat plate rectangular wing of large aspect ratio. The circulation distribution method was used to obtain the wake roll up on large aspect ratio flat plate wings at angle of attacks upto 10^0.

CHAPTER - 1

INTRODUCTION

1.1 Preliminary remarks

The knowledge of the trailing vortex wake is required because of the increasing importance of interactions between aircraft in crowded air corridors and the need to minimize these interactions by accelerating the dissipation of the trailing vortices.

A wing of finite span in flight generates trailing vortices which rollup into two "discrete" vortices. During the rolling up process the trailing vorticity is displaced vertically downwards, assuming that the aircraft is in horizontal flight, under the influence of the wing circulation and the self-induced downwash velocities.

A starting point for the calculation of the trailing vortex wake is the realistic evaluation of the vorticity distribution on the wing and in the near wake. The calculation of a vorticity distribution on the wing planform and its trailing wake leads to an important result; the accurate evaluation of wing aerodynamic characteristics including the nonlinear effects.

For the vortex flow behind a wing of finite span at angle of attack, there exists a pressure differential between the top and bottom surfaces as a byproduct of the

lift force. The vorticity is shed as a result of the difference in the direction of the flow between the wing surfaces at the trailing edge.

For high Reynolds number flow past a thin wing at moderate angles of attack, convection dominates diffusion and the vorticity is confined to a thin, free shear layer; under the influence of the self induced velocity, the shear layer has tendency to roll-up into vortex cores. In the downstream direction the vorticity is continuously fed into vortex cores resulting in a growth both in strength & dimension. Further downstream of the wing the roll up process will be completed and most of the vorticity is contained within the cores. At this stage the velocity gradients in the cores are large and the viscous effects become more important, consequently instability may occur which can result in the break up of the trailing vortex system. We are considering only initial stage of the wake roll-up - potential flow is considered with embedded vortex sheets. Thus we are able to predict viscous phenomenon using potential solution without solving Navier-strokes equations

1.2 Literature Review

In this section earlier attempts to model lifting-surface flows are reviewed and evaluation of the present method is discussed.

The earliest analytical method was presented by Prandtl in 1918 (See e.g. Karamcheti /2/) and is known as the lifting line theory. He considered rectangular wings having large aspect ratio at small angles of attack. The bound vortex sheet was approximated by a single bound vortex line having variable strength. Spatial conservation of vorticity requires a continuous sheet of trailing vortices to be shed from the bound vortex line. The resulting model in assumed to lie in a plane parallel to the free stream. In addition the model was simplified by assumptions concerning the spanwise component of the bound vortex line. The model is very simple and limited to rectangular wings having large aspect ratios and low angles of attack.

Using the method of matched asymptotic expansion, Van Dyke /14/ and Thurber /16/ refined Prandtl's analysis to obtain better approximations. Kerney /36/ corrected Van Dyke's expression for the lift-curve slope. However these expansions possess a number of non-uniformities near the wing tips, discontinuities in planform, and root juncture of a swept back wing among others.

One of the earliest models for rectangular wings having low aspect ratios was presented by Bollay /5/. In the limiting case of a rectangular wing of zero aspect ratio (finite span but infinite chord), he assumed that the wing surface is equivalent to a distribution of spanwise, bound vortices. The trailing vortices are shed rearwards from the wingtips at half the angle of attack in a plane perpendicular to the wing surface.

Assuming the lift distribution and the downwash to be constant across the span, he expressed the total normal force coefficients as a nonlinear function of the angle of attack. He also extended the theory to wings having finite but small aspect ratios. Here, the trailing vortices from the wing tips are again straight but follow the direction of the resultant velocities at the wing tips. The no-penetration boundary condition was satisfied along the mid-chord, leading to an integeral equation. The form of the function giving the vorticity in terms of the distance from the leading edge was assumed. This method yields surprisingly good results for wings having aspect ratio less than one, but it does not predict the distribution or shape of the trailing vortices, and it cannot be applied to other planforms.

Multhopp /6/ presented a method, based on the linear potential equation obtained by the use of continuity and momentum equations for steady inviscid flow. This method uses fields of doublets over the projection of the wing on a plane parallel to the free stream. The downwash velocity condition is satisfied on the projection of the wing. This results in an integral equation relating the local-incidence and the distributed-load coefficient. The Kutta condition is satisfied by assuming that the load functions disappear toward the trailing edge. Finally the integral equation is solved by selecting a limited number of independent load distributions and satisfying the integral equation by a linear combination of these distributions at a certain number of so called "pivotal points". This method is limited to small angle of attack and large aspect ratio.

Similar methods were developed to model flow over very highly swept wings. These were based on the slender-body approximations. One such method is due to Lawrrence /7/, who also presented an extensive summary of previous methods. Lawrence did not attempt to model separation at sharp leading edges and/or wing tips, which can occur even at moderate angles of attack.

Apparently, Legendre made the first attempt to include leading-edge separation in his model of flows over delta wings. In his model, isolated vortices were placed over the wing. Their strength and position were determined by forcing the flow to be tangential to the wing surface at the leading edge. Brown and Michael /8/ improved this model by adding feeding vortex sheet extending from the leading edge to the isolated vortices above the wing. The strengths and positions of the vortices are obtained by requiring the flow to be tangential at the leading edge and the resultant force on the feeding sheets and the vortices to be zero. They did not make the pressure difference across the feeding sheets zero everywhere. Mangler and Smith /9/ modified this model further by assuming a curved shape for the feeding vortex sheets, and by forcing the pressure difference across these sheets to vanish at selected points. In these methods the shape of the vortex sheets at the leading edge is prescribed, the flow is assumed to be conical, and the slender body assumption is used. Consequently these methods are restricted to slender

delta wings and most importantly small angle of attack. These assumptions do not appear to be justified for the delta wings used in the wind tunnel tests.

In an attempt to treat wings having general planforms and arbitrary aspect-ratios, Gersten assumed that trailing vortices are shed from each point of the lifting surface at one half of the angle of attack. Such an approach leads to a non-linear relationship between the total loads and the angle of attack. Garner and Lehrian /13/ combined the method of Multhopp and Gersten.Their model is based on essentially the same assumptio which were used by Gersten.

Theoretical and semi-empirical methods were presented by Sacks et al /23/. The methods are based on the assumption that the lift coefficient is the sum of two terms. The first is the lift coefficient obtained by the method of Lawrence, while the second is due to the contribution of the leading edge separation. They considered delta wings of small aspect ratios and hence used the slender body approximation. The vortex sheet shed from the leading edge is represented by a finite number of vortex filament. Here, the basic unknowns are the strengths and position of these vortex filaments. One equation was obtained by satis-fying the Kutta condition at the leading edge while the other was obtained from shedding rate. The shedding rate was determined by either a semi-emperical or a theoretical method. The results of theoretical method over predicted the lift coefficient, while those of the semi-empirical method gave satisfactory results.

Finkleman /35/ extended this method and obtained a solution for the interacting Canard-wing system. Other methods were developed on the basis of treating the shape of the trailing vortices by the two dimensional analysis associated with the intersection of the vortex sheet and the Trefftz plane Rossow /44/.

Polhamus /31/ developed a method to predict the total lift and the drag due to lift for sharp edge delta and delta-like planforms. The method is restricted to thin wings having no camber and no twist. In addition the leading edge is assumed to have sufficient sharpness so that the separation is fixed at it and no leading edge suction is developed.

Polhamus /30/ extended this method to account for compressibility by using the Prandtl-Glauert transformation. Bradley, et al /45/ extended Polhamus's method to more general planforms. Although Polhamus's method predicts the total lift coefficient with sufficient accuracy, it is incapable of predicting the pitching moment and the shape of the wake.

Kuo & Morino /43/ presented a method for determining the distributed and total aerodynamic loads on lifting bodies having arbitrary shapes and sharp trailing edges in a steady, subsonic potential flow. The Prandtl Glauert transformation is used to reduce the linearized compressible flow equation to Laplace's equation. Green's theorem is used to obtain an

integral equation relating the velocity potential to its normal derivative on the surface enclosing the lifting body and its wake at the trailing edge. The shape of the wake is prescribed. Morino and Kuo /47/ extended this method to account for unsteadiness in the flow.

In brief, the most common drawback of all the analytical methods presented above is that none adequately models the wake. Hence they are restricted to small angles of attack. In addition they are restricted to wings having certain planforms, aspect ratios, and/or small thickness ratio.

Discrete-vortex methods are based on approximating the continuous distribution of the bound vorticity (representing the lifting surface) by either a finite number of horseshoe vortices or a vortex lattice composed of a finite number of vortex filaments and the continuous distribution of free vorticity (representing the wake) by a finite number of vortex lines which extend downstream. This technique has been known for a long time. The earliest models were presented by Prandtl /2/ and Bollay /5/ but their further development and refinement only became practical with the advent of digital computers. These methods can be divided into two types. Linear and non-linear discrete vortex methods.

Numerical methods of the LINEAR DISCRETE-VORTEX type were presented by several investigators such as Rubbert /12/, Hedman /20/ and Belotserkovskii /21/, for solving the steady flow problem Later these methods were extended to the unsteady-

flow problem (oscillatory case) by combining the vortex-lattice with a doublet-lattice by Kalman, et al /22/, Albano and Rodden /27/, Rodden, et al /38/, Giesing et al /36/ Ashley and Rodden /34/, Hua /41/ and Rodden /49/. Only steady flow problem will be discussed here.

In this approach, the so-called vortex lattice method (VLM), the lifting surface is replaced by a number of panels arranged in streamwise columns. Each panel is replaced by a horseshoe vortex with its bound part positioned on the quarter chord line of the panel, which is the location of the aerodynamic centre of a two dimensional plate in a steady incompressible inviscid flow. With this arrangement a vortex lattice represents the lifting surface. The wake attached to the lifting surface is represented by rectilinear-vortex lines which extend downstream to infinity. The direction of these lines is prescribed to be parallel either to the free stream velocity or to the root chord of the lifting surface. With this configuration, the only unknown is the circulation distribution. This is obtained by satisfying the no penetration boundary condition at a certain number of points (known as control points) on the wing surface. The control points are centered spanwise at the $\frac{3}{4}$ chord length of each panel. The reason for the selection of this location for control point is based on numerical experiments. James /28/ and Hough /46/ indicated that this location yields fast convergence of the aerodynamic loads as the number of panels is increased. Once the circulation distribution is obtained the forces due to the bound

vortices can be calculated. It is noted that a bound vortex line runs between the leading row of control points and the leading edge of a delta wing and between the out board columns of control points and the wing tip for other wings. Thus separation at the leading edge and wing tip is not taken into account. Hence it is restricted to small angle of attack. It is worth mentioning that some investigators introduced compressibility effects into this technique by using Prandtl-Glauert transformation e.g. Hedman /20/ and Kalman et al /22/.

Hess /39/ used a finite-strength vorticity distribution over the wing surface instead of vortex lines. He used a step function for the spanwise variation of vorticity, while he used a constant strength around each chordwise strip. This method is also limited to small angles of attack.

All the previous models suffer from a common basic fault, none of them models the leading-edge and wing-tip vortex system adequately. For the intended applications, these vortex systems strongly influence the flow in the immediate neighbourhood of a significant portion of lifting surface; thus methods which do not describe vortex systems accurately cannot be expected to predict the aerodynamics characteristics of the wing accurately

In the NON-LINEAR DISCRETE VORTEX type, the first attempt to model the wake was made by Ermolenko /19/, who considered rectangular wings having small aspect ratios. He replaced the wing surface by a system of spanwise vortex lines. The circulatior

are constant along each vortex line but vary from line to line. The vortices in the wing tip wake are considered to be rectilinear and to lie in two vertical planes which are perpendicular to the lifting surface. Each trailing vortex is directed parallel to the projection of the resultant velocity onto these planes at the point where the spanwise lines intersect the wing tips. The boundary conditions are satisfied on the average along spanwise lines distributed at the three-quarter chord lines of each panel. This method is subject to the same limitations as Bollay's method /5/.

Belotserkovskii /25/ greatly improved Ermolenko's method and developed the first successful model of wing-tip wake. He also replaced the wake by a finite number of discrete vortex lines, but in contrast with the earlier methods, he made each line consist of a finite number of segments, where the last one is semi-infinite segment. Then through an iterative procedure, he aligned each finite segment with the velocity at its mid-point. He showed the method to be highly reliable in predicting the total and distributed loads on parallelogram wings at large angle of attack.

Butter and Hancock /33/ replaced the wing by a single lifting-line bound vortex which represent the circulation distribution around the wing while the trailing vortex sheet is approximated by a number of discrete line vortices. Starting with a planar system and following step-by-step process, working downstream aft of the wing trailing edge, the deformation of the trailing vortex sheet is determined.

Mook and Maddox /48/ used a vortex lattice method and considered leading separation. They modified the steady portion of the program of Giesing, Kalman and Rodden /36/ by superposing a system of discrete vortex lines on the existing lattice. They determined the shape of the lines trailing from the leading edge. However the method cannot account for wing tip and trailing edge vortex sheets being free of forces.

Through the advance of computer technology, a number of fully three dimensional models have been developed for the prediction of wake roll-up. The vortex-lattice method has found wide applications for computing the attached flow loading of lifting surface. Rom and Zorea /42/ developed a computational procedure to relax the wake. They use finite number of line vortices to represent the trailing vortex sheet. The wake geometry is evaluated in an iterative fashion starting from an assumed initial wake position. Sucio and Morino /51/ developed a method that uses constant doublet panels on the wing and the wake to calculate the wake roll-up behind rectangular wings. The use of constant doublet panels for the wake modelling is equivalen to using vortex filaments. In recent years the constant doublet panel method has been widely applied to helicopter applications to model the blade and wake /57/.

For the cases when the vortex wake passes close to lifting surface, the filament wake model may not be adequate to describe the flow details. This is true for leading edge sheets of low aspect ratio wings. It is also noted that a higher order panel

method solution for the wake roll-up behind a large aspect ratio wing is not available in literature.

Yeh /61/ used linear vortex panel method to calculate the three dimensional wake roll-up behind large aspect ratio symmetric wing in steady inviscid incompressible flow. He obtained the wing spanwise circulation distribution from lifting line theory and wake geometry was evaluated in an iterative fashion. The capability of the method to model a rectangular wing with a deflected flap was also studied.

Higher order panel methods for three dimensional vortex calculation have been developed by Johnson et al /54/, Hoeijmakers and Co-workers /59/ and Kandil et al /60/. These methods have been used to study leading and side edge separation for low aspect ratio wing. The method developed at Boeing /54/ and NLR /58/ use second order doublet distribution.

In the method of Kandil et al /60/, vortex panels (triangular panels in the wake) with a first order vorticity distribution are used in the near field calculations. In the far field calculations, the distributed vorticity is lumped into equivalent concentrated vortex lines. We choose to modify this method and apply it to large aspect ratio wing.

An excellent review of the literature on vortex wakes is given by Hoeijmakers /59/. Many of the studies use a two-dimensional time dependent analogy to study the wake roll-up for large aspect ratio case. The technique is developed under

the assumption that the flow varies in the streamwise direction and that there is no direct influence due to the upstream wing. The two dimensional time dependent problem can be considered as a marching problem in the sense that vortex sheet is determined at each cross flow plane and is convected with its own induced velocity in subsequent cross flow planes. The work by Fink and Soh /53/ appears to be most successful in producing smooth wake roll-up by using the discrete vortex method. Murman and Stremel /56/ utilized the "Cloud-in Cell" method to capture the vortex wake motion. A sophisticated second order doublet panel method (curved segments) developed at NLR /59/ is capable of describing complicated vortex sheet motion and vortex cores are also included to model highly rolled-up regions.

All users of the vortex representation have met difficulties of convergence i ,e. growing randomness of location of equivalent vortices so that the line joining these crossed itself and could no longer serve to represent a sheet. This inconsistency appeared to become more pronounced as segmentation was refined. Brikhoff /11/ asserted the inevitability of such randomization as a consequence of the Hamilton principle applied to a two-dimensional system of discrete vortex filaments. Von Karman /1/ had already demonstrated strongly growing instability with decreasing separation for the special case of linear array of point vortices of equal strength.

A suitable problem for testing a new approach is that of the calculation of roll-up of the trailing vortex sheet well behind an elliptically loaded lifting surface. This has challenged many writers. Westwater /4/ was the first to use the Roshenhead /3/ method for this problem. He confined his attention to points far enough downstream of the wing for the influence of the equivalent bound vortex to be negligible, thus converting the problem to a two dimensional one; namely a trefftz plane calculation. Fortuitously, Westwater used only ten discrete vortices, a small enough number to escape serious irregularity of vortex position in the limited period of his calculation. Attempt to reproduce Westwater's result by Takami /15/ and Moore /32/ were not successful. For much finer subdivision than that used by Westwater, these authors found that the vortices moved Chaotically and that the sheet or rather the straight line joining appropriate vortices, crossed through itself. Moore /32/ showed that this phenomenon was not due to round off errors. If at some instant the vortex strength was reversed the chaotic motion would unscramble and the vortices would return to their original position. Several authors then put forward schemes intended to overcome the difficulty, Moore /50/ used a different scheme. If the vortices near the tip are too far or the distance between the vortices is greater than critical distance, they are combined to form a tip vortex or line vortex with its coordinates at the centroid of the two vortices and the

circulation is equal to the combined circulation of original pair. We have used this method for our problem.

1.3 Present Scope

In the present work an attempt is made to calculate the wake roll-up behind large aspect ratio wings, for the accurate computation of aerodynamic coefficients over the lifting surfaces.

Vorticity distribution over the panels in the near wake is determined, and then induced velocities are calculated at the corner point or average point of triangular panels chosen to model the wake. These velocities have been used to obtain the shape of free wake. Now aerodynamic coefficients are calculated using these new coordinates for wake surface rather than a planar wake.

The present wake model bears no small perturbation assumptions and all of the equations engaged are solved analytically. Moreover the method is capable of calculating the wake geometry for a variety of planforms and shapes when spanwise circulation distribution is known either from numerical calculation or experiment.

The first chapter deals with the requirement of trailing vortices, some attempts by various authors to model the lifting surface flows and a brief summary of the problem considered is discussed.

In the second chapter the axes system for the problem, mathematical formulation or governing equations and boundary

conditions are discussed.

The third chapter discusses the method of solutions for the wake rollup problem and the manner in which the boundary conditions are satisfied.

Fourth chapter describes the computer program detailing the function subprograms and subroutines, indicating the various inputs and outputs. A list of variables used in the program is also attached.

The last chapter gives the results of computation and discussion of these results.

CHAPTER - 2

PROBLEM SPECIFICATION AND MATHEMATICAL FORMULATION

The accurate calculation of the position and strength of the vortex wake behind a blade in motion is a critical problem for rotorcraft applications. A detailed model of the vortex wake would permit substantial improvements in many aspects of rotary wing design such as performance, acoustics, vibration and response. Trailing vortices are of interest to minimize the interaction between the two aircraft flying in vicinity with each other. Purpose of the present investigation is to compute the wake roll-up behind large aspect ratio wing, for the accurate calculation of aerodynamic coefficients over the lifting surfaces.

Consider the flow of a steady freestream of speed U_∞ at an angle of attack α past a thin wing of large aspect ratio. Since the flow field considered here is the high Reynolds number flow past a thin wing at a moderate angle of attack, the viscous boundary layer and wake are essentially confined to a thin region. Outside the boundary layer and wake velocity gradients are small enough that the shear stresses acting on a fluid element can be neglected. For a region near the centre of rolled up region, however the velocity gradients are large and the viscous effects become dominant. In the present study only the initial roll up stage is analyzed and, consequently the fluid is considered to be inviscid.

The problem is formulated relative to a wing fixed frame of reference xyz. The x-axis is the wing centreline and the xy plane is the wing plane of symmetry with z-axis in the spanwise direction (Fig. 1). The dimension-less free stream velocity is expressed by

$$\underline{e}_\infty = \cos\alpha \ \hat{i} - \sin\alpha \ \hat{j} \tag{2.1}$$

where $\hat{i}$, $\hat{j}$, $\hat{k}$ are the base unit vectors of the xyz frame of reference and α is the angle of attack.

The continuity equation for an incompressible flow is

$$\nabla . \underline{V} = 0 \tag{2.2}$$

and the irrotationality of flow demands

$$\nabla \times \underline{V} = 0 \tag{2.3}$$

where $\underline{V}$ is the velocity vector. Equation (2.3) holds everywhere in the flow field except on the wake surface and on the lifting line where rotational regions are confined. If we define the velocity potential Φ and perturbation velocity potential ϕ such that

$$\underline{V} = \underline{e}_\infty + \nabla\phi = \nabla\Phi \tag{2.4}$$

Then Eq. (2.3) is satisfied identically. Substituting Eq. (2.4) into (2.2), the Laplace equation for both Φ and ϕ is obtained i,e.,

$$\nabla^2 \Phi = 0 \quad , \quad \nabla^2 \phi = 0 \tag{2.5}$$

The no-penetration on the wing surface $S(\underline{r}) = 0$ relative to wing fixed frame of reference is given by

$$(\underline{e}_\infty + \nabla\phi) . \ \nabla S = 0 \text{ on } S(\underline{r}) = 0 \tag{2.6}$$

the no-penetration condition is applied to enforce the flow tangency on the wake surface

$$(\underline{e}_\infty + \nabla \phi) \cdot \quad \nabla f = 0 \quad \text{on } f(\underline{r}) = 0 \tag{2.7}$$

where $f(\underline{r}) = 0$ is the equation of wake surface.

The no-pressure jump condition on $f(\underline{r})$ is obtained from incompressible Bernoulli's equation

$$cp(\underline{r}) = - \nabla \phi . [\nabla \phi + 2 \underline{e}_\infty] \tag{2.8}$$

where cp $(\underline{r})$ is the pressure coefficient at any point $(\underline{r})$. Forming the pressure jump from Eq. (2.8) and equating the result to zero, we obtain

$$\Delta cp = cp_1 - cp_2 = -(\nabla \phi_1 - \nabla \phi_2) . (\nabla \phi_1 + \nabla \phi_2 + 2 \underline{e}_\infty) = 0 \tag{2.8a}$$

where subscripts 1 and 2 refers to upper and lower surfaces on the wing, respectively.

Rearranging (2.8a) and setting

$$\phi_1 - \phi_2 = \Delta \phi \tag{2.8b}$$

$$\Delta cp = - 2 (v_f . \nabla)(\Delta \phi) = -2 \frac{D}{Dt} (\Delta \phi) = 0 \tag{2.8c}$$

where v_f is the velocity of wake element relative to xyz frame of reference

$$\underline{v_f} = \tfrac{1}{2} (\Delta \phi_1 + \Delta \phi_2) + \underline{e}_\infty$$

Eq. (2.8c) represents theorem of Kelvin and Helmhaltz

$$\frac{D\Gamma}{Dt} = -\frac{D}{Dt}\iint \underline{w} \cdot \underline{n}_A \, dA = 0 \quad \text{on} \quad f(\underline{r}) = 0 \qquad (2.9)$$

of conservation of circulation and outflow of vorticity, respectively. In Eq. (2.9), $\underline{n}_A$ is a unit normal to the surface A bounded by a closed curve around which circulation is calculated. Eq. (2.9) simply states that the rate of change of circulation around a closed curve or the rate of change of outflow of vorticity through the surface bounded by this closed curve is zero (following the same fluid particles).

For uniqueness of the solution one has to impose the Kutta condition along the edges of separation. Here Kutta condition is represented by

$$\Delta cp/_{TE} = 0 \qquad (2.10)$$

finally the infinity condition requires that

$$\nabla \phi \longrightarrow 0 \quad \text{away from } f(\underline{r}) \text{ and } S(\underline{r}) \qquad (2.11)$$

The basic unknowns in the present problem are the vorticity distribution and free vortex sheet. They are determined by satisfying the Eqs. (2.1-2.11). Eq. (2.7) requires the flow to be tangent to wake surface while (2.8a) requires this tangential flow to be parallel to the vorticity direction. Therefore if position of f is adjusted so that flow direction is parallel to the vorticity direction on the surface f, the boundary conditions of Eq. (2.7) and (2.8a) are automatically satisfied.

CHAPTER - 3

METHOD OF SOLUTION

3.1 General

With the linear vortex lattice method (VLM) the so called horse-shoe elements are used to form the lattice as well as the lines modelling the wake adjoining the trailing edge. The directio of these lines is prescribed, not obtained as part of the solution and no attempt is made to model the tip or leading edge vortex system. Consequently the only unknowns are the circulation of horse-shoe elements. These are found from the no-penetration boundary condition and consequertly the entire problem is linear. These methods yield accurate results for small angle of attack only.

A steady non-linear hybrid vortex (NHV) method /60/ is considered for large aspect ratio wings at large angles of attack. In this method vortex panels with linear vorticity distribution are used on the wing as well as in the near field of the wake. For the far field calculations, the distributed vorticity over each far field panel is lumped into equivalent concentrated vortex lines. In this way accuracy is satisfied in the near field, while computational efficiency is maintained in the far field. The coupling of a continuous vortex-sheet representation and a concentrated vortex line representation for solving the non-linear lifting surface problem is referred to as "non-linear hybrid vortex" (NHV) method.

The circulation distribution method /61/ is presented to calculate the wake roll-up for a steady flow past a high aspect ratio wing at low angle of attack, in which the linear vorticity distribution on the wing is replaced by a quadratic circulation distribution over the lifting surface. The flow field considered here is incompressible and inviscid. The present wake model bears no small perturbation assumptions and all the equations engaged are solved analytically. Moreover the method is capable of calculating the wake geometry for a variety of planforms and shapes when the spanwise circulation distribution is known either from numerical calculations or experiments (VLM is currently used). As the number of panels in the spanwise direction increases the wake sheet becomes more flexible and tends to roll-up more. To prevent chaotic motion at the tip, the method due to moore /50/ is used to model the tip core.

3.2 Vorticity Distribution method

A higher order panel method is used to calculate the three dimensional wake roll-up behind a large aspect ratio wings in steady incompressible flow.

For a steady symmetric flow the governing Eqs. are(2.1-2.11). The vorticity distribution over each bound vortex panel is obtained by satisfying the no-penetration condition over the control points, continuity condition at each common node of bound vortex panel, Kutta condition at the trailing edge and symmetry condition along the root chord assuming wake to be planar (Fig. 2).

Equating the outflow of vorticity from bound vortex panels to the free vortex panels along the separation edges, induced velocity at each common nodal point over the wake is calculated in the near region which is taken two spans in length. In the far field the distributed vorticity is reduced to concentrated vortex lines and simple Biot-Savart law is used to calculate induced velocity due to vortex filaments, see Appendix A. Wake geometry is then evaluated in an iterative fashion by satisfying conservation of circulation, flow tangency and zero pressure jump for all wake panel surfaces in the near region.

Planar quadrilateral vortex panels are used to represent the bound vortex sheet. On each panel a local linear distribution of vorticity in term of five undetermined coefficients ($a_1 - a_5$) is specified in local axes system, in which ζ and ξ axes are located in the panel plane such that the ζ-axis coincides with the side 1-4 of the quadrilateral panel. The η axis is perpendicular to the plane such that ζ, ξ and η form a right handed local coordinate system, See Fig. 3a.

$$w_\zeta = a_1 + a_2 \zeta + a_3 \xi \tag{3.1}$$

$$w_\xi = -a_2 \xi - a_4 - a_5 \zeta \tag{3.2}$$

This type of vorticity distribution satisfies solenoidal property of vorticity

$$\nabla . \underline{w} = 0 \tag{3.3}$$

Planar triangular panels are used to model free vortex sheet where highly nonplanar and twisted surfaces are encountered. The local vorticity distribution is still given by Eqs. (3.1) and (3.2). The corners of this panel serves as nodal point. The ζ-axis now coincides with side 1-3 of the panel, the ξ-axis is in the panel plane and η axis is perpendicular to the plane such that ζ, ξ, and η axes again form a right handed local coordinate system, See Fig. 3b.

The velocity induced by a distribution of vorticity on the surface σ at any point P(x,y,z) in the local panel coordinates can be calculated by means of Biot-Savart law to yield

$$\underline{V}\ (x,y,z) = -\frac{1}{4\pi}\iint_{\sigma}\frac{(\underline{r}-\underline{s})\ X\ \underline{w}}{(\underline{r}-\underline{s})^3}\ d\sigma \qquad (3.4)$$

where $\underline{r} = x\ e_\xi + y e_\eta + z e_\zeta$ is the position vector of a point P, and $s = w_\xi e_\xi + w_\zeta e_\zeta$ position vector of a point on σ. With the vorticity distribution

$$\underline{w} = w_\xi\ e_\xi + w_\zeta\ e_\zeta \qquad (3.5)$$

the induced velocity in the near field at any point is given by

$$\underline{V}\ (x,y,z) = -\frac{1}{4\pi}\iint_{\sigma}\frac{y w_\zeta\ e_\xi + ((z-\zeta)w_\xi - (x-\xi)w_\zeta)\ e_\eta - y w_\xi\ e_\zeta}{((x-\xi)^2 + y^2 + (z-\zeta)^2)^{3/2}}\ d\zeta \qquad (3.6)$$

Each rectangular panel over the wake surface is divided into two triangular panels. Assuming the same vorticity distribution over both the panels (Fig. 1), Eq. (3.6) can be expressed as

$$\underline{V}(x,y,z) = -\frac{1}{4\pi}\sum_{i=1}^{2}\iint \frac{yw_\zeta e_\xi + ((z-\zeta)w - (x-\xi)w)e_n - yw_\xi e_\zeta}{((x-\xi)^2 + y^2 + (z-\zeta)^2)^{3/2}}\, d\zeta \quad (3.7)$$

Substituting Eqs. (3.1) and (3.2) into (3.7) the induced velocities are calculated in local axes system in terms of the coefficients of a's, see Appendix B. At each control point of bound vortex panel no-penetration condition Eq. (2.6) is enforced (Appendix B and C) in terms of five unknowns per panel. Control point is defined as the average point. Additional equations are obtained by satisfying conditions of vorticity continuity, Kutta and symmetry conditions, see Appendix C.

The number of equations from these four conditions is given by 5NB + 2NZX(NX-1) + 2NXX(NZ-1) in term of 5NB unknowns, where NB is number of bound vortex panels. The vorticity distribution coefficients over bound vortex panels are obtained by solving this overdetermined set of equations using method of Least-Squares. Vorticity distribution coefficients over wake surface are derived in term of vorticity distribution coefficients of bound vortex panels, see Appendix D.

3.3 Circulation Distribution Method

To calculate the three dimensional wake geometry in a steady incompressible flow behind a symmetric wing of large aspect ratio for a given spanwise circulation, method uses triangular vortex panels with a linear vorticity distribution for a near wake modelling. To model this problem the wake is

first initialized as a flat sheet of zero thickness, extended from the wing TE which is divided into three regions-adjoining, near and for region.

The adjoining region is described as a small region (1/10 of span) of planar vortex sheet where the wake surface lies in the direction of x-axis and stays fixed. The region is introduced to model the satisfaction of Kutta condition, that the flow will leave the trailing edge smoothly.

In the near region approximately two spans in length, the wake surface is split into a network of flat, triangular elements (panels) with linearly distributed vorticity in local spanwise direction and constant vorticity along the streamwise direction (local flow direction) for each panel.

In the far region, straight semi-infinite vortex filaments of equivalent strength are shed from the trailing edge of vortex panel sheet to infinity. Such representation for the far wake is introduced for economic feasibility while accuracy is maintained in the near region as well.

The wake geometry is then evaluated in an iterative fashion by satisfying conservation of circulation, the flow tangency condition and zero pressure jump for all wake panel surfaces in the near region. The iteration continues until the wake shape converges or equivalently the wake sheet truly becomes a stream surface in the near region. Straight semi-infinite vortex filaments in the far wake are assumed to be in the uniform stream direction.

The governing Eqs. are again (2.1-2.11). The spanwise circulation distribution $\Gamma(z)$ over the lifting surface is obtained by VLM approach. Once the spanwise circulation $\Gamma(z)$ is obtained the vorticity shed by the wing or the strength of the trailing vortex sheet can be expressed as

$$w = - \frac{d\Gamma}{dz} \tag{3.8}$$

The direction of shed vorticity is taken perpendicular to lifting line.

For a piecewise linear distribution of vorticity in the spanwise direction, along with the fact that the change of circulation $(\Gamma_i - \Gamma_{i+1})$ must be shed behind and into the wake. Equation (3.8) can be written with the use of trapezoidal rule

$$(w_i^n + w_{i+1}^n) \left(\frac{z_{i+1}^n - z_i^n}{2} \right) = - (\Gamma_{i+1} - \Gamma_i) \tag{3.9}$$

The value of vorticity at each nodal point can be obtained by starting from the symmetry plane and marching in the spanwise direction with the fact that

$$w_i = 0 \text{ at } z = 0 \ (i=1) \tag{3.10}$$

and referring to Fig. 4, Eq. (3.9) reflects that the vorticity distribution is adjusted such that the shaded area under the vorticity curve is always equal to change of circulation provided that the vorticity is continuous at the common node

between two adjecent panels. Once the vorticity at each of the common node is known, it can be expressed as

$$\underline{w} = (A + B\,\xi)\,e_x \tag{3.11}$$

The velocity induced by a distribution of vorticity on the surface σ at the point P (x_m, y_m, z_m) in the local panel coordinates can be calculated by using Eq. (3.4), Fig. 5.

$$\underline{V}(x_m, y_m, z_m) = -\frac{1}{4\pi} \int_0^{\xi_1} \int_{\zeta_{LE}(\xi)}^{\zeta_{TE}(\xi)} \frac{(A+B\,)(y_m\, e_\zeta - (z_m - \xi)\, e_\eta)}{((x_m-\xi)^2 + y_m^2 + z_m - \zeta)^{2)^{3/2}}}\, d \tag{3.12}$$

with substitution

$$(x_m - \xi) = (y_m^2 + (z_m - \zeta)^2)^{\frac{1}{2}} \tan\theta \tag{3.13}$$

$$= K \tan\theta$$

Equation (3.12) on integration gives

$$\underline{V}(x_m, y_m, z_m) = \frac{1}{4\pi} \int_0^{\xi_1} \left[\frac{(A+B\xi\,)\,(y_m\, e_\zeta - (z_m - \zeta) e_\eta)}{K^2\,((x_m - \xi)^2 + y_m^2 + (z_m - \zeta)^2)^{\frac{1}{2}}} \right]_{\zeta_{LE}(\xi)}^{\zeta_{TE}(\xi)}$$

3.4 Free Vortex wake

The induced velocity at a point on the wake surface is calculated by summing the contribution from three major sources. They are

1) Bound vortex segment (Appendix A)
2) Triangular panels in the near region (Sec. 3.2 & 3.3)
3) Straight semi-infinite vortex filaments in the far region (Appendix A)

The induced velocities calculated due to near wake region from Eqs. (3.7) and (3.14) have to be transformed to global system of reference as follows :

$$\begin{bmatrix} v_x \\ v_y \\ v_z \end{bmatrix} = \begin{bmatrix} d_{\xi x} & d_{\xi y} & d_{\xi z} \\ d_{\eta x} & d_{\eta y} & d_{\eta z} \\ d_{\zeta x} & d_{\zeta y} & d_{\zeta z} \end{bmatrix} \begin{bmatrix} v_x \\ v_y \\ v_z \end{bmatrix}_{loc} \qquad (3.15)$$

where d with suffix is the cosine of angle between its two subscripts.

To satisfy the boundary conditions over free vortex panels an iterative technique is followed. During a typical iterative cycle vorticity distribution is calculated. This is followed by aligning the surface, after perturbation velocities are calculated at the nodal point 1 and control point of panel for vorticity distribution and circulation distribution methods respectively. For calculating the induced velocity at the point results are evaluated at a distance of 10^{-6}

Each of the triangular panel is considered to be a stream surface composed of the streamlines that are parallel to one another with respect to side 1-3. Once the induced velocity at a nodal point or control point is determined the streamline which contains that point is moved in the same direction as that of local velocity.

To demonstrate the approach, the unit vector of streamline at a control point, $\underline{e}_{cp}$ is given by

$$\underline{e}_{cp} = \frac{u_R}{V_R} e_x + \frac{v_R}{V_R} e_y + \frac{w_R}{V_R} e_z \qquad (3.16)$$

Where u_R, v_R, w_R, are the components of induced velocity in x, y & z direction respectively and $V_R = (u_R^2 + v_R^2 + w_R^2)^{\frac{1}{2}}$ Side 1-3 is then moved in the direction parallel to unit vector.

$$x_1 (L+1, J) = x_3 (L, J) = x_1 (L, J) + |l_{13}| \frac{u_R}{V_R}$$

$$y_1 (L+1, J) = y_3 (L, J) = y_1 (L, J) + |l_{13}| \frac{v_R}{V_R}$$

$$z_1 (L+1, J) = z_3 (L, J) = z_1 (L, J) + |l_{13}| \frac{w_R}{V_R}$$

Where (L,J) and (L+1, J) refers to upstream and downstream nodes of side 1-3, l_{13} is the length of side 1-3 (Fig. 5).

The best approximation for the angle at which flow leaves the trailing edge is half the angle of attack. The wake is over-released by taking the first row of panels in the direction of chord for first iteration. The computation is initiated by specifying the rest of the wake to be planar. Align the second row of panel (Fig. 6) with local velocities. The downstream wake shape is adjusted so that the nodal points will have the same y and z coordinate as that of second row. The vorticity distribution is calculated again due to new wake geometry. Align the next row with local velocities and process continues until last row of panels is moved. The semi-infinite filaments of far wake are left parallel to free stream velocity.

Starting from the second iteration the process is altered due to the fact that the geometry of the upstream wake will be affected. Calculate the resultant velocities at all of the nodal points and move the downstream nodal points simultaneously in the direction of local velocity. Repeat the same process until wake shape is converged.

3.5 Tip Core modelling

Refinement of the wake roll up /50/ is done by dividing the spiral into inner and outer portions. Vortex sheet is represented by NP number of points in the spanwise direction. We assume that a turn of spiral is represented by N point vortices. This N has to be determined by trial and error, actually N/NP should be 0.1 to 0.15.

$$\text{Let } \theta_c = \frac{360}{N} \tag{3.17}$$

We first calculate induced velocities and new coordinates of y and z, and then angle θ between the two vectors of adjecent panels is determined. If θ exceeds θ_c then two panels are combined to form a new tip vortex placed at the centroid of those two vortices with circulation that equals the combined circulation of original pair.

We start our calculations from the wing root. Initially $\theta < \theta_c$ over the tip, which is called outer part of the spiral and takes about 20% of the vortices. When $\theta > \theta_c$ then all the vortices are combined to form a tip vortex or inner portion of the spiral, which also consumes almost the same amount of vortice: $\theta = \theta_c$ can be included in either inner part of the spiral or

outer part. It should be noted that once the condition $\theta > \theta_c$ is achieved then for all the points on the right side, the same condition has to be satisfied. Vortex sheet will came nearer and nearer to the tip vortex as go on increasing NP.

Referring to Fig. 11, let

$$L_i = X_{i-1} - X_i = (y_{i-1} - y_i)\, j + (z_{i-1} - z_i)\, k$$

$$= y_i\, j + z_i\, k$$

where X_i is a two dimensional vector which represent the coordinates (y(i), z(i)

and

$$L_{i+1} = X_i - X_{i+1} = y_{i+1}\, j + z_{i+1}\, k$$

the angle between the two vectors L_i and L_{i+1} is given by

$$\theta = \cos^{-1} \frac{y_i\, y_{i+1} + z_i\, z_{i+1}}{(y_i^2 + z_i^2)^{\frac{1}{2}} (y_{i+1}^2 + z_{i+1}^2)^{\frac{1}{2}}}$$

whose direction cosines are $\langle y_i, z_i \rangle$ and $\langle y_{i+1}, z_{i+1} \rangle$.

CHAPTER - 4

DESCRIPTION OF COMPUTER PROGRAM

A computer program is developed to implement the method of solution for both the methods. Vorticity distribution method has been used to calculate the normal force coefficient over flat plate at an angle of attack assuming wake to be planar. The wake rollup could not be solved because of the limitation on the computing power available. The computer program consists of several function subprograms and subroutines.

The subroutine CORT calculates the nodal point of panels over the flat plate wing with given aspect ratio and number of panels in both the direction as input.

Induced velocities are calculated to apply the no-penetration condition over the average point of each panel. This has been achieved by using function subprograms SIMPSN and CINT'S. Next letter of CINT i,e. 5th denotes the j corresponding to a_j such as CINT1R will give the y-component of induced velocity per unit a_1 for right wing and CINT1L for left wing. SIMPSN integrates all these functions by Simpson rule.

Local coordinate axis system is needed for the calculation of perturbation velocities, otherwise it is difficult to integrate those expressions of induced velocity in global system of reference. This way lower and upper limit for integrals of induced velocity will be same for all the panels, provided the size of panel over which integral is taken is same. By the shifting of the origin at one of the nodal point (corner point) coordinates of panels in their own axis system are calculated

and then used for the calculation of induced velocities. These induced velocities are transformed back to the wing fixed frame of reference by rotating the axis system. The induced velocities calculated do not require any transformation as the wing taken is a flat plate.

CINT1R to CINT5R are used for the calculation of induced velocity in y-direction and CINT6R to CINT8R are used to calculate the induced velocities in x and z-directions. Function subprograms ZO and ZU are the equations of line which have been used to convert quadrilateral panels to triangular panel with local origin at the left and right mode respectively.

Continuity of vorticity in x and z directions, Kutta condition along the trailing edge and symmetry condition for a symmetric flow along the root chord are applied, details of which are given in Appendix - C. All conditions including no-penetration condition have been stored in the matrix A(m,n), where m is the total number of equations in term of n(5 times the number of bound vortex panels) variables B is a column vector. This overdetermined set of equations (since number of equations are more than the number of variables) can be solved using the method of Least-squares by reducing them to their normal equations. This scheme was not acceptable to the DEC-1090 system for some cases of increased number of panels as it required much more memory space. Therefore standard library subroutine IMSL, LLSQAR was selected to solve set of

equations by the method of Least-Squares. Now the vorticity distribution coefficients so obtained are stored in matrix B which overwrites the column vector of right hand side. This problem is solved assuming wake to be planar.

Computer program for the circulation distribution method is divided into three major parts and each part consists of several subroutines and function subprograms.

The first part deals with the wing geometry, wing panelling (bound vortex panels), wake panelling (free vortex panels) and calculation of circulation distribution over the lifting surface. The various input to this part are aspect ratio, angle of attack, number of panels in the spanwise direction of flow over lifting surface and free surface.

Subroutine CORD calculates the coordinates of each panel and control point over the lifting surface in order to calculate circulation distribution, while coordinates of triangular panel over the force vortex surface are determined by the subroutine GEMTRY assuming wake to be planar. Subroutine GMQUAD serves the same purpose but the length of panels in the streamwise direction is varied according to quadratic law. Panels in the direction of span are distributed according to cosine spacing for both subroutines GEMTRY and GMQUAD.

No-penetration condition of tangential flow is applied at the control point of each panel over the flat plate. Coefficient matrix (W) obtained from this condition is solved by subroutine

FINV which has been tested against the standard NAG subroutine, FO1AAF. Both of these (FO1AAF and FINV) calculate the inverse (UNIT) of matrix (W) and this UNIT is multiplied to the right hand side of simultaneous equations to obtain the unknowns of circulation.

Second part deals with the wake. The wake geometry is generated by dividing the straight wake into NW rows and NZ columns (Semispan) to form (NW)(NZ) rectangular elements(Fig-6), Each rectangular element is then divided into two triangular panels. Once the spanwise circulation is obtained, vorticity distribution over each triangular panel is calculated. Function subprogram SIMPSN integrates CINT1L and CINT1R to give y-component of induced velocity due to left and right wing and corresponding z-components are obtained from CINT2L and CINT2R. To calculate the velocities in the global axis system, induced velocities calculated are multiplied by the transformation matrix. Induced velocity at a point over the wake surface is the sum of contribution from bound vortex panels,far wake region and near wake with triangular vortex panels. Contribution due to bound and far wake is calculated by VELY, VELZ, VLINFY and VLINFZ. Function subprogram VELY and VELZ will give induced velocities in y and z-directions due to finite vortex element with given end points while VLINFY and VLINFZ calculate velocities due to semi-infinite vortex filament in y and z-directions respectively. Aligning the wake surface in the direction of local flow velocity is done itself in the main program.

In the third part of program number of vortices per turn of rollup is tested. If number of vortices per turn falls from some specified level then those vortices are combined to form a tip vortex and coordinates of other vortices which do not satisfy this condition are written as it is.

Vorticity Distribution Method

VARIABLE	DESCRIPTION
A	mxn matrix, with m number of equations in term of n unknowns
ALPHA	angle of attack in degrees
B	column vector (See IMSL : LLSQAR)
D	is a 3x1 matrix for the three components of unit normal at the receiver panel
EXL	value of ξ
F	is 3x3 matrix obtained from the dot product of global and local axis system
G	is N X NUNK matrix for the no-penetration condition over the average point of bound vortex panels
IDGT	number of significant digits for IMSL
IER	error parameter
IT	do loop index, performing iterations
ITER	maximum number of iterations allowed
N	total bound vortex panels
NEQ	total number of equations
NUNK	number of unknowns
NW	panels in the direction of wake over the wake surface
NX	number of panels in the direction of flow over flat plate
NP	number of nodal points per unit semi-span

VARIABLE	DESCRIPTION
NZ	semi-spanwise number of panels
S12	distance between the points 1 and 2
S13	distance between the points 1 and 3
VR1	a column vector with arrays equal to number of bound vortex panels and calculates induced velocity in y-direction for the right hand side of wing per unit a_1
VL1	- similar to VR1 but for left wing - induced velocity per unit a_1 in local coordinate system
XP	width of panel in x-direction
XAy1	XP for first row over the wake (adjoining region
XAy2	XP for 2^{nd} row
XAy3	XP for 3^{rd} row
XX	x-coordinate in local axis system for left as well as right wing
yyL	y-coordinate for left wing, when observer is facing the flow
yyR	y-coordinate for right wing in local axis system
ZZL	z-coordinate for left wing
ZZR	z-coordinate for right wing
ZETA	value of ζ
ZP	width of panel in z-direction

Circulation Distribution Method

VARIABLE	DESCRIPTION
A	lower limit of integeration
AA	constant term of the linearly varying vorticity expression
ALPHA	angle of attack in degrees
AR	aspect ratio
AREA	area of half flat plate
B	upper limit of integ ration
BB	coefficient of linearly varying vorticity term
C	It is a column vector. Right hand side of simultaneous equations obtained from no-penetration condition
CR	root chord
CT	tip chord
E2	width of panel in spanwise direction
E3	margin left around the singularity on one side
E4	margin left on the right side of singularity
F's	F is a 3x3 matrix obtained from the dot product of local and global axis and elements are like F(1,1) as F11
GM	circulation obtained by joining the panels in the direction of flow
GN	circulation over each panel
II	row number for free vortex panels

VARIABLE	DISCRIPTION
IT	iteration number
ITER	maximum number of iterations allowed
NB	total number of bound vortex panels
NF	free vortex panels
NP	total nodal points per semi-span
NW	number of panels in the direction of flow
NX	number of panels in the flow direction over lifting surface
Ny	spanwise number of panels
S13	distance between the points 1 and 3
THETA	angle between the line joining both sides of nodal point in order to obtain the smooth roll-up
THETAc	critical angle, if THETA exceeds THETAc vortices are combined
TU	total velocity at the control point of a triangular panel in x-direction
TV	total velocity in y-direction at the control point of a triangular panel
TW	total velocity in z-direction
UNIT	inverse of matrix w obtained from no-penetration condition over each panel of lifting surface
VB	y-component of induced velocity due to bound vortex panels

VARIABLE	DISCRIPTION
VF	y-component of induced velocity due to far wake (semi-infinite vortices)
VW	y-component due to near wake region
VLy	induced velocity in y-direction due to left wing in local axis system at one control point due to single triangular panel and obtained by integ rating function CINT1L
VLz	- z-direction due to left wing -
VRy	- y-direction due to right wing -
VRz	- z-direction due to right wing -
W	z-component of induced velocity due to bound vortex panels
WF	z-component of induced velocity at a triangular panel due to all the far wake vortices
WW	- due to near wake -
XP	width of each panel in x-direction
XX	x-coordinate in local axis system
yyL	y-coordinate in local axis system for left wing
yyR	y-coordinate in local axis system for right wing
ZZL	z-coordinate for left wing
ZZR	z-coordinate for right wing

CHAPTER - 5

RESULTS AND DISCUSSION

The methods of vorticity distribution and circulation distribution are implemented using a computer program. The wake shape from vorticity distribution method could not be obtained as the necessary computing power was not available. Spanwise variation of pressure coefficients over flat plate rectangular wing of aspect ratio 1.0 at an angle of attack 15° are obtained and presented in Fig. 12. The results are compared with those of Kandil et al /52/ who have considered the wake roll up.

The difference between the two curves at a section perpendicular to the free stream direction, as shown in Fig. 12 is due to the planar wake for our analysis.

In the program for circulation distribution method the initial wake geometry is automatically generated by dividing the straight wake into NW rows and Nz columns to form (NW)(Nz) rectangular elements. Each rectangular element is then divided into two triangular panels. The panels in the near wake are distributed using cosine spacing in the spanwise direction to emphasize the details near the wing tip. For all the numerical runs presented, the results of the wake shape are shown only for the right half of the wing, since the flow considered is symmetric.

The convergence properties of the circulation distribution method are studied for a rectangular flat plate wing of AR=8.0 at

5-deg. angle of attack and panels in the spanwise direction are varied from 6 to 18 as shown in Fig. 13. It is seen that in the third iteration the nodes of the wake shape at 1.69 span lengths behind the trailing edge virtually fall on top of one another and form a defined contour. The wake geometry shows divergence after three iterations in each case. Such divergence is due to truncation errors. This has been checked by reversing the direction of vortices after three iterations and original wake sheet was not produced.

It is also learned that as the number of spanwise panels increase bringing the outboard panel closer to the tip the wake sheet becomes more flexible and tends to roll-up more. This is because the present method is limited to calculations with less than one turn of rollup.

Simpson rule is used to evaluate the integral, Eq. (3.14), for the expression of induced velocity. Singularity contributes to zero induced velocity, so we can leave an equal margin on both the sides of singularity to calculate the contribution of the panel towards induced velocity having singular effect. The results of Fig. 13 are computed by leaving an interval of $1/30^{th}$ of panel width (spanwise). The results are computed by selecting two different intervals $1/30^{th}$ and $1/50^{th}$ of panel width and are plotted in Fig. 14. It is seen that the wake shape is not changed by selecting different intervals, however the panel end points near the wake tip show different magnitude.

For the above and the following calculations the length of the near wake taken is two spans. Fig. 15 illustrates the pattern of rolled-up wake sheet in the streamwise direction for a rectangular wing of AR = 8.0 at 5-deg. angle of attack for five different downstream stations, x_w = 0.29, 0.59, 0.89, 1.19 and 1.49 span lengths measured from trailing edge; panel arrangement of Nx = 1, Nz = 12, Nw = 7 is used. The streching and spiral motions are seen on the wake panels over the tip region during the roll-up process while the wake sheet remains flat at the middle of the wing, but y-coordinate increase in the streamwise direction.

The effect of changing Nx, the number of panels over the lifting surface (used to calculate the circulation distribution) in the streamwise direction, over wake geometry is negligible as shown in Fig. 16.

The results of wake shape for flat plate rectangular wing of AR = 8.0 at two different angles of attack, α = 5 and 10 deg. are shown in Fig. 17. A comparison of the wake roll up with the results of Sucio and Morino /51/ at 5 chord lengths downstream of the trailing edge, demonstrates the validity in predicting the wake roll-up. The agreement is satisfactory in the sense that Sucio and Morino used constant doublet panels to model the wake; this is equivalent to using vortex filaments. Sucio and Morino's result for the location of the vortex centres appear to agree well with experimental observations oc Chigier and Corsiglia /40/

For spanwise panelling Nz = 6-18 the near wake exhibit no more than one turn of roll-up at any streamwise location. Followi Moore /50/ we tried to model the core by increasing the number of panels in the spanwise direction. Increasing number of panels in the spanwise direction beyond 20 results in overlapping of panels or in other words jumping of panels over one another results in the tip region and no definite contour was obtained.

LIST OF REFERENCES

1. Vom T. Karman (1911) Hydrodynamics by H. Lamb (1945) Dover Publication P-225.

2. Prandtl (1918) Principles of Ideal-fluid aerodynamics by Karamcheti, K. (1966) John Wiley & Sons, Inc., N.Y.

3. Roshenhead, L. (1931) The formation of vortices from a surface of discontinuity. Proc. R.Soc. Lond. A-134,pp. 170-192.

4. Westwater, F.L. (1935) Rolling up of the surface of discontinuity behind an aerofoil of finite span. ARC R&M no. 1692.

5. Bollay, W. (1937) A theory for rectangular wings of small aspect ratio. Journal of Aeronautical Sciences, vol. 4, 294-296.

6. Multhopp, H. (1950) Methods for calculating the lift distribution of wings (subsonic lifting-surface theory) ARC R&M No 2884.

7. Lawrence, H. (1951) The lift distribution on low aspect ratio wings at subsonic speeds. Journal of the Aeronautical Sciences, Vol. 18, 683-695.

8. Brown, C.E. and Michael, W.H. (1954) Effect of leading edge separation on the lift of a delta wing. Journal of Aeronautical Sciences, Vol. 21, 690-694.

9. Mangler, K.W. and Smith, J.H.B. (1957) Calculation of the flow past slender delta wings with leading edge separation, RAE Report No 2593.

10. Gersten, K. (1961) Calculation of non-linear aerodynamic stability derivatives of aeroplanes. AGARD Report No 342.

11. Birkhoff, G. (1962) Helmholtz and Taylor instability Proceedings of the Symposium on Applied Mathematics, Vol. 13, 55-76, American Mathematical Society.

12. Rubbert, P.E. (1962) Theoretical characteristics of arbitrary wings by a nonplanar Vortex Lattice Method. The Boing Company Report D6-9244.

13. Garner, H.C. & Lehrian (1963) Nonlinear theory of steady forces on wings with leading-edge flow separation, ARC R&M No 3375.

14. Van Dyke, M. (1964) Lifting line theory as a singular perturbation problem. Arch. Mech. Stos., Vol. 16, No. 3.

15. Takami, H. (1964) A numerical experiment with discrete vortex approximation with reference to the rolling up of a vortex sheet. Department of Aeronautics and Astronomy, Stanford University, report SUDAER 202.

16. Thurber, J.K. (1965) An asymptotic method for determining the lift distribution of a swept-back wing of finite span. comm. Pure Appl. Math.

17. Ashley, H. and Landahl, M. (1965) Aerodynamics of wings and bodies. Addison-Wesley Publishing Company I.C., Mass.

18. Kuchemann, D. (1965) Report on the I.U.T.A.M. symposium on concentrated vortex motions in fluids. Journal of Fluid Mech Vol. 21, 1-20.

19. Ermolenko, S.D. (1966) Nonlinear theory of small aspect ratio wings. Soviet Aeronautics (in English) Vol. 9, 5-11.

20. Hedman, S.G. (1966) Vortex Lattice Method for calculation of quasi steady state loadings on thin elastic wings. The Aeronautical Research Institute of Sweden. Report 105, Stockholm.

21. Belotserkovskii, S.M. (1967). Theory of thin wings in subsonic flow. Translated from Russian, Plenum Press, N.Y., 67.

22. Kalman, T.P., Rodden, W.P. and Giesing, J.P. (1967) Aerodynamic influence coefficients by the doublet lattice method for interfering non planar lifting surfaces oscillating in subsonic flow (Part I). McDonnell Doughlas Corporation, Report No. DAC-67977.

23. Sack, A.H., Lundberg, R.E., and Hanson, C.W. (1967) A theoretical investigation of the aerodynamics of slender wing body combinations exhibiting leading-edge separation NASA CR-719.

24. Landahl, M.T., and Stark, V.J.E. (1968) Numerical lifting-surface theory problems and progress. AIAA Journal, Vol. 6, 2049-2060.

25. Belotserkovskill, S.M. (1968) Calculation of the flow around wings of arbitrary planforms over a wide range of angles of attack. NASA TT F-12, 291, May 1969.

26. Smith, J.H.B. (1968) Improved calculations of the leading edge separation from slender, thin, delta wings. Proc. R.Soc. Lond., A 306, 67-90.

27. Albano, E., and Rodden, W.P. (1969), A doublet-lattice method for calculating lift distributions on oscillating surfaces in subsonic flows. AIAA Journal, Vol. 7, 279-285.

28. James, R.M. (1969) On the remarkable accuracy of the vortex lattice discretization in thin wing theory. McDonnell Doughlas Aircraft Co., Report DAC-67211.

29. Cunnigham, A.M. (1971) An efficient subsonic collocation metho for solving lifting-surface problems. Journal of Aircraft, Vol. 8, 168-176.

30. Polhamus, E.C. (1971) Charts for predicting the subsonic vortex-lift characteristics of Arrow, Delta & Diamond wings NASA TND - 6243.

31. Polhamus, E.C. (1971) Prediction of vortex-lift characteristic by a leading edge suction analogy. Journal of Aircraft, Vol. 8, 193-199.

32. Moore, D.W. (1971) The discrete vortex approximation of a vortex sheet. Airforce office of Scientific Research Report 1084-69, California Institute of Technology.

33. Butter, D.J. and Hancock, G.J. (1971) A numerical method for calculating the trailing vortex system behind a swept wing at low speeds, The Aeronautical Journal, Vol. 75, 564-568.

34. Ashley, H. and Rodden, W.P. (1972) Wing-body aerodynamic interaction. Annual review of Fluid Mechanics, Vol.4, 431-472.

35. Finkleman, D. (1972) Nonlinear vortex interaction on wing-canard configurations. Journal of Aircraft, Vol. 9, 399-406.

36. Giesing, J.P.,Kalman, T.P. and Rodden, W.P. (1972) subsonic steady and oscillatory aerodynamics for multiple interferring wings and bodies. Journal of Aircraft, Vol. 9, 693-702.

37. Kerney, K.P. (1972) A correction to lifting line theory as a singular perturbation problem. AIAA Journal, Vol.10,1683-168

38. Rodden, W.P., Giesing, J.P. and Kalman, T.P. (1972) Refinement of the nonplanar aspects of the subsonic doublet-lattice lifti surface method. Journal of Aircraft Vol. 9, 69-73.

39. Hess, J.L. (1972) Calculation of potential flow about arbitrary three dimensional lifting bodies. McDonnel Douglas Corporation,Report No MDC J5679-01.

40. Chigier, N.A. and Corsiglia, V.R. (1972) wind-Tunnel studies of wing wake turbulence. Journal of Aircraft Vol. 9,820-825.

41. Hua, H.M. (1973) A finite element method for calculating aerodynamic coefficients of a subsonic airplane. Journal of Aircraft, Vol. 10, 422-426.

42. Rom, J., and Zorea, C. (1973) The calculation of the lift distribution and the near wake behind high and low aspect ratio wings in subsonic flow. Technion-Israel Institute of Technology, Haifa, TAE Report 168.

43. Kuo, C.C., and Morino, L. (1973) steady subsonic flow around finite thickness wings. Boston University, Department of Aerospace Engineering, Boston, Mass., TR-73-02.

44. Kossow, V.J. (1973) On the inviscid roll-up structure of lift generated vortices. Journal of Aircraft, Vol. 10, 647-65

45. Bradley, R.G. Smith, C.W. and Bhateley, I.C. (1973) Vortex-lift prediction for complex wing planforms. Journal of Aircraft, Vol. 10, 379-381.

46. Hough, G.R. (1973) Remarks on vortex-lattice method. Journal of Aircraft, Vol. 10, 314-317.

47. Morino, L. and Kuo, C.C. (1974) subsonic potential aerodynamics for complex configurations : A general theory. AIAA Journal, Vol. 12, 191-197.

48. Mook, D.T. and Maddox, S.A. (1974) Extension of a vortex lattice method to include the effects of leading-edge separation. Journal of Aircraft, Vol. 11, 127-128.

49. Rodeen, W.P., Giesing, J.P., Kalman, T.P., and Rowan, J.C. (1974) Comment on : A finite element method for calculating aerodynamic coefficients of a subsonic airplane. Journal of Aircraft, Vol. 11, 366-367.

50. Moore, D.W. (1974) A numerical study of the roll up of a finite vortex sheet, J. Fluid Mech., Vol. 63, 225-235.

51. Sucio, E.O. and Morino, L. (1976). A nonlinear Finite element analysis of wings in steady incompressible flows with wake Roll up. AIAA paper 76-64, 1976.

52. Kandil, O.A., Mook, D.T., and Nayfeh, A.H. (1976) Nonlinear Prediction of the Aerodynamic loads on lifting surfaces. Journal of Aircraft, Vol. 13, 22-28.

53. Fink, P.T. and Soh, W.K. (1978) A new approach to roll up calculations of vortex sheets. Proc. Roy. Soc. of London, Ser A 362, 195-209.

54. Johnson, F.T., Tinoco, F.N., Lu, P., and Epton, MA. (1980) Three dimensional flow over wings with leading edge vortex separation. AIAA Journal, Vol. 18, 367-380.

55. Lavin, D. and Katz, J. (1981) vortex lattice method for the calculation of the nonsteady separated flow over delta wings, Journal of Aircraft, Vol. 18, 1032-1037.

56. Murman, E.M. and Stremel, P.M. (1987) A vortex wake capturing method for potential flow calculations. AIAA Paper 82-0947,198

57. Summa, J.M. (1982) Advanced Rotor analysis method for the aerodynamics of vortex/blade interactions in Hover. Eighth European Forum, paper - 28, France.

58. Hoeijmaker, H.W.M. (1983) Computational vortex flow Aerodynami AGARD CP 342.

59. Hoeijmaker, H.W.M. and Vaatstra, W. (1983) A higher order pane method applied to vortex sheet roll up. AIAA Journal, Vol. 21, 516-523.

60. Kandil, O.A., Chu, L., and Tureaud, T., (1984) A nonlinear hybrid vortex method for wings at large angles of attack. AIAA Journal Vol. 22, 329-336.

61. Yeh, D.T., and Plotkin, A. (1986) Wake roll up behind a large aspect ratio wing. AIAA Journal, Vol. 24, 1417-1423.

APPENDIX - A

Calculation of induced velocity due to vortex filaments

The far wake is modelled by straight semi-infinite vortex filaments that are in the uniform stream direction. Circulation Γ for this is derived in terms of the unknown parameter a's of bound vortex panels (Fig. 7) as follows :

$$\Gamma_1 = - \int_0^{\zeta_1} w_x \, d\zeta$$

$$\Gamma_2 = - \int_0^{\zeta_2} w_x \, d\zeta$$

$$\Gamma_3 = - \int_0^{\zeta_3} w_x \, d\zeta$$

$$w_x = w_\zeta \, d_{\zeta x} + w_\xi \, d_{\xi x}$$

$$= w_\xi = - a_2 \xi - a_4 - a_5 \zeta$$

$$\Gamma_1 = - \int_0^{\zeta_1} (-a_2 \xi - a_4 - a_5 \zeta) \, d\zeta$$

$$= -\left(-a_2 \xi \; \zeta_1 - a_4 \; \zeta_1 - a_5 \; \frac{\zeta_1^2}{2}\right)$$

Similarly,

$$\Gamma_2 = a_2 \xi \; \zeta_2 + a_4 \; \zeta_2 + a_5 \; \frac{\zeta_2^2}{2}$$

and $$\Gamma_3 = a_2 \xi \; \zeta_3 + a_4 \; \zeta_3 + a_5 \; \frac{\zeta_3^3}{2}$$

The velocity induced (Fig. 8a) at any point C(x,y,z) due to bound vortex is calculated using Biot-Savart law as follows :

$$d\underline{V} = \frac{\Gamma_n \sin\theta \, dl}{4\pi r^2} \qquad (A-1)$$

Integrating

$$V = \frac{\Gamma_n}{4\pi r_p} (\cos\theta_1 - \cos\theta_2) \qquad (A-2)$$

$$\cos\theta_1 = \frac{\underline{r}_0 \cdot \underline{r}_1}{|\underline{r}_0||\underline{r}_1|} \quad , \quad \cos\theta_2 = \frac{\underline{r}_0 . \underline{r}_2}{|\underline{r}_0||r_2|}$$

$$r_p = \frac{|\underline{r}_1 \times \underline{r}_2|}{|\underline{r}_0|}$$

$$\underline{V} = \frac{\Gamma_n}{4\pi} \frac{\underline{r}_1 \times \underline{r}_2}{|\underline{r}_1 \times \underline{r}_2|^2} \left[\underline{r}_0 \cdot \left(\frac{\underline{r}_1}{|r_1|} - \frac{\underline{r}_2}{|r_2|}\right)\right]$$

$$\underline{r}_0 = (x_2-x_1)\,\hat{i} + (y_2-y_1)\,\hat{j} + (z_2-z_1)\,\hat{k}$$

$$\underline{r}_1 = (x-x_1)\,\hat{i} + (y-y_1)\,\hat{j} + (z-z_1)\,\hat{k}$$

$$\underline{r}_2 = (x-x_2)\,\hat{i} + (y-y_2)\,\hat{j} + (z-z_2)\,\hat{k}$$

$$\underline{V} = \frac{\Gamma_n}{4\pi}\left[\frac{(x_2-x_1)(x-x_1) + (y_2-y_1)(y-y_1) + (z_2-z_1)(z-z_1)}{((x-x_1)^2 + (y-y_1)^2 + (z-z_1)^2)^{1/2}} - \right.$$

$$\left. \frac{(x_2-x_1)(x-x_2) + (y_2-y_1)(y-y_2) + (z_2-z_1)(z-z_2)}{((x-x_2)^2 + (y-y_2)^2 + (z-z_2)^2)^{1/2}}\right]$$

$$[((y-y_1)(z-z_2)-(y-y_2)(z-z_1))\,\hat{i}-((x-x_1)(z-z_2)-(x-x_2)(z-z_1))\,\hat{j}+((x-x_1)(y-y_2)-(x-x_2)(y-y_1))\hat{k}]/[((y-y_1)(z-z_2)-(y-y_2)(z-z_1))^2+((x-x_1)(z-z_2)-(x-x_2)(z-z_1))^2+((x-x_1)(y-y_2)-(x-x_2)(y-y_1))^2] \quad (A-3)$$

For a horse-shoe vortex

From Fig. 8(b) $\underline{V} = \underline{V}_{AB} + \underline{V}_{\infty A} + \underline{V}_{B\infty}$

where

$$\underline{V}_{AB} = \underline{V}$$

$$\underline{V}_{\infty A} = \frac{\Gamma_n}{4\pi}\,\frac{(z-z_1)\,\hat{j}+(y-y_1)\hat{k}}{(z-z_1)^2+(y-y_1)^2}\left[1+\frac{(x-x_1)}{((x-x_1)^2+(y-y_1)^2+(z-z_1)^2)^{\frac{1}{2}}}\right] \quad (A-4)$$

$$\underline{V}_{B\infty} = \frac{\Gamma_n}{4\pi}\,\frac{(z-z_2)\,\hat{j}+(y-y_2)\hat{k}}{(z-z_2)^2+(y-y_2)^2}\left[1+\frac{(x-x_2)}{((x-x_2)^2+(y-y_2)^2+(z-z_2)^2)^{\frac{1}{2}}}\right] \quad (A-5)$$

APPENDIX - B

Evaluation of integrals of induced velocity

From Eq. (3.7)

$$\underline{V}(x,y,z) = -\frac{1}{4\pi}\sum_{i=1}^{2}\iint \frac{y w_\zeta \hat{e}_\xi + ((z-\zeta)w_\xi - (x-\xi)w_\zeta)\hat{e}_\eta - y w_\xi \hat{e}_\zeta}{((x-\xi)^2 + y^2 + (z-\zeta)^2)^{3/2}} d\zeta$$

$$v_x = -\frac{1}{4\pi}\iint \frac{y w_\xi}{r^3}\, d\zeta\, d\xi$$

$$v_y = -\frac{1}{4\pi}\iint \frac{(z-\zeta)w_\xi - (x-\xi)\, w_\zeta}{r^3}\, d\zeta\, d\xi$$

$$v_z = \frac{1}{4\pi}\iint \frac{y w_\xi}{r^3}\, d\zeta\, d\xi$$

where $r = [(x-\xi)^2 + y^2 + (z-\zeta)^2]^2$

$$w_\xi = a_1 + a_2\zeta + a_3\xi$$

$$w_\zeta = -a_2\xi - a_4 - a_5\zeta$$

$$v_x = -\frac{1}{4\pi}\sum_{i=1}^{2}\iint \frac{y(a_1+a_2\zeta+a_3\xi)}{((x-\xi)^2 + y^2+(z-\zeta)^2)^{3/2}}\, d\zeta\, d\xi$$

Substituting

$$(x-\xi) = [y^2+(z-\zeta)^2]^{\frac{1}{2}}\tan\theta = K\tan\theta$$

and integrating

$$v_x = \frac{1}{4\pi} \sum_{i=1}^{2} \int_0^{\xi_1} \left[\frac{y(z-\zeta)}{rk^2} a_1 + \left(\frac{y(z-\zeta)}{rk^2} + \frac{y}{r} \right) a_2 + \frac{\xi y(z-\zeta)}{rk^2} a_3 \right]_{\zeta_1(\xi)}^{\zeta_2(\xi)} d\xi \qquad (3\text{-}1)$$

For calculating induced velocity due to i=1, $\zeta_1(\xi) = 0$ is Eq. of line BC (Fig. 6b) $\zeta_2(\xi) = 0$ is the equation of AB in local coordinate system with origin at A. For i=2 origin is shifted to B and $\zeta_1(\xi) = 0$ $\zeta_2(\xi) = 0$ are equations of CD and BC, ξ_1 is the distance

$$vy = \frac{1}{4\pi} \sum_{i=1}^{2} \iint \frac{(2-\zeta)(-a_2\xi - a_4 - a_5\zeta) - (x-\xi)(a_1 + a_2\xi + a_3\zeta)}{r^3} d\zeta\, d\xi \qquad (B\text{-}2)$$

$$= I_1 a_1 + I_2 a_2 + I_3 a_3 + I_4 a_4 + I_5 a_5$$

Solving with the same substitution as $(x-\xi) = K \tan$

$$I_1 = -\frac{1}{4\pi} \sum_{i=1}^{2} \int_0^{\xi_1} \left[\frac{(x-\xi),\ (z-\zeta)}{rk^2} \right]_{\zeta_1(\xi)}^{\zeta_2(\xi)} d \qquad (B\text{-}3.1)$$

$$I_2 = \frac{1}{4\pi} \sum_{i=1}^{2} \int_0^{\xi_1} \left[\frac{(2\xi - x)}{r} - \frac{(x-\xi)z(z-\zeta)}{rk} \right]_{\zeta_1(\xi)}^{\zeta_2(\xi)} d\xi \qquad (B\text{-}3.2)$$

$$I_3 = \frac{1}{4\pi} \sum_{i=1}^{2} \int_0^{\xi_1} \frac{(x-\xi)\,\xi\,(z-\zeta)}{rk^2} \Big]_{\zeta_1(\xi)}^{\zeta_2(\xi)} d\xi \qquad (B\text{-}3.3)$$

$$I_4 = \frac{1}{4\pi} \sum_{i=1}^{2} \int_{0}^{\xi_1} \left[\frac{1}{4} \right]_{\zeta_1(\xi)}^{\zeta_2(\xi)} d\xi \qquad \text{(B-3.4)}$$

$$I_5 = -\frac{1}{4\pi} \sum_{i=1}^{2} \int_{0}^{\xi_1} \left[-\frac{z}{r} - \log \left| \frac{r+(z-\zeta)}{k} \right| + \frac{z-\zeta}{r} \right]_{\zeta_1(\xi)}^{\zeta_2(\xi)} d\xi \qquad \text{(B-3.5)}$$

It is easy to apply simpson's rule for evaluating these integrals rather than looking for closed form expressions.

$$v_2 = \frac{1}{4\pi} \sum_{i=1}^{2} \iint \frac{yw_\xi}{r^3} \, d\zeta \, d\xi \qquad \text{(B-4)}$$

$$= \frac{1}{4\pi} \sum_{i=1}^{2} \int_{0}^{\xi_1} \left[\frac{y(z-\zeta)}{rk^2} a_2 + \frac{y(z-\zeta)}{rk^2} a_4 + \left(\frac{y}{r} + \frac{yz(z-\zeta)}{rk^2} \right) a_5 \right]_{\zeta_1(\xi)}^{\zeta_2(\xi)} d\xi \qquad \text{(B-5)}$$

Quadrilateral panels over the flat plate are not subdivided unlike free vortex panels over the wake, then summation from Eq. (A-5) is dropped and the equations $\zeta_1(\xi) = 0$, $\zeta_2(\xi) = 0$ becomes the Eq. of lines AB and CD respectively (Fig. 6b). Second integral of A-5 remains the same from 0 to ξ_1.

APPENDIX - C

Boundary Conditions over bound vortex panels

The boundary condition equations are satisfied at certain nodes of bound vortex panels to obtain the undetermined coefficients of the local vorticity distribution over bound vortex panels.

The no-penetration condition Eq. (2.6) is enforced at the average point of the bound vortex panels. At m^{th} control point Eq. (2.6) is of the form

$$\sum_{k=1}^{N}\sum_{j=1}^{5}\begin{bmatrix} d_{nx} & d_{ny} & d_{nz}\end{bmatrix}_m \begin{bmatrix} d_{\xi x} & d_{\eta x} & d_{\zeta x} \\ d_{\xi y} & d_{\eta y} & d_{\zeta y} \\ d_{\xi z} & d_{\eta z} & d_{\zeta z}\end{bmatrix}_k \begin{bmatrix} u_j \\ v_j \\ w_j\end{bmatrix}_{(m,k)} \times a(j,k)$$

$$= -\begin{bmatrix}\cos\alpha & \sin\alpha & 0\end{bmatrix} \begin{bmatrix} d_{nx} \\ d_{ny} \\ d_{nz}\end{bmatrix} \qquad (c\text{-}1)$$

Where α is the angle of attack and suffix m refers to the receiver panel and k to the sender panel, d_{nx}, d_{ny}, d_{nz} are the cosines of angle between normal at m^{th} control point and x,y,z axis respectively.

For a flat plate rectangular wing if we are calculating the induced velocity due to bound vortex, (C-1) reduces to

$$\sum_{k=1}^{N}\sum_{j=1}^{5} (v_j)_{m,k} \times a(j,k) = \sin\alpha \qquad (C\text{-}2)$$

$$\begin{matrix} d_{\xi x} & d_{\eta x} & d_{\zeta x} \\ d_{\xi y} & d_{\eta y} & d_{\zeta y} \\ d_{\xi z} & d_{\eta z} & d_{\zeta z} \end{matrix}$$

otherwise has to be evaluated

Where d with suffix in the cosine of the angle between its two subscripts on sender panel and u_j, v_j, w_j are the velocity components per unit a_j.

In addition we write equation of vorticity continuity at each common node of bound vortex panels i,e. w_z and w_x should be continuous at each global node, (Fig. 9),

$$w_z = w_\xi d_{\zeta z} + w_\xi d_{\xi z}$$

$$w_x = w_\zeta d_{\zeta x} + w_\xi d_{\xi x}$$

For example

$$\begin{aligned} w_z\,(I,4) &= w_z\,(II,1) \\ w_z\,(I,2) &= w_z\,(II,1) \\ w_z\,(III,3) &= w_z\,(IV,2) \\ w_z\,(II,2) &= w_z\,(IV,4) \end{aligned} \qquad \text{(C-3)}$$

and four equations from continuity at common node (I,3), i.e.

$$\begin{aligned} w_z\,(I,3) &= w_z\,(II,2) \\ w_z\,(III,4) &= w_z\,(IV,1) \\ w_z\,(I,3) &= w_z\,(III,4) \\ w_z\,(II,2) &= w_z\,(IV,1) \end{aligned} \qquad \text{(C-4)}$$

Continuity in x-direction is obtained by replacing z by x from (c-3) and (C-4).

Kutta condition, Eq. (2.10) is enforced at the nodes along the edges of separation, such as (III,2), (III,3), (IV,2) & (IV,3), Ref. Fig. 9, where

$$w_x v_z - w_z v_x = 0$$

or

$$w_x \cos\beta - w_z \sin\beta = 0 \qquad \text{(C-5)}$$

where β is the angle with z-axis. For a flat plate rectangular wing this β is taken as 90°.

Kutta condition at these four nodes is

$$\begin{aligned} w_z\ (III,2) &= 0 \\ w_z\ (III,3) &= 0 \\ w_z\ (IV,2) &= 0 \\ w_z\ (IV,3) &= 0 \end{aligned} \qquad \text{(C-6)}$$

The last set of equations is obtained from symmetry condition for a symmetric flow along the root chord, that vorticity in x-direction is zero.

$$w_x = 0$$

$$= w_\zeta d_{\zeta x} + w_\xi d_{\xi x}$$

$$= w_\xi \qquad \text{for a flat plate rectangular wing}$$

$$w_x\ (I,1) = 0$$

$$w_x\ (I,2) = 0$$

$$w_x\ (III,1) = 0 \qquad \text{(C-7)}$$

$$w_x\ (III,2) = 0$$

The overdetermined set of equations obtained from (C-2) to (C-7) is solved by the method of least squares.

APPENDIX - D

Calculation of wake unknowns in terms of vorticity distribution coefficients of bound vortex panels.

It is difficult to solve the unknowns (vorticity distribution coefficients) of wake panels individually. If we satisfy continuity and symmetry condition over the wake panels it gives under-determined set of equations which cannot be solved. Therefore unknowns for free vortex panels are derived in terms of unknowns (a's) of bound vortex panels. This has been achieved by applying the condition that out flow of vorticity is equal to inflow of vorticity to free vortex panels (Fig. 10).

Outflow of vorticity in z-direction = vorticity from panel 1 + vorticity from panel 5

$$= - \int_0^{\zeta_1} (w_x)_1 \, dz - \int_0^{\zeta_1} (w_x)_5 \, dz \qquad \text{(D-1)}$$

Inflow of vorticity = vorticity in z-direction to panel 9

$$= - \int_0^{\xi_1} (w_x)_9 \, dz \qquad \text{(D-2)}$$

$$(w_x)_9 = (w_\xi d_{\xi x} + w_\zeta d_{\zeta x})_9 = (w_\zeta)_9$$

$$(w_x)_{1 \text{ or } 5} = (w_\zeta d_{\xi x} + w_\xi d_{\xi x})_{1 \text{ or } 5} = (w_\xi)_{1 \text{ or } 5}$$

Equating (D-1) and (D-2)

$$\int_0^{\xi_1} (w_\zeta)_9 \, dz = \int_0^{\zeta_1} (w_\xi)_1 \, dz + \int_0^{\zeta_1} (w_\xi)_5 \, dz$$

$$\int_0^{\xi_1} (a_1 + a_2 \zeta + a_3 \xi) \, d\xi = - \int_0^{\zeta_1} (a_2 \xi + a_4 + a_5 \zeta) \, d\zeta$$

$$- \int_0^{\zeta_1} (a_2 \xi + a_4 + a_5 \zeta)_5 \, d\zeta$$

$$(a_1 \xi_1 + a_2 \zeta\xi_1 + a_3 \frac{\xi_1^2}{2})_9 = -(a_2 \xi\zeta_1 + a_4 \zeta_1 + a_5 \frac{\zeta_1^2}{2})_1$$

$$-(a_2 \xi\zeta_1 + a_4 \zeta_1 + a_5 \frac{\zeta_1^2}{2})_5 \quad \text{(D-3)}$$

Since flow leaves the TE at an angle of 90°, $\zeta_1 = \xi_1$ for a rectangular wing.

Equating coefficients of ζ and ξ, from D-3

$$(a_2)_9 = -(a_2)_1 - (a_2)_5 \quad \text{(D-4)}$$

$$(a_1 + a_3 \frac{\xi_1}{2})_9 = (a_4 + a_5 \frac{\zeta_1}{2})_1 - (a_4 + a_5 \frac{\zeta_1}{2})_5 \quad \text{(D-5)}$$

At pt A, $\xi_1 = 0$

$$(a_1)_9 = -(a_4)_1 - (a_4)_5 \quad \text{(D-6)}$$

and $$(a_3)_9 = -(a_5)_1 - (a_5)_5 \quad \text{(D-7)}$$

Similarly if we equate the outflow of vorticity from bound vor tex panels (1 and 5) to the inflow of vorticity to free vortex panel (9) in x-direction.

we get,

$$\int_0^{\zeta_1} (w_z)_9 \, dx = \int_0^{\xi_1} (w_z)_1 \, dx + \int_0^{\xi_1} (w_2)_5 \, dx \quad \text{(D-8)}$$

$$(w_z)_9 = w_\xi = (-a_2\xi - a_4 - a_5\zeta)_9$$

$$(w_z)_{1 \text{ or } 5} = w_\zeta = (a_1 + a_2\zeta + a_3\xi)_{1 \text{ or } 5}$$

From (D-8)

$$\int_0^{\zeta_1} (-a_2\xi - a_4 - a_5\zeta)_9 \, d\zeta = \int_0^{\xi_1} (a_1 + a_2\zeta + a_3\xi)_1 \, d\xi + \int_0^{\xi_1} (a_1 + a_2\zeta + a_3\xi)_5 \, d\xi \qquad \text{(D-9)}$$

Integrating

$$(-a_2\xi\zeta_1 - a_4\zeta_1 - a_5\frac{\zeta_1^2}{2})_9 = (a_1\xi_1 + a_2\zeta\xi_1 + a_3\frac{\xi_1^2}{2})_1 + (a_1\xi_1 + a_2\zeta\xi_1 + a_3\frac{\xi_1^2}{2})_5 \qquad \text{(D-10)}$$

Subtracting (D-4) from D-10)

$$(a_4 + a_5\frac{\zeta_1}{2})_9 = -(a_1 + a_3\frac{\xi_1}{2})_1 - (a_1 + a_3\frac{\xi_1}{2})_5 \qquad \text{(D-11)}$$

For a large aspect ratio wing at point A

$$\zeta_1 = \xi_1 = 0$$

$$(a_4)_9 = -(a_1)_1 - (a_1)_5 \qquad \text{(D-12)}$$

$$(a_5)_9 = -(a_3)_1 - (a_3)_5 \qquad \text{(D-13)}$$

Outflow of vorticity from panel 9 equated to inflow of vorticity to panel 10 can be written as follows

$$\int_0^{\xi_1} (w_x)_9 \, d\xi = \int_0^{\xi_1} (w_x)_{10} \, d\xi \qquad \text{(D-14)}$$

$$\int_0^{\zeta_1} (w_z)_9 \, d\zeta = \int_0^{\zeta_1} (w_z)_{10} \, d\zeta \qquad \text{(D-15)}$$

(D-14) gives

$$(a_1 \xi_1 + a_2 \zeta\xi_1 + a_3 \frac{\xi_1^2}{2})_9 = (a_1 \xi_1 + a_2 \zeta\xi_1 + a_3 \frac{\xi_1^2}{2})_{10} \quad \text{(D-16)}$$

$$(a_2)_9 = (a_2)_{10} \quad \text{(D-17)}$$

and $$(a_1 + a_3 \frac{\xi_1}{2})_9 = (a_1 + a_3 \frac{\xi_1}{2})_{10} \quad \text{(D-18)}$$

and from D-15

$$(-a_2 \xi \zeta_1 - a_4 \zeta_1 - a_5 \frac{\zeta_1^2}{2})_9 = (-a_2 \xi \zeta_1 - a_4 \zeta_1 - a_5 \frac{\zeta_1^2}{2})_{10} \quad \text{(D-19)}$$

From D-17 and D-19

$$(a_4 + a_5 \frac{\zeta_1}{2})_9 = (a_4 + a_5 \frac{\zeta_1}{2})_{10} \quad \text{(D-20)}$$

Continuity condition at the points F and B (Fig.10) in z-direction gives

$$(w_z)_9 \Big/_{F\&B} = (w_z)_{10} \Big/_{F\&B} \quad \text{(D-21)}$$

At point B $$(-a_2 \xi_1 - a_4)_9 = -(a_4)_{10} \quad \text{(D-22)}$$

At point F $$(-a_4 - a_5 \zeta_1)_9 = (a_2 \xi_1 - a_4 - a_5 \zeta_1)_{10} \quad \text{(D-23)}$$

Subtracting (D-22) from (D-23)

$$(a_2 \xi_1 - a_5 \zeta_1)_9 = (a_2 \xi_1 - a_5 \zeta_1)_{10} \quad \text{(D-24)}$$

From D-17 and D-24

$$(a_5)_9 = (a_5)_{10} \quad \text{(D-25)}$$

From D-24 and D-25

$$(a_4)_9 = (a_4)_{10} \tag{D-26}$$

Continuity in x-direction at same points F and B gives

$$(w_x)_9 \,/_{F\&B} = (w_x)_{10} \,/_{F\&B} \tag{D-27}$$

at point B $(a_1 + a_3 \xi_1)_9 = (a_1)_{10}$ (D-28)

at point F $(a_1 + a_2 \zeta_1)_9 = (a_1 + a_2 \zeta_1 + a_3 \xi_1)_{10}$ (D-29)

Subtracting

$$(a_2 \zeta_1 - a_3 \xi_1)_9 = (a_2 \zeta_1 - a_3 \xi_1)_{10} \tag{D-30}$$

From D-17 and D-30

$$(a_3)_9 = (a_3)_{10} \tag{D-31}$$

Add D-27 to D-28

we get $(a_1)_9 = (a_1)_{10}$ (D-32)

Similarly vorticity distribution coefficients for panel 10 and 17 are obtained by applying the continuity of vorticity in x and z-direction at points F and G (Fig. 10)

continuity in z-direction

$$(w_z)_{10} \,/_{F,G} = (w_z)_{17} \,/_{F,G} \tag{D-33}$$

$$(w_\xi)_{10} \,/_{F,G} = (w_\xi)_{17} \,/_{F,G} \tag{D-34}$$

pt G $(a_2 \xi_1 - a_4 - a_5 \zeta_1)_{10} = -(a_4)_{17}$ (D-35)

pt F $(-a_4 - a_5 \zeta_1)_{10} = (-a_4 - a_2 \xi_1)_{17}$ (D-36)

Subtracting

$$(a_2)_{10} = (a_2)_{17} \quad \text{(D-37)}$$

Continuity in x-direction

$$(w_\zeta)_{10} / _{F,G} = (w_\zeta)_{17} / _{F,G} \quad \text{(D-38)}$$

pt G $(a_1 + a_2 \zeta_1 - a_3 \xi_1)_{10} = (a_1)_{17}$ (D-39)

pt F $(a_1 + a_2 \zeta_1)_{10} = (a_1 + a_3 \xi_1)_{17}$ (D-40)

Subtracting

$$(a_3)_{10} = (a_3)_{17} \quad \text{(D-41)}$$

Applying outflow conditions

we will get

$$(a_1)_{10} = (a_1)_{17}$$

$$(a_2)_{10} = (a_2)_{17}$$

$$(a_3)_{10} = (a_3)_{17}$$

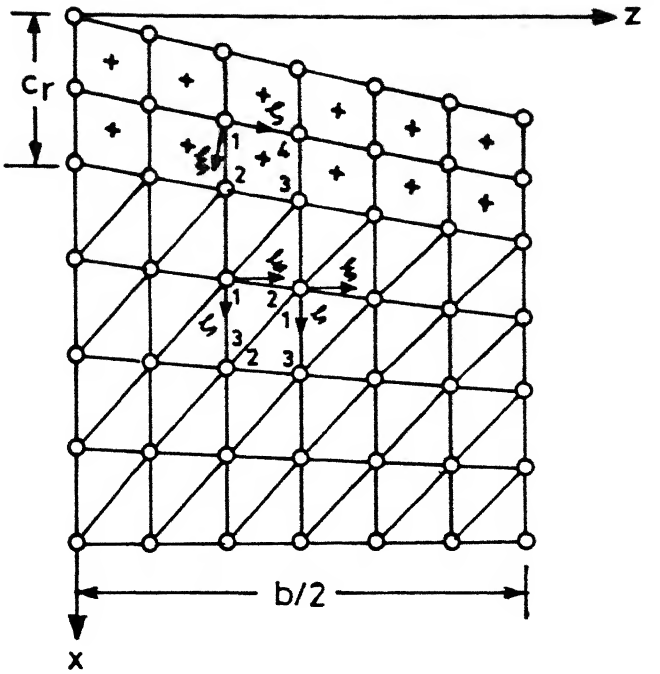

Fig. 1 Arrangement of bound and free vortex panels.

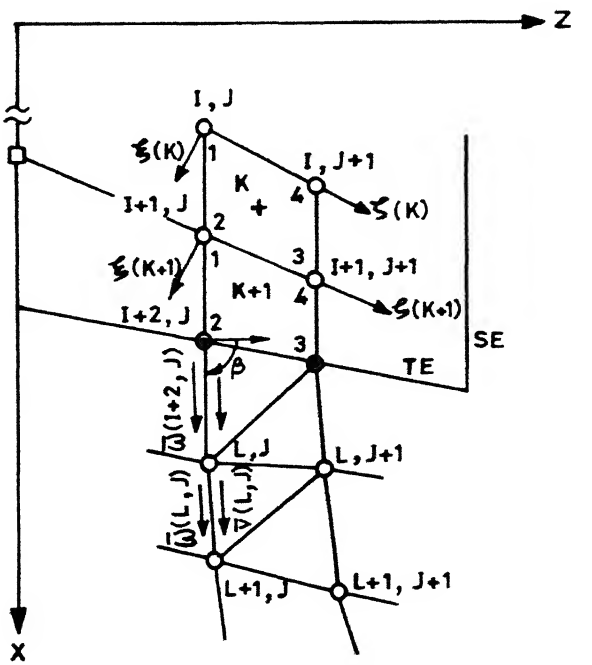

+ No-Penetration Condition
o Continuity of Vorticity Condition
• Kutta Condition
□ Symmetry Condition
Kinematic and Dynamic Condition

Fig. 2 Details of boundary conditions.

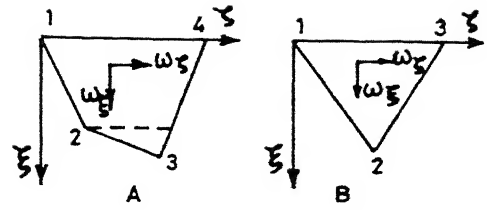

Fig. 3 Quadrilateral and triangular vortex panels.

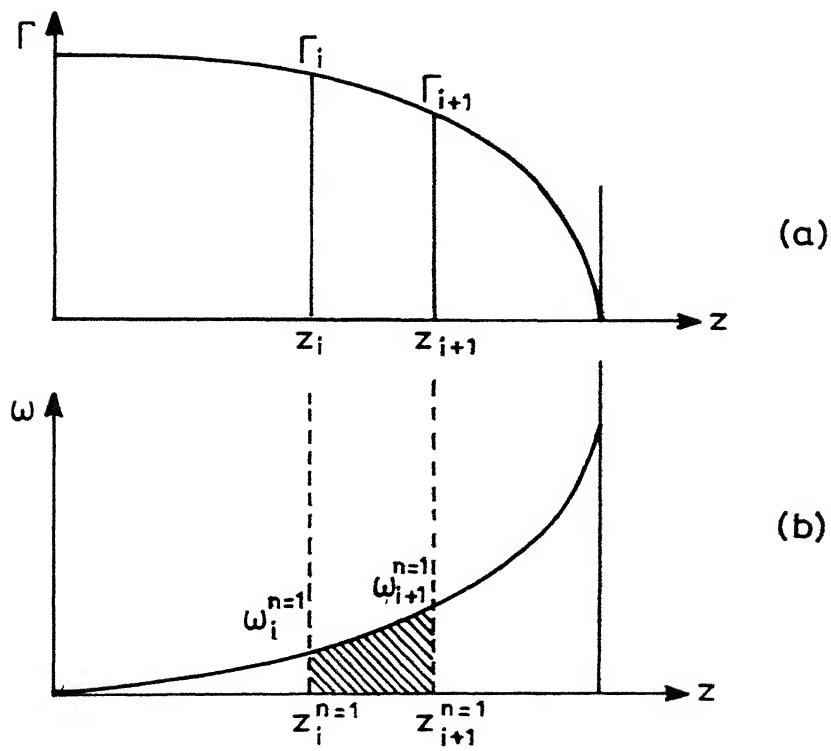

Fig. 4 Spanwise circulation and shed vorticity distribution.

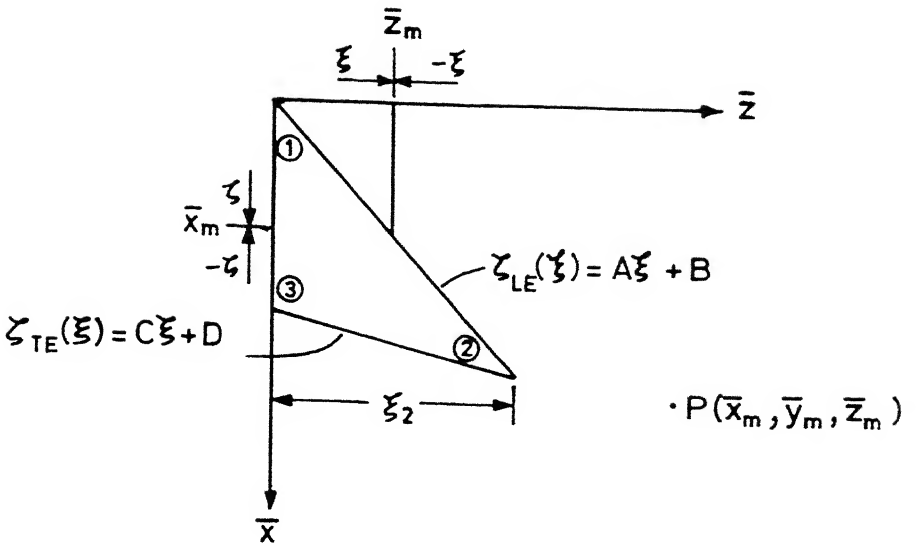

Fig. 5 Geometry of a triangular panel

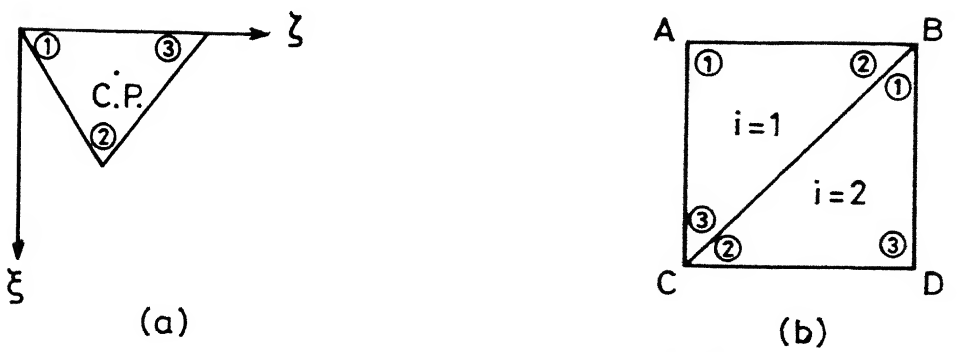

Local panel numbering system

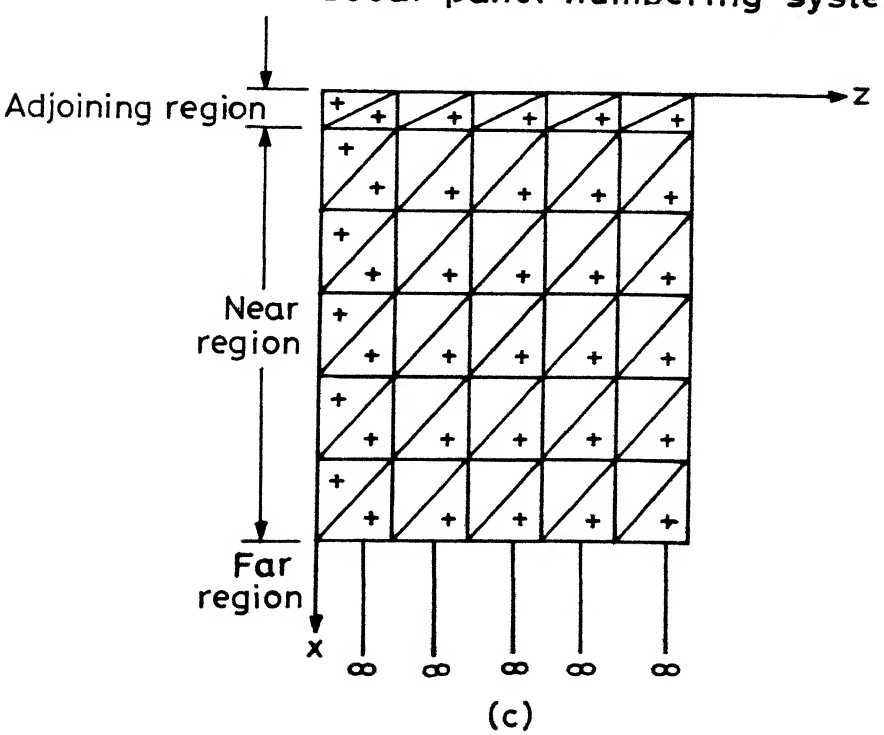

Fig. 6 Location of control points and regions.

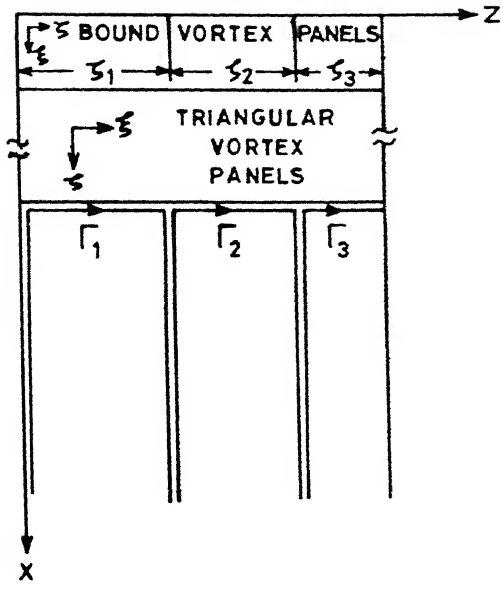

Fig. 7 Far wake modelling.

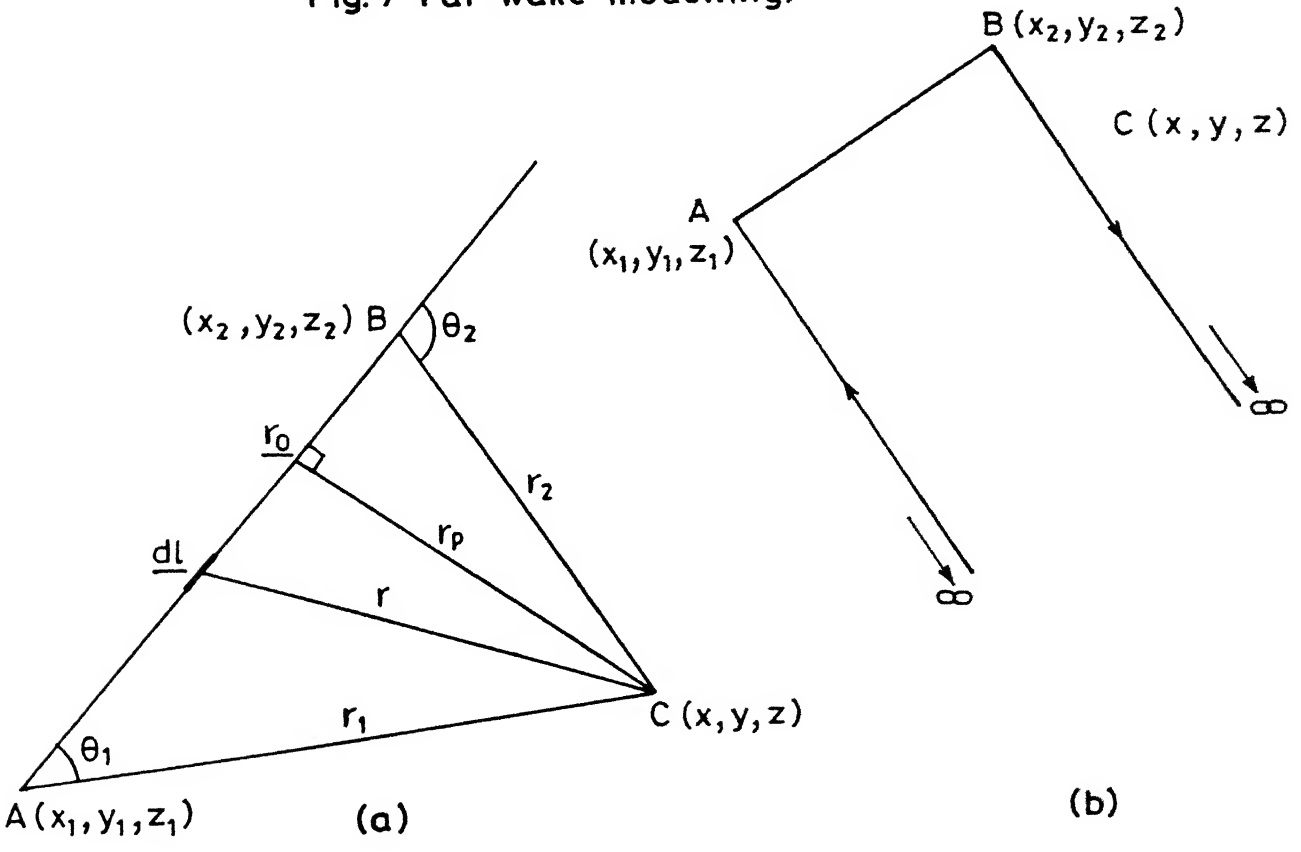

Fig. 8 Induced velocity calculation due to horse-shoe vortex.

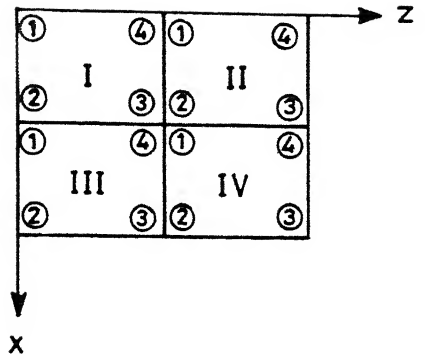

Fig. 9 Details of boundary conditions.

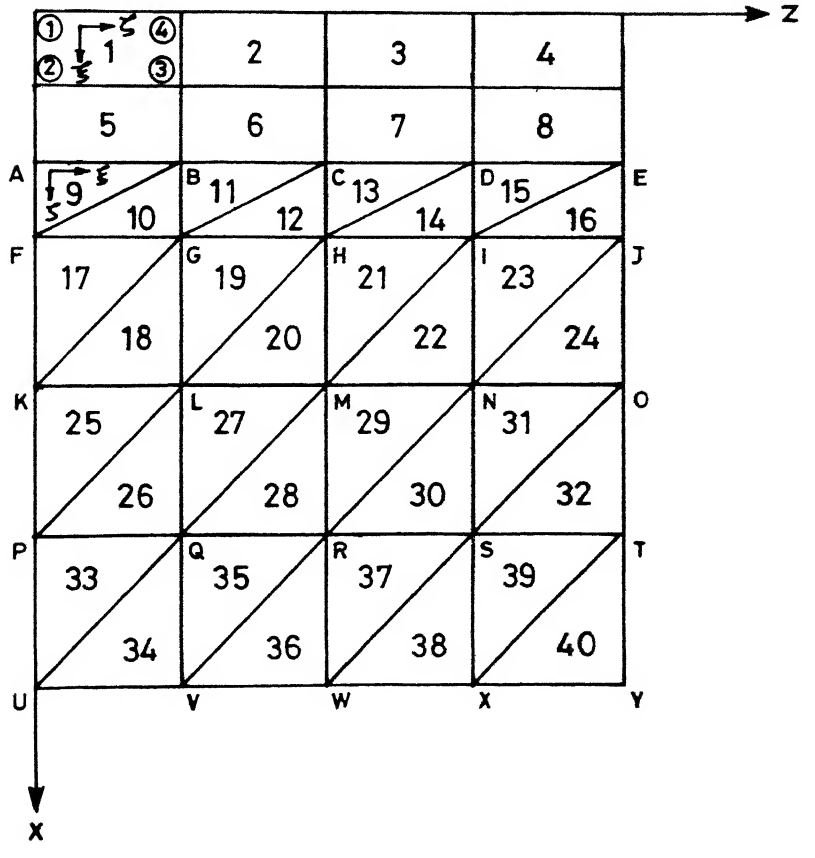

Fig. 10 Equating outflow of vorticity to inflow.

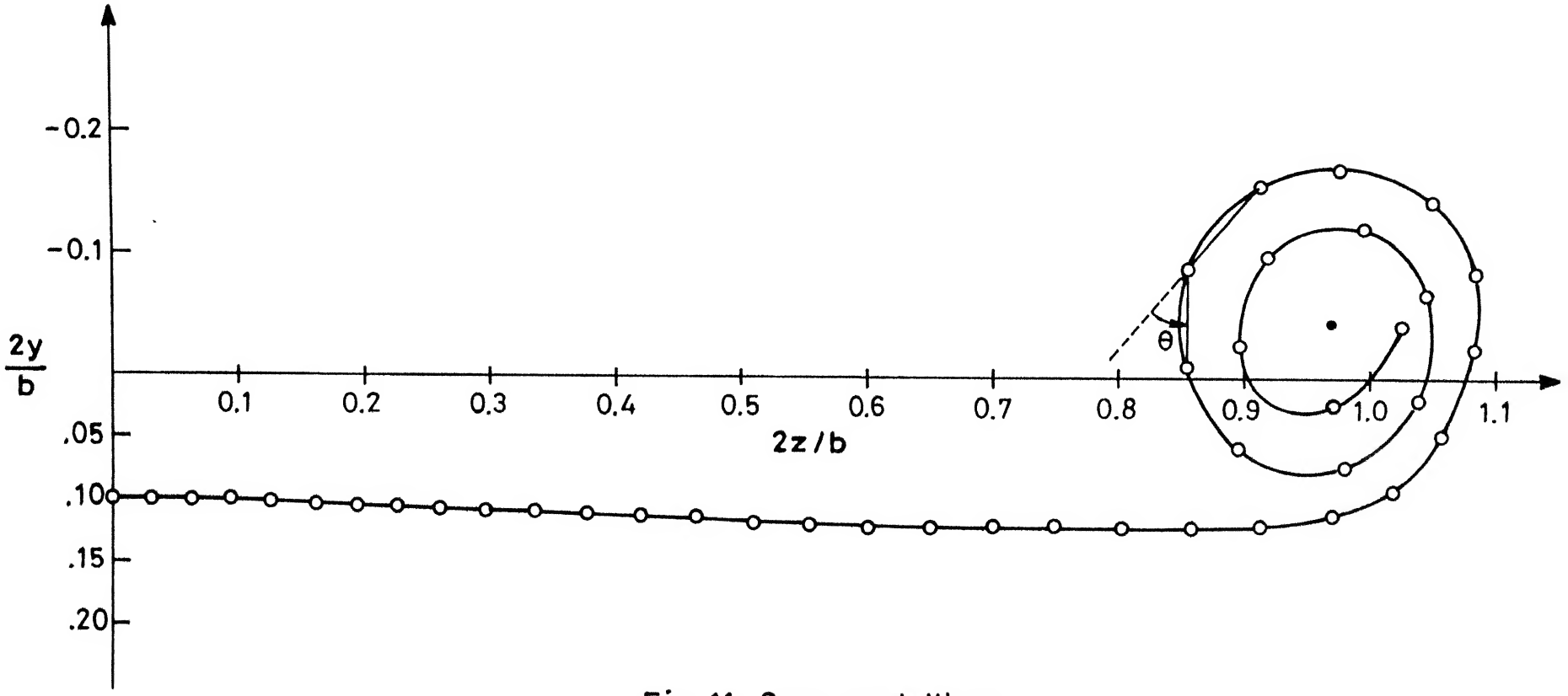

Fig. 11 Core modelling.

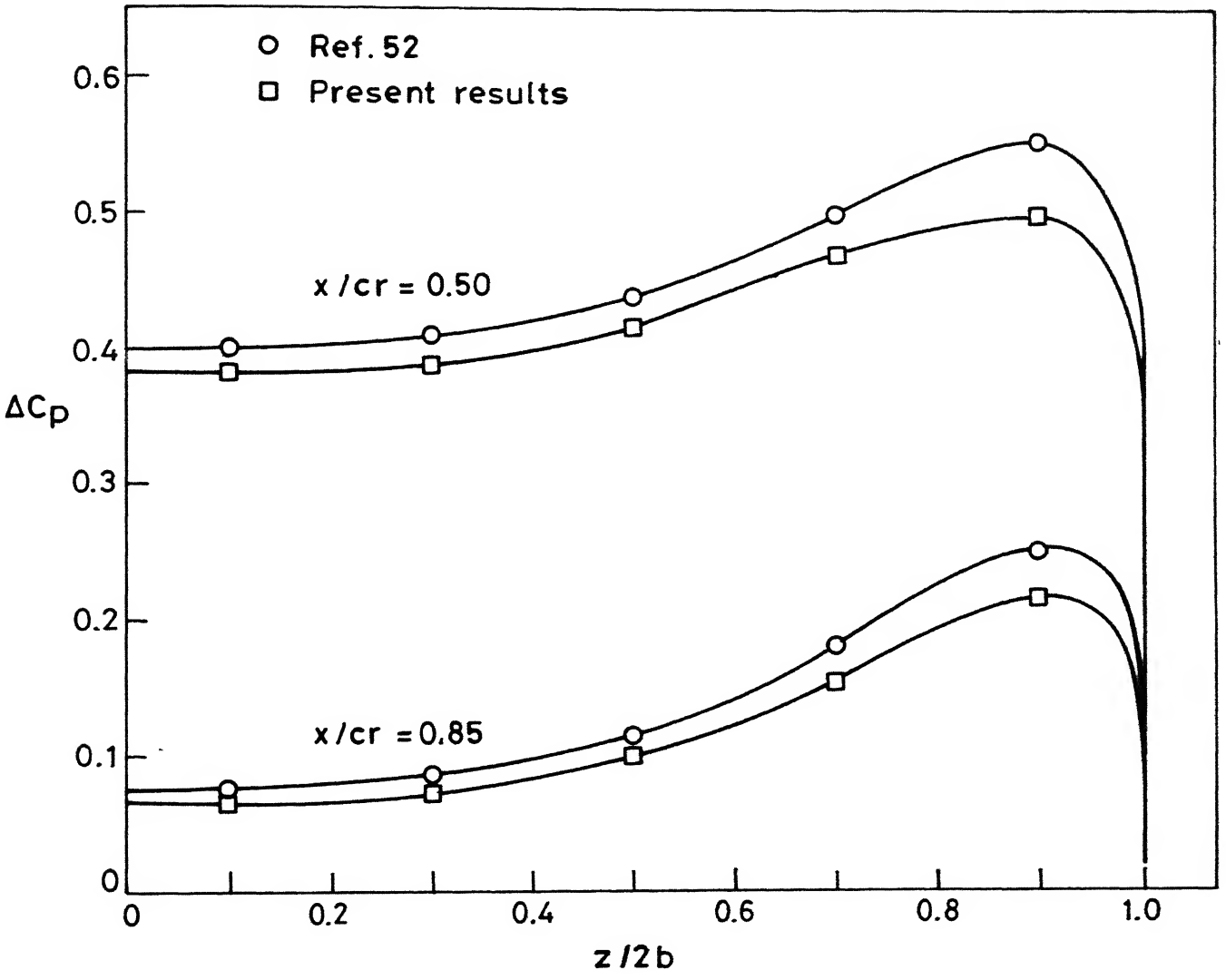

Fig. 12 Spanwise variation of pressure coefficient : AR = 1.0, α = 15 deg , NX = 5 , NZ = 5 .

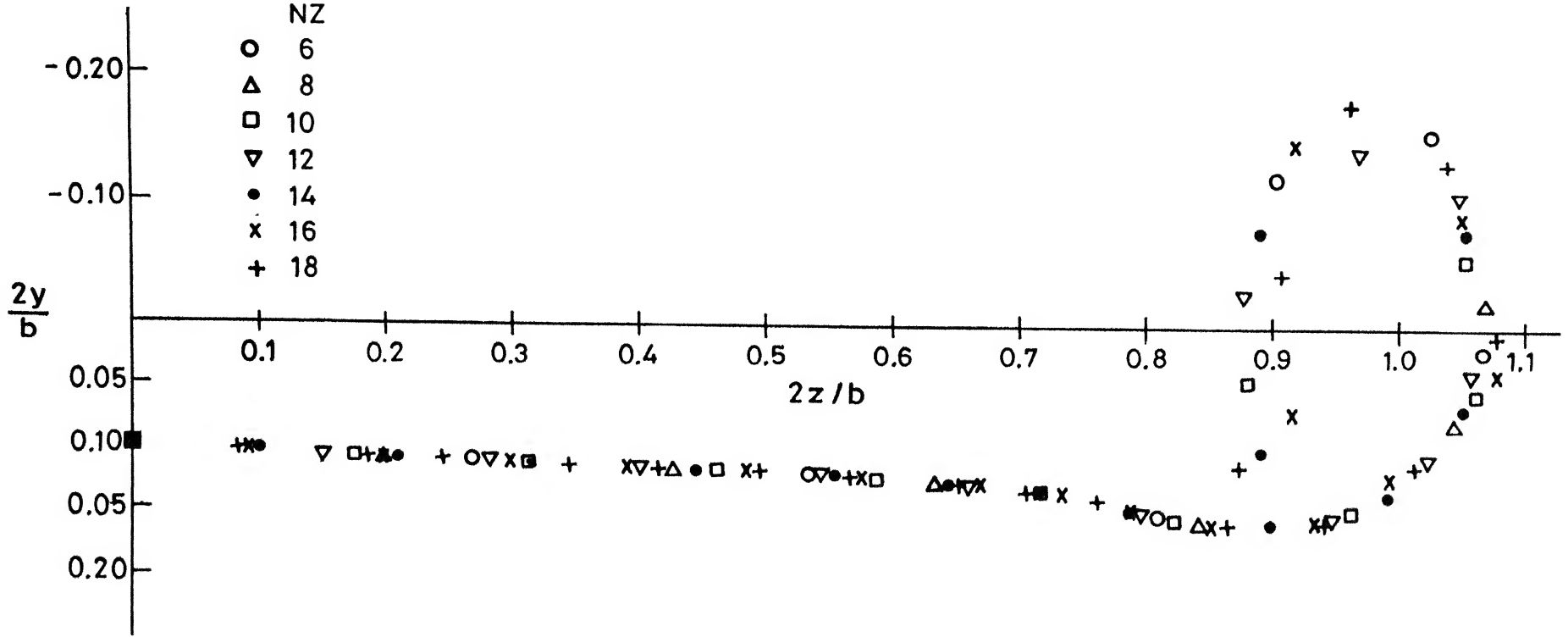

Fig. 13 Convergence study for a rectangular wing: AR = 8.0, $\alpha = 5^{\circ}$, $x_w/b = 1.69$
NX = 1, NW = 4.

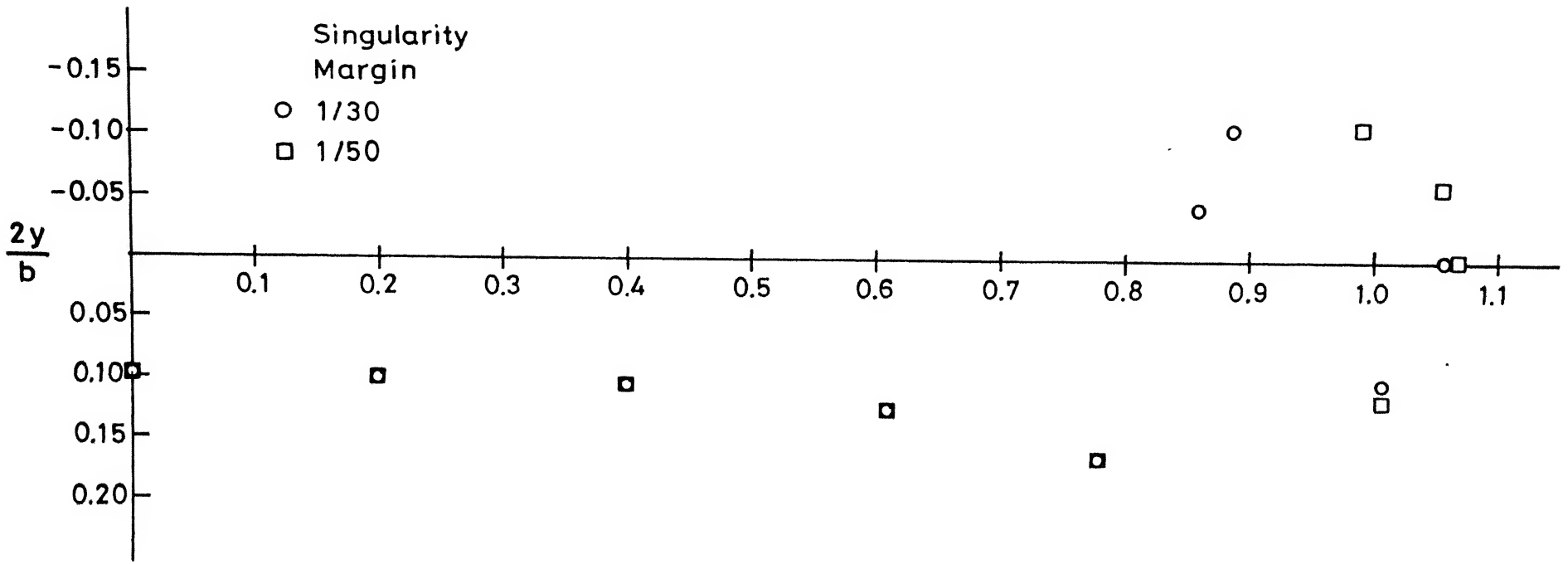

Fig. 14 Wake geometry evaluation leaving different margin around singularity for a rectangular wing : AR = 8.0, $\alpha = 5^{\circ}$, $x_w/b = 1.69$ NX = 1, NZ = 8, NW = 4.

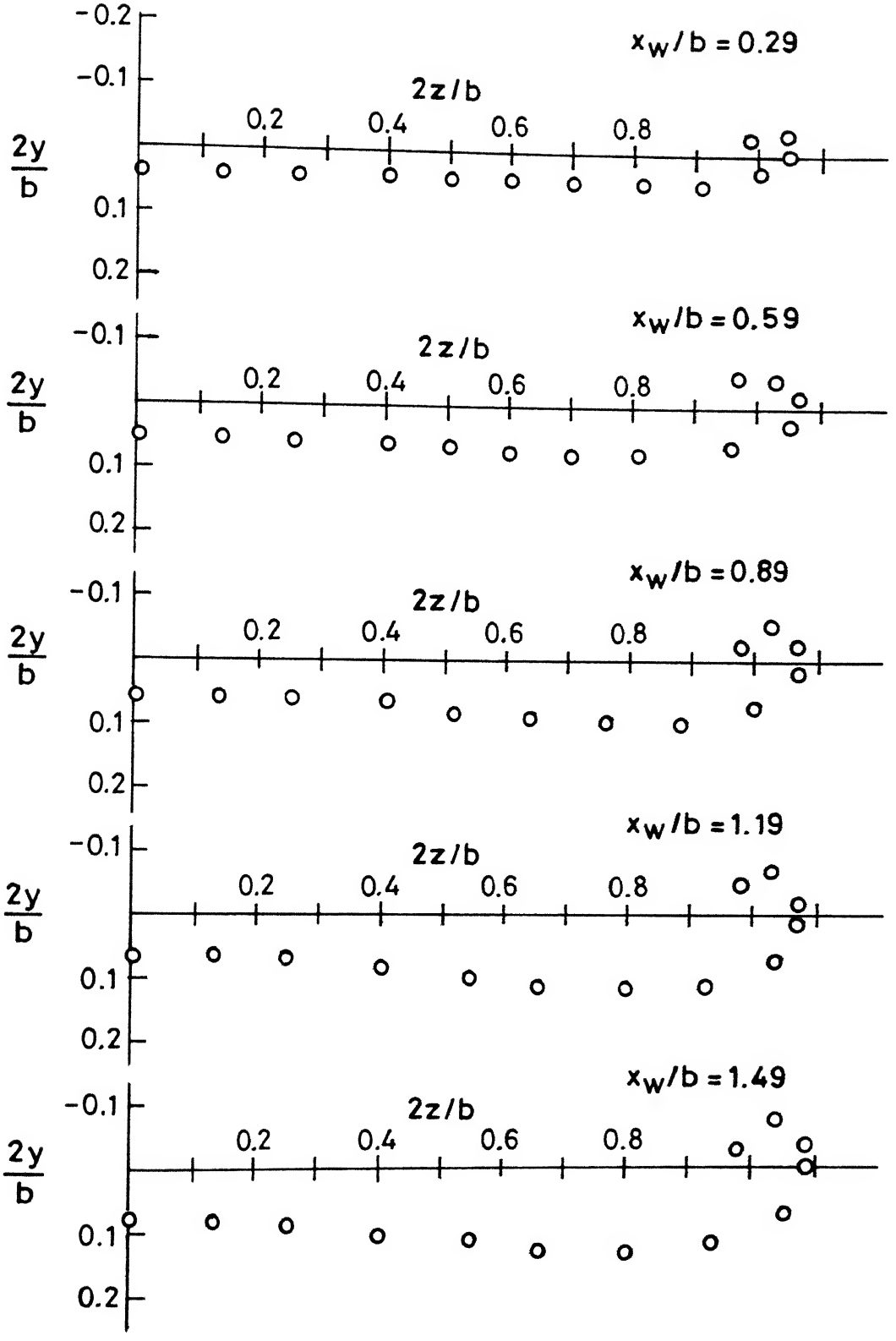

Fig. 15 Wake geometry at different downstream stations for a rectangular wing : AR = 8.0, α = 5°, NX = 1, NZ = 10, NW = 7.

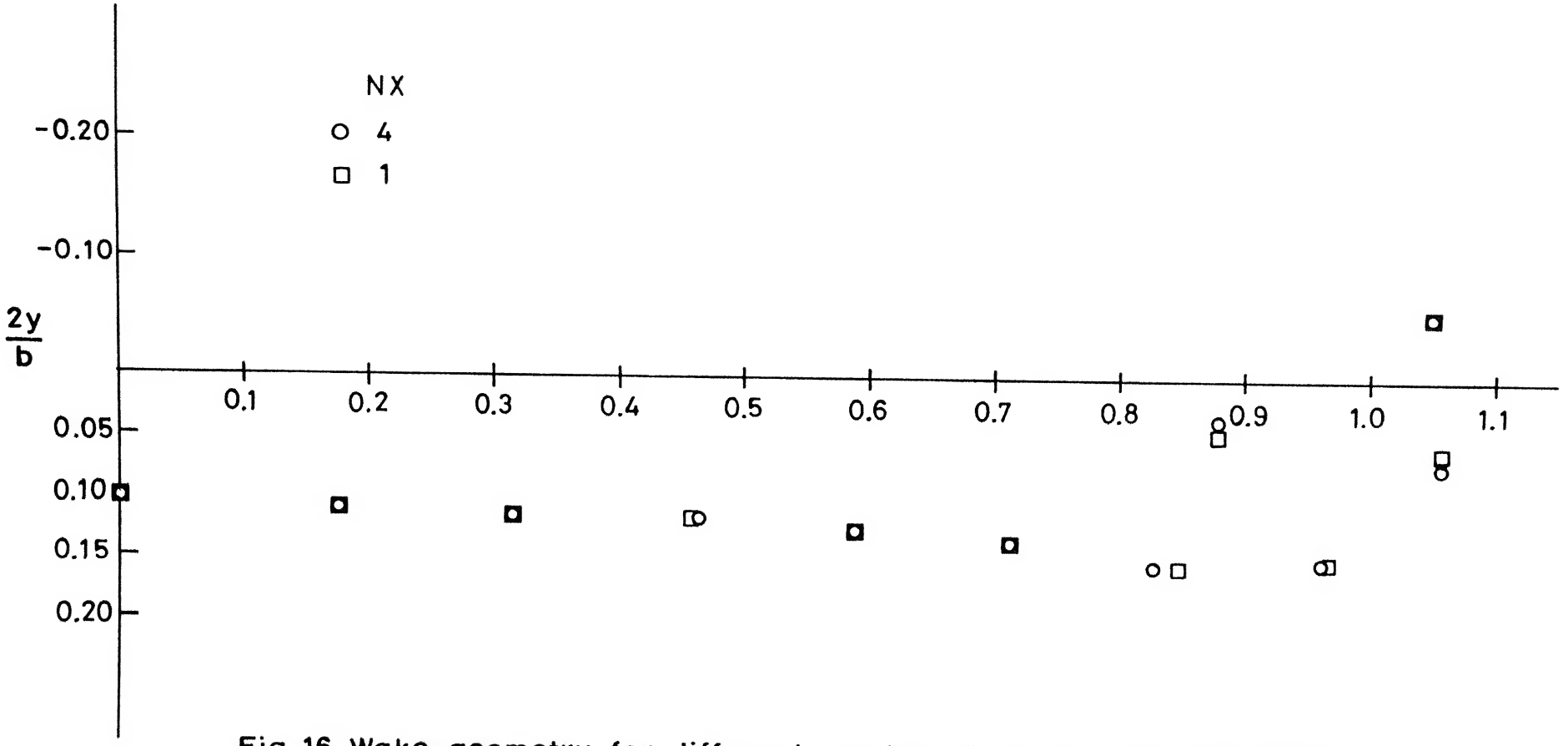

Fig. 16 Wake geometry for different number of panels over the lifting surface for a rectangular wing: AR = 8.0, $\alpha = 5^\circ$, $x_w/b = 1.69$ NZ = 10, NW = 4 .

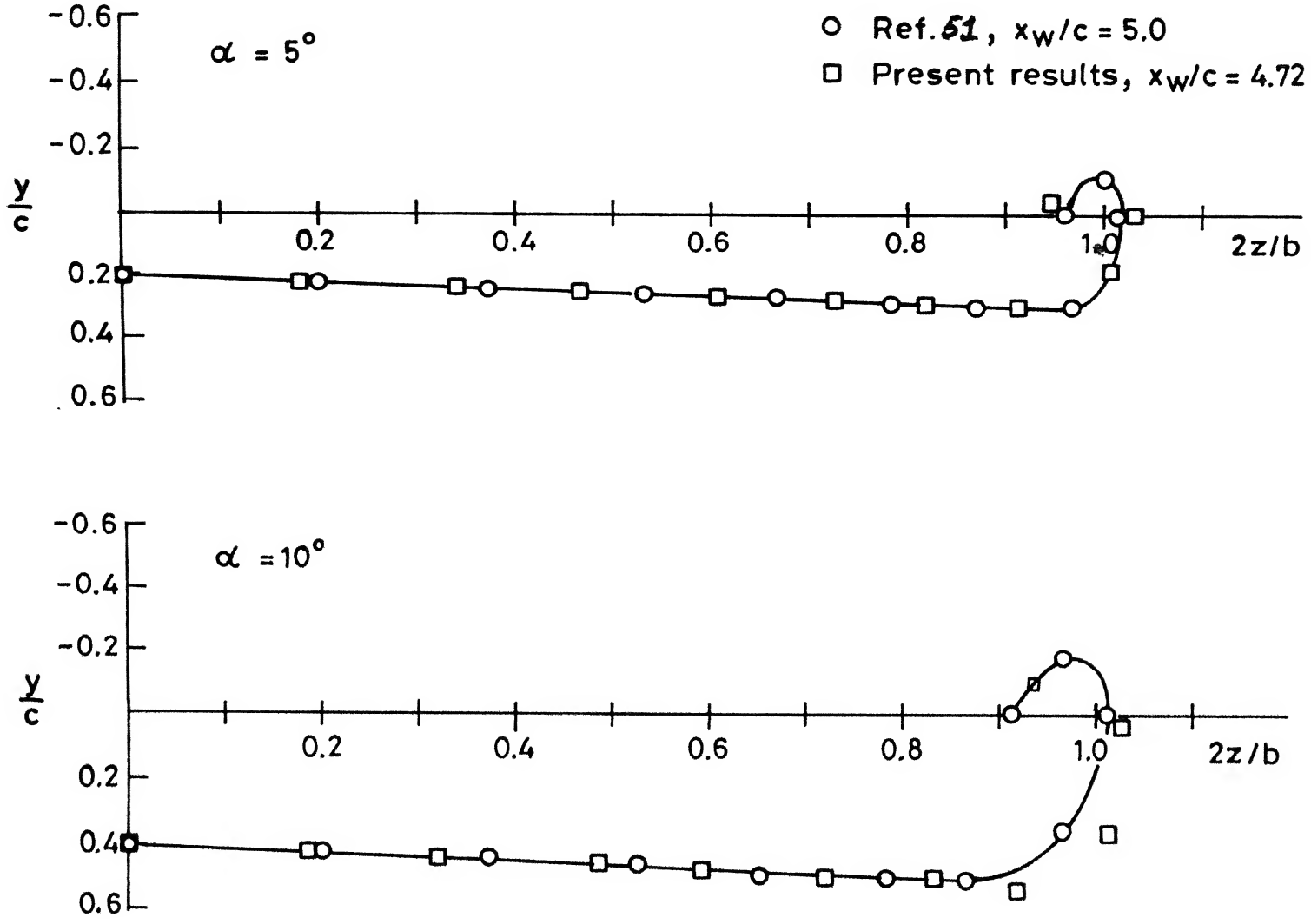

Fig. 17 Wake shape at different angle of attack for a rectangular wing : AR = 8.0, NX = 1, NZ = 10, NW = 7.

```
C
C       VORTICITY DISTRIBUTION METHOD
        ------------------------------
        DIMENSION X1(20),Z1(20),XM(20),ZM(20),V1(20),YN(20),S12(20)
       1,ZP(20),ZL(20),X2(20),X3(20),X4(20),Z2(20),Z3(20),Z4(20)
       2,V2(20),V3(20),V4(20),V1(20),VJ(20),VK(20),VR1(20),VL1(20)
       3,VR5(20),VL5(20),VR2(20),XN(20),Y1(20),YM(20),A(60,40),F(3,3)
       4,VU2(20),V44(20),VR5(20),Y2(20),Y3(20),V5(20),B(60),S13(20)
       5,XW1(20),XW2(20),XW3(20),XWM(20),YW1(20),YW2(20),YW3(20)
       6,YWM(20),ZW1(20),ZW2(20),ZW3(20),ZWM(20),WKAREA(20000),D(3)
       7,VL2(20),VR3(20),VL3(20),VR4(20),VL4(20),C(20),VIW(20),E(3)
       8,VKW(20),VJW(20),CI2(20),CJ2(20),CK2(20),GM(20),VR(20)
       9,S32(20),G(8,40),H(8,40)
        COMMON/ASO/XX,ZT,ZJ
        COMMON/ASOL/ZZL,YYL
        COMMON/ASOR/ZZR,YYR
        COMMON/ASP/XP,ZP
        EXTERNAL CINT1R,CINT1L,CINT2R,CINT2L,CINT3R,CINT3L,CINT5L,
       1CINT5R,CINT4L,CINT4R,WAKE,CINT6R,CINT6L,CINT7R,CINT7L
       1,CINT8R,CINT8L,STMPSN,ZJ,ZU
        OPEN(UNIT=23,DEVICE='DSK0')
        OPEN(UNIT=42,DEVICE='DSK')
        OPEN(UNIT=29,DEVICE='DSK')
        OPEN(UNIT=28,DEVICE='DSK')
        OPEN(UNIT=32,DEVICE='DSK')
        NX=2
        NZ=4
        NW=4
        PAI=3.141592674
        NAZ=NZ-1
        NAX=NX-1
        N=NX*NZ
        NP=(NZ+1)*NW
        ALPHA=5.
        CALL GMQUAD(X1,X2,X3,X,Y1,Y2,Y3,Y,Z1,Z2,Z3,Z,NP)
        ITER=3
        DO 28 IT=1,ITER
        WRITE(28,*) IT
        WRITE(32,*)IT
        WRITE(42,*)IT
        NAZ=NZ-1
        NAX=NX-1
        N=NX*NZ
        NP=(NZ+1)*NW
        NUNK=5*N
        NEQ=NUNK+2*NAX*NZ+2*NAZ*NX
        NER=NZ*NAX
        XC=0.12900000
        ZC=0.5
        XP=(XC-XA)/NX
        ZP=(ZC-ZA)/NZ
        W2=XP*ZP/2.
        W4=ZP
        W5=ZP*ZP/2.
        DO 10 K=1,N
        CALL CORT(X1,X2,X3,X4,XM,Z1,Z2,Z3,Z4,ZM)
        DO 100 J=1,N
        CALL CORT(X1,X2,X3,X4,XM,Z1,Z2,Z3,Z4,ZM)
        XN(J)=XM(K)-X1(J)
        ZR(J)=ZM(K)-Z1(J)
        ZL(J)=ZM(K)+Z1(J)
        XX=XN(J)
        ZZL=ZL(J)
        ZZR=ZR(J)
        ZT=ZP
        YYL=0.0
```

```
      YYR=0.0
      VR1(J)=SIMPSN(0,XP,10,CINT1R)
      VL1(J)=SIMPSN(0,XP,10,CINT1L)
      V1(J)=VR1(J)+VL1(J)
      VR2(J)=SIMPSN(0,XP,10,CINT2R)
      VL2(J)=SIMPSN(0,XP,10,CINT2L)
      VW2(J)=WAKE(W2,X2,X3,XM,Y2,Y3,Y,Z2,Z3,ZM)
17    V2(J)=VR2(J)+VL2(J)+VW2(J)
      VR3(J)=SIMPSN(0,XP,10,CINT3R)
      VL3(J)=SIMPSN(0,XP,10,CINT3L)
      V3(J)=VR3(J)+VL3(J)
      VR4(J)=SIMPSN(0,XP,10,CINT4R)
      VL4(J)=SIMPSN(0,XP,10,CINT4L)
      VW4(J)=WAKE(W4,X2,X3,XM,Y2,Y3,Y,Z2,Z3,ZM)
18    V4(J)=VR4(J)+VL4(J)+VW4(J)
      VR5(J)=SIMPSN(0,XP,10,CINT5R)
      VL5(J)=SIMPSN(0,XP,10,CINT5L)
      VW5(J)=WAKE(W5,X2,X3,XM,Y2,Y3,Y,Z2,Z3,ZM)
19    V5(J)=VR5(J)+VL5(J)+VW5(J)
      G(K,5*(J-1)+1)=V1(J)
      G(K,5*(J-1)+2)=V2(J)
      G(K,5*(J-1)+3)=V3(J)
      G(K,5*(J-1)+4)=V4(J)
      G(K,5*(J-1)+5)=V5(J)
100   CONTINUE
      WRITE(29,*)((G(K,J),J=1,NUNK))
10    CONTINUE
      IF(II.EQ.1)GO TO 44
      DO 22 I=1,N
      DO 23 NL=1,NCL
      V1(NL)=0.0
      V2(NL)=0.0
      V3(NL)=0.0
      V4(NL)=0.0
      V5(NL)=0.0
      DO 24 IP=1,NW
      DO 25 M=1,2
      J=(IP-1)*NCL+NL
      IF(NL.EQ.NCL) GO TO 22
      XX=XM(I)-XW1(J)
      ZZR=ZM(I)-ZW1(J)
      ZZL=ZM(I)+ZW1(J)
      YYR=YM(I)-YW1(J)
      YYL=YM(I)+YW1(J)
      XO=1.333
      XAY1=XO/8.
      XAY2=(XO+XO**2)/8.
      XAY3=(XO+XO**2+XO**4)/8.
      XAY4=(XO+XO**2+XO**4+XO**8)/8.
      IF(IP.EQ.1)XP=XAY1
      IF(IP.EQ.2)XP=XAY2-XAY1
      IF(IP.EQ.3)XP=XAY3-XAY2
      IF(IP.EQ.4)XP=XAY4-XAY3
      IF(M.EQ.1)ZT=0.0
      IF(M.EQ.1)ZO=ZO(XE)
      IF(M.EQ.2)ZT=ZU(XE)
      IF(M.EQ.2)ZO=XP
      S13(J)=SQRT((XW3(J)-XW1(J))**2+(YW3(J)-YW1(J))**2
     1+(ZW3(J)-ZW1(J))**2)
      S23=SQRT((X3(I)-X2(I))**2+(Y3(I)-Y2(I))**2+(Z3(I)-Z2(I))**2)
      S21=SQRT((X1(I)-X2(I))**2+(Y1(I)-Y2(I))**2+(Z1(I)-Z2(I))**2)
      F1X=((Y3(I)-Y2(I))*(Z1(I)-Z2(I))
     1-(Z3(I)-Z2(I))*(Y1(I)-Y2(I)))/(S23*S21)
      F1Y=((Z3(I)-Z2(I))*(X1(I)-X2(I))
     1-(X3(I)-X2(I))*(Z1(I)-Z2(I)))/(S23*S21)
```

```
      S12=((X3(I)-X2(I))*(Y1(I)-Y2(I))
     1-(Y3(I)-Y2(I))*(X1(I)-X2(I)))/(S23*S21)
   6  E(1)=T1X
      E(2)=T1Y
      E(3)=T1Z
      F(1,1)=(XW3(J)-XW1(J))/S13(J)
      F(1,2)=(YW3(J)-YW1(J))/S13(J)
      F(1,3)=(ZW3(J)-ZW1(J))/S13(J)
      F(2,1)=-(YW3(J)-YW1(J))/S13(J)
      F(2,2)=(XW3(J)-XW1(J))/S13(J)
      F(2,3)=0.0
      F(3,1)=-(ZW3(J)-ZW1(J))/S13(J)
      F(3,2)=0.0
      F(3,3)=(XW3(J)-XW1(J))/S13(J)
      DO 35 IU=1,3
      D(IU)=0.0
      DO 37 JU=1,3
      D(IU)=E(JU)*F(JU,IU)+D(IU)
  37  CONTINUE
C     TYPE *,D(IU)
  35  CONTINUE
      V1(NL)=V1(NL)+(SIMPSN(0,ZP,20,CINT1R)-SIMPSN(0,ZP,20,CINT1L))
     1*D(2)
      V2(NL)=V2(NL)+(SIMPSN(0,ZP,20,CINT6R)-SIMPSN(0,ZP,20,CINT6L))
     1*D(1)+(SIMPSN(0,ZP,20,CINT2R)-SIMPSN(0,ZP,20,CINT2L))*D(2)
     1+(SIMPSN(0,ZP,20,CINT8R)-SIMPSN(0,ZP,20,CINT8L))*D(3)
      V3(NL)=V3(NL)+(SIMPSN(0,ZP,20,CINT3R)-SIMPSN(0,ZP,20,CINT3L))
     1*D(2)
      V4(NL)=V4(NL)+(SIMPSN(0,ZP,20,CINT7R)-SIMPSN(0,ZP,20,CINT7L))
     1*D(1)+(SIMPSN(0,ZP,20,CINT4R)-SIMPSN(0,ZP,20,CINT4L))*D(2)
     1+(SIMPSN(0,ZP,20,CINT6R)-SIMPSN(0,ZP,20,CINT6L))*D(3)
      V5(NL)=V5(NL)+(SIMPSN(0,ZP,20,CINT8R)-SIMPSN(0,ZP,20,CINT8L))
     1*D(1)+(SIMPSN(0,ZP,20,CINT5R)-SIMPSN(0,ZP,20,CINT5L))*D(2)
     1+(SIMPSN(0,ZP,20,CINT7R)-SIMPSN(0,ZP,20,CINT7L))*D(3)
  25  CONTINUE
  24  CONTINUE
      WRITE(29,*)V1(NL),V2(NL),V3(NL),V4(NL),V5(NL)
      H(I,5*(NL-1)+1)=V1(NL)
      H(I,5*(NL-1)+2)=V2(NL)
      H(I,5*(NL-1)+3)=V3(NL)
      H(I,5*(NL-1)+4)=V4(NL)
      H(I,5*(NL-1)+5)=V5(NL)
  23  CONTINUE
      WRITE(29,*)(H(I,J),J=1,NUNK)
  22  CONTINUE
  44  DO 21 II=1,N
      DO 21 JJ=1,NUNK
      A(II,JJ)=G(II,JJ)+H(II,JJ)
  21  CONTINUE
      WRITE(23,*)((A(I,J),J=1,NUNK),I=1,N)
      XP=(XC-XA)/NX
      PAUSE1
C     CONTINUITY IN Z-DIRECTION
      DO 20 L=1,NAZ
      DO 20 K=1,NX
      DO 20 M=1,2
      IF(M.EQ.1)ZETA=ZP;IF(M.EQ.1)EXL=0.0
      IF(M.EQ.2)ZETA=ZP;IF(M.EQ.2)EXL=XP
      I=N+M+2*(K-1)+2*NX*(L-1)
      LL=5*NZ*(K-1)+5*(L-1)
      DO 11 J1=1,NUNK
      A(I,J1)=0.0
  11  CONTINUE
      A(I,1+LL)=1
      A(I,2+LL)=ZETA
```

```
      A(I,3+LL)=EXL
      IF(M.EQ.1)ZETA=0.0;IF(M.EQ.1)EXL=0.0
      IF(M.EQ.2)ZETA=ZP;IF(M.EQ.2)EXL=XP
      A(I,6+LL)=-1
      A(I,7+LL)=-ZETA
      A(I,8+LL)=-EXL
20    CONTINUE
      PAUSE2
      WRITE(23,*)((A(I,J),J=1,NUNK),I=N+1,2*N)
C     X-DIRECTION
      DO 30 L=1,NX
      DO 30 K=1,NZ
      DO 30 M=1,2
      IF(M.EQ.1)ZETA=0.0;IF(M.EQ.1)EXL=XP
      IF(M.EQ.2)ZETA=ZP;IF(M.EQ.2)EXL=XP
      I=M+2*NX*(NZ-1)+M+2*(K-1)+2*NX*(L-1)
      LL=5*NZ*(L-1)+5*(K-1)
      DO 12 J2=1,NUNK
      A(I,J2)=0.0
12    CONTINUE
      A(I,2+LL)=EXL
      A(I,4+LL)=1
      A(I,5+LL)=ZETA
      IF(M.EQ.1)ZETA=0.0;IF(M.EQ.1)EXL=0.0
      IF(M.EQ.2)ZETA=ZP;IF(M.EQ.2)EXL=0.0
      A(I,2+5*NZ+LL)=-EXL
      A(I,4+5*NZ+LL)=-1
      A(I,5+5*NZ+LL)=-ZETA
30    CONTINUE
      PAUSE3
      WRITE(23,*)((A(I,J),J=1,NUNK),I=2*N+1,3*N)
C     SYMMETRY CONDITION
      DO 40 IQ=1,NX
      DO 40 M=1,2
      IF(M.EQ.1)ZETA=0.0;IF(M.EQ.1)EXL=0
      IF(M.EQ.2)ZETA=0.0;IF(M.EQ.2)EXL=XP
      I=M+2*NZ*(NX-1)+2*NX*(NZ-1)+2*(IQ-1)+M
      J=5*NZ*(IQ-1)
      DO 13 J3=1,NUNK
      A(I,J3)=0.0
13    CONTINUE
      A(I,2+J)=EXL
      A(I,4+J)=1
      A(I,5+J)=ZETA
40    CONTINUE
      PAUSE4
      WRITE(23,*)((A(I,J),J=1,NUNK),I=3*N+1,4*N)
C     KUTTA CONDITION
      DO 50 LQ=1,NZ
      DO 50 M=1,2
      IF(M.EQ.1)ZETA=0.0;IF(M.EQ.1)EXL=XP
      IF(M.EQ.2)ZETA=ZP;IF(M.EQ.2)EXL=XP
      I=M+2*NX*(NZ-1)+2*NZ*(NX-1)+2*NX+M+2*(LQ-1)
      J=5*NZ*(NX-1)+1+5*(LQ-1)
      DO 14 J4=1,NUNK
      A(I,J4)=0.0
14    CONTINUE
      BETA=80
      A(I,J)=SIND(BETA)
      A(I,1+J)=ZETA*SIND(BETA)+EXL*COSD(BETA)
      A(I,J+2)=EXL*SIND(BETA)
      A(I,J+3)=COSD(BETA)
      A(I,J+4)=ZETA*COSD(BETA)
50    CONTINUE
      WRITE(23,*)((A(I,J),J=1,NUNK),I=4*N+1,5*N)
```

```
      DO 69 IP=1,NAZ
      DO 69 JQ=1,NX
      DO 69 M=1,2
      IF(M.EQ.1)ZETA=ZP
      IF(M.EQ.1)EXL=0.
      IF(M.EQ.2)ZETA=0.
      IF(M.EQ.2)EXL=XP
      I=NUNK+(IP-1)*2*NX+(JQ-1)*2+M
      J=(JQ-1)*5*NZ+(IP-1)*5
      DO 89 J6=1,NUNK
      A(I,J6)=0.
89    CONTINUE
      A(I,J+2)=EXL
      A(I,J+4)=1
      A(I,J+5)=ZETA
      IF(M.EQ.1)ZETA=0.
      IF(M.EQ.1)EXL=0.
      IF(M.EQ.2)ZETA=0.
      IF(M.EQ.2)EXL=XP
      A(I,J+7)=-EXL
      A(I,J+9)=-1
      A(I,J+10)=-ZETA
69    CONTINUE
      WRITE(23,*)((A(I,J6),J6=1,NUNK),I=NUNK+1,NUNK+2*NX*NAZ)
C     CONT IN Z-DIRECTION
      DO 70 JQ=1,NAX
      DO 70 IL=1,NZ
      DO 70 M=1,2
      I=NUNK+2*NX*NAZ+(JQ-1)*2*NZ+(IL-1)*2+M
      J=(JQ-1)*5*NZ+(IL-1)*5
      DO 94 J7=1,NUNK
      A(I,J7)=0.0
94    CONTINUE
      IF(M.EQ.1)ZETA=0.
      IF(M.EQ.1)EXL=XP
      IF(M.EQ.2)ZETA=ZP
      IF(M.EQ.2)EXL=XP
      A(I,J+1)=1
      A(I,J+2)=ZETA
      A(I,J+3)=EXL
      LL=5*NZ
      IF(M.EQ.1)ZETA=0.
      IF(M.EQ.1)EXL=0.
      IF(M.EQ.2)ZETA=ZP
      IF(M.EQ.2)EXL=0.
      A(I,J+1+LL)=-1.
      A(I,J+2+LL)=-ZETA
      A(I,J+3+LL)=-EXL
70    CONTINUE
      WRITE(23,*)((A(I,J7),J7=1,NUNK),I=NUNK+2*NX*NAZ+1,NUNK
     1+2*NAZ*NX+2*NAX*NZ)
C
C     TYPE*,NEQ
      DO 101 I=1,NEQ
      IF(I.LE.N)B(I)=-1.0
      IF(I.GT.N)B(I)=0.0
101   CONTINUE
      PAUSE5
      M=NEQ
      NA=NUNK
      NB=1
      IA=NEQ
      IB=NEQ
      IDGT=8
C     IER=128
```

```
      CALL GLSJAR(A,B,J,MA,MB,IA,IB,IDGT,WKAREA,IER)
      DO 102 I=1,MBUK
      WRITE(42,*)(B(I))
102   CONTINUE
      PAUSE6
C     CONTRIBUTION OF BOUND VORTEX PANELS OVER THE WAKE
      X0=1.333
      XAY1=X0/8.
      XAY2=(X0+X0**2)/8.
      XAY3=(X0+X0**2+X0**4)/8.
      XAY4=(X0+X0**2+X0**4+X0**8)/8.
      DO 71 I=1,MP
      VI(I)=0.0
      VJ(I)=0.0
      VK(I)=0.0
      DO 72 J=1,M
      XR(J)=XW1(I)-X1(J)
      ZR(J)=YW1(I)-Z1(J)
      ZL(J)=ZW1(I)+Z1(J)
      YY(J)=YW1(I)-Y1(J)
      XX=XR(J)
      ZZR=ZR(J)
      ZZL=ZL(J)
      YYL=YY(J)
      YYR=YYL
      ZT=ZP
      ZO=1.0
      K=(J-1)*5
      V1(J)=B(J+1)*(SIMPSN(0,XP,50,CINT6R)
     1-SIMPSN(0,XP,50,CINT6L))
      V2(J)=B(K+2)*(SIMPSN(0,XP,50,CINT7R)
     1-SIMPSN(0,XP,50,CINT7L))
      V3(J)=B(K+3)*(SIMPSN(0,XP,50,CINT8R)
     1-SIMPSN(0,XP,50,CINT8L))
C     TYPE *,V1(J),V2(J),V3(J)
      VI(I)=V1(J)+V2(J)+V3(J)+VI(I)
      V1(J)=B(K+1)*(SIMPSN(0,XP,50,CINT1R)
     1-SIMPSN(0,XP,50,CINT1L))
      V2(J)=B(K+2)*(SIMPSN(0,XP,50,CINT2R)
     1-SIMPSN(0,XP,50,CINT2L))
      V3(J)=B(K+3)*(SIMPSN(0,XP,50,CINT3R)
     1-SIMPSN(0,XP,50,CINT3L))
      V4(J)=B(K+4)*(SIMPSN(0,XP,50,CINT4R)
     1-SIMPSN(0,XP,50,CINT4L))
      V5(J)=B(K+5)*(SIMPSN(0,XP,50,CINT5R)
     1-SIMPSN(0,XP,50,CINT5L))
C     TYPE *,V1(J),V2(J),V3(J),V4(J),V5(J)
      VJ(I)=V1(J)+V2(J)+V3(J)+V4(J)+V5(J)+VJ(I)
      V2(J)=B(K+2)*(SIMPSN(0,XP,50,CINT8L)
     1-SIMPSN(0,XP,50,CINT8R))
      V4(J)=B(K+4)*(SIMPSN(0,XP,50,CINT6R)
     1-SIMPSN(0,XP,50,CINT6L))
      V5(J)=B(K+5)*(SIMPSN(0,XP,50,CINT7R)
     1-SIMPSN(0,XP,50,CINT7L))
C     TYPE *,V2(J),V4(J),V5(J)
      VK(I)=V2(J)+V4(J)+V5(J)+VK(I)
72    CONTINUE
      WRITE(20,*)VI(I),VJ(I),VK(I)
71    CONTINUE
      PAUSE7
      NAKC=5*NZ
      DO 73 I=1,NAKC
      C(I)=0.0
      DO 74 J=1,NX
      C(I)=B(I+5*(J-1)*NZ)+C(I)
```

```
71        CONTINUE
          WRITE(32,*)C(J)
73        CONTINUE
          NCL=NZ+1
          DO 75 J=1,NP
          XW1(J)=0.0
          YW1(J)=0.0
          ZW1(J)=0.0
          DO 76 JK=1,NM
          DO 76 JP=1,NCL
          DO 84 M=1,2
          J=(JK-1)*NCL+JP
          IF(JK.EQ.1)XP=XAY1
          IF(JK.EQ.2)XP=XAY2-XAY1
          IF(JK.EQ.3)XP=XAY3-XAY2
          IF(JK.EQ.4)XP=XAY4-XAY3
          NOP=NCL*JK
          IF((JP.EQ.1).AND.(M.EQ.2)) GO TO 84
          IF((JP.EQ.NCL).AND.(M.EQ.1)) GO TO 84
          XX=XW1(I)-XW1(J)
          ZZR=ZW1(I)-ZW1(J)
          ZZL=ZW1(I)+ZW1(J)
          YYR=YW1(I)-YW1(J)+1.0E-04
          YYL=YW1(I)+YW1(J)+1.0E-04
          IF(M.EQ.1)ZQ=ZO(XE)
          IF(M.EQ.1)ZT=0.0
          IF(M.EQ.2)ZQ=XP
          IF(M.EQ.2)ZT=ZU(XE)
          S13(J)=SQRT((XW3(J)-XW1(J))**2+(YW3(J)-YW1(J))**2
         1+(ZW3(J)-ZW1(J))**2)
          S12(J)=SQRT((XW2(J)-XW1(J))**2+(YW2(J)-YW1(J))**2
         1+(ZW2(J)-ZW1(J))**2)
          T1X=((YW3(I)-YW1(I))*(ZW2(I)-ZW1(I))
         1-(YW2(I)-YW1(I))*(ZW3(I)-ZW1(I)))/(S12(I)*S13(I))
          T1Y=((ZW3(I)-ZW1(I))*(XW2(I)-XW1(I))
         1-(XW3(I)-XW1(I))*(ZW2(I)-ZW1(I)))/(S12(I)*S13(I))
          T1Z=((XW3(I)-XW1(I))*(YW2(I)-YW1(I))
         1-(YW2(I)-YW1(I))*(YW3(I)-YW1(I)))/(S12(I)*S13(I))
          IF(JP.EQ.1) GO TO 86
          S32(I)=SQRT((XW3(I)-XW2(I))**2+(YW3(I)-YW2(I))**2
         1+(ZW3(I)-ZW2(I))**2)
          T1X=((YW1(I)-YW3(I))*(ZW2(I)-ZW3(I))
         1-(YW2(I)-YW3(I))*(ZW1(I)-ZW3(I)))/(S13(I)*S32(I))
          T1Y=((ZW1(I)-ZW3(I))*(XW2(I)-XW3(I))
         1-(ZW2(I)-ZW3(I))*(XW1(I)-XW3(I)))/(S13(I)*S32(I))
          T1Z=((XW1(I)-XW3(I))*(YW2(I)-YW3(I))
         1-(XW2(I)-XW3(I))*(YW2(I)-YW3(I)))/(S13(I)*S32(I))
86        E(1)=T1X
          E(2)=T1Y
          E(3)=T1Z
          F(1,1)=(XW3(J)-XW1(J))/S13(J)
          F(1,2)=(YW3(J)-YW1(J))/S13(J)
          F(1,3)=(ZW3(J)-ZW1(J))/S13(J)
          F(2,1)=-(YW3(J)-YW1(J))/S13(J)
          F(2,2)=(XW3(J)-XW1(J))/S13(J)
          F(2,3)=0.0
          F(3,1)=-(ZW3(J)-ZW1(J))/S13(J)
          F(3,2)=0.0
          F(3,3)=(XW3(J)-XW1(J))/S13(J)
          DO 80 IU=1,3
          D(IU)=0.0
          DO 90 JU=1,3
          D(IU)=E(JU)*F(JU,IU)+D(IU)
90        CONTINUE
C         TYPE *,D(IU)
```

```
80      CONTINUE
        IF(M.EQ.1)JL=(JP-1)*5
        IF(M.EQ.2)JL=(JP-2)*5
        IF(M.EQ.2)ZP=-ZP
        ZP=ZP+0.01
        V1(J)=-C(JL+4)*(SIMPSN(0,ZP,50,CINT6R)
       1-SIMPSN(0,ZP,50,CINT6L))
        V2(J)=-C(JL+2)*(SIMPSN(0,ZP,50,CINT7R)
       1-SIMPSN(0,ZP,50,CINT7L))
        V3(J)=-C(JL+5)*(SIMPSN(0,ZP,50,CINT8R)
       1-SIMPSN(0,ZP,50,CINT8L))
C       TYPE *,V1(J),V2(J),V3(J)
        VIW(I)=V1(J)+V2(J)+V3(J)+VIW(I)
        VIW(I)=VIW(I)*D(1)
        V1(J)=-C(JL+4)*(SIMPSN(0,ZP,50,CINT1R)
       1-SIMPSN(0,ZP,50,CINT1L))
        V2(J)=-C(JL+2)*(SIMPSN(0,ZP,50,CINT2R)
       1-SIMPSN(0,ZP,50,CINT2L))
        V3(J)=-C(JL+5)*(SIMPSN(0,ZP,50,CINT3R)
       1-SIMPSN(0,ZP,50,CINT3L))
        V4(J)=-C(JL+1)*(SIMPSN(0,ZP,50,CINT4R)
       1-SIMPSN(0,ZP,50,CINT4L))
        V5(J)=-C(JL+3)*(SIMPSN(0,ZP,50,CINT5R)
       1-SIMPSN(0,ZP,50,CINT5L))
C       TYPE *,V1(J),V2(J),V3(J),V4(J),V5(J)
        VJW(I)=V1(J)+V2(J)+V3(J)+V4(J)+V5(J)+VJW(I)
        VJW(I)=VJW(I)*D(2)
        V2(J)=-C(JL+2)*(SIMPSN(0,ZP,50,CINT8R)
       1-SIMPSN(0,ZP,50,CINT8L))
        V4(J)=-C(JL+1)*(SIMPSN(0,ZP,50,CINT6R)
       1-SIMPSN(0,ZP,50,CINT6L))
        V5(J)=-C(JL+3)*(SIMPSN(0,ZP,50,CINT7R)
       1-SIMPSN(0,ZP,50,CINT7L))
C       TYPE *,V1(J),V2(J),V3(J)
        VKW(I)=V2(J)+V4(J)+V5(J)+VKW(I)
        VKW(I)=VKW(I)*D(3)
84      CONTINUE
76      CONTINUE
        WRITE(20,*) VIW(I),VJW(I),VKW(I)
75      CONTINUE
        PAUSE10
C
CC      CALCULATION FOR THE CONTRIBUTION OF FAR WAKE
C
        OPEN(UNIT=21,DEVICE='DSK')
        READ(21,*)(GM(I),I=1,NZ)
120     MAP=NP-NZ+1
        DO 81 LL=1,NP
        CI2(LL)=0.0
        CJ2(LL)=0.0
        CK2(LL)=0.0
        DO 82 J=MAP,NP
        I=J-(NW-1)*(NZ+1)-1
        P=XW1(LL)-XW2(J)
        Q=XW1(LL)-XW3(J)
        R=ZW1(LL)-ZW2(J)
        SS=ZW1(LL)-ZW3(J)
        T=YW1(LL)-YW2(J)
        U=YW1(LL)-YW3(J)
        V=ZW1(LL)+ZW2(J)
        WW=ZW1(LL)+ZW3(J)
        POR=(R*U-SS*T)**2+(P*U-Q*T)**2+(P*SS-Q*R)**2
        ROP=(WW*U-V*T)**2+(Q*U-P*T)**2+(Q*V-P*WW)**2
        OIM=GM(I)*ALPHA*PAI/180.
        UVW=(((Q-P)*P+(SS-R)*R+(U-T)*T)/SQRT(P*P+R*R+T*T)-((Q-P)*Q+
```

```
     1(SS-R)*SS+(U-T)*U)/SQRT(Q*Q+SS*SS+U*U))*DIM
     WVU=(((P-Q)*Q+(V-WW)*WW+(U-T)*T)/SQRT(Q*Q+WW*WW+T*T)-((P-Q)*P
     1+(V-WW)*V+(U-T)*U)/SQRT(P*P+V*V+U*U))*DIM
     D1=SQRT(P*P+R*P+T*T)
     D2=SQRT(Q*Q+SS*SS+U*U)
     CI2(LL)=((R*U-SS*T)/PQR)*UVW+((WW*U-V*T)/RQP)*WVU+CI2(LL)
     CK2(LL)=((Q*T-P*U)/PQR)*UVW+((P*T-Q*U)/RQP)*WVU+(T/(T*T+R*R))*
     1(1.+P/D1)*DIM-(U/(U*U+SS*SS))*(1.+Q/D2)*DIM+CK2(LL)
     CJ2(LL)=((P*SS-Q*R)/PQR)*UVW+((Q*V-P*WW)/RQP)*WVU-(R/(T*T-R*R))*
     1(1.+P/D1)*DIM+(S/(U*U-SS*SS))*(1.+Q/D2)*DIM+CJ2(LL)
87   CONTINUE
     WRITE(20,*)CI2(LL),CJ2(LL),CK2(LL)
81   CONTINUE
     DO 51 II=1,NW
     DO 51 JJ=1,NCL
     I=(II-1)*NCL+JJ
     V1(I)=(V1(I)+VIW(I)+CI2(I))+COSD(ALPHA)
     V2(I)=(VJ(I)+VJW(I)+CJ2(I))-SIND(ALPHA)
     V3(I)=(VK(I)+VKW(I)+CK2(I))
     VR(I)=SQRT(V1(I)**2+V2(I)**2+V3(I)**2)
     S13(I)=SQRT((XW3(I)-XW1(I))**2+(YW3(I)-YW1(I))**2+(ZW3(I)-ZW1(I)
     1)**2)
     VI(I)=V1(I)/VR(I)
     VJ(I)=V2(I)/VR(I)
     VK(I)=V3(I)/VR(I)
     IF(I.GT.NCL) GO TO 107
108  XW3(I)=XW1(I)+VI(I)*S13(I)
     YW3(I)=YW1(I)+VJ(I)*S13(I)
     ZW3(I)=ZW1(I)+VK(I)*S13(I)
     GO TO 109
107  XW1(I)=XW3(I-NCL)
     YW1(I)=YW3(I-NCL)
     ZW1(I)=ZW3(I-NCL)
     XW3(I)=XW1(I)+VI(I)*S13(I)
     YW3(I)=YW1(I)+VJ(I)*S13(I)
     ZW3(I)=ZW1(I)+VK(I)*S13(I)
109  IF(JJ.NE.1)GO TO 111
     IF(I.EQ.1)XW2(I)=XC
     IF(I.EQ.1)YW2(I)=0.0
     IF(I.EQ.1)ZW2(I)=ZP
     IF((JJ.EQ.1).AND.(I.NE.1))XW2(I)=XW3(I-NCL+1)
     IF((JJ.EQ.1).AND.(I.NE.1))YW2(I)=YW3(I-NCL+1)
     IF((JJ.EQ.1).AND.(I.NE.1))ZW2(I)=ZW3(I-NCL+1)
     GO TO 110
111  XW2(I)=XW3(I-1)
     YW2(I)=YW3(I-1)
     ZW2(I)=ZW3(I-1)
110  XWM(I)=(XW1(I)+XW2(I)+XW3(I))/3.
     YWM(I)=(YW1(I)+YW2(I)+YW3(I))/3.
     ZWM(I)=(ZW1(I)+ZW2(I)+ZW3(I))/3.
     WRITE(28,*)(XW1(I),XW2(I),XW3(I),XWM(I),ZW1(I),ZW2(I)
     1,ZW3(I),ZWM(I),YW1(I),YW2(I),YW3(I),YWM(I))
51   CONTINUE
     PAUSE12
28   CONTINUE
     STOP
     END
     FUNCTION SIMPSN(A,B,NM,F)
     Y=A
     H=(B-A)/FLOAT(NM)
     IP=4
C    S=F(Y)+F(Y+NM*H)
     F1=F(Y)
     F2=F(B)
     S=F1+F2
```

```
      I=1
2     IF(I.E).N) GO TO 3
      Y=Y+I*H
      S=C4(Y)
      I=I+1
      IP=6-IP
      GO TO 2
3     S=S*H/3
      ST=PSM=S
      RETURN
      END
C
      FUNCTION CINT1R(XE)
C
      COMMON/ASD/XX,ZT,ZQ
      COMMON/ASFR/ZZR,YYR
      CINT1R=-((ZZR-ZT)*(XX-XE)/(((XX-XE)**2+YYR**2)*SQRT(((XX-XE)**2)
     1+YYR**2+(ZZR-ZT)**2))-(ZZR-ZQ)*(XX-XE)/(((XX-XE)**2+YYR**2)
     1*SQRT(((XX-XE)**2)+YYR**2+(ZZR-ZQ)**2)))
      RETURN
      END
C
      FUNCTION CINT1L(XE)
C
      COMMON/ASD/XX,ZT,ZQ
      COMMON/ASFL/ZZL,YYL
      CINT1L=-((ZZL-ZT)*(XX-XE)/(((XX-XE)**2+YYL**2)*SQRT(((XX-XE)**2)
     1+YYL**2+(ZZL-ZT)**2))-(ZZL-ZQ)*(XX-XE)/(((XX-XE)**2+YYL**2)
     1*SQRT(((XX-XE)**2)+YYL**2+(ZZL-ZQ)**2)))
      RETURN
      END
C
      FUNCTION CINT2L(XE)
C
      COMMON/ASD/XX,ZT,ZQ
      COMMON/ASFL/ZZL,YYL
      CINT2L=(2*XE-XX)/SQRT((XX-XE)**2+YYL**2+(ZZL-ZT)**2)-ZZL*(ZZL-
     1ZT)*(XX-XE)/(SQRT((XX-XE)**2+YYL**2+(ZZL-ZT)**2)*SQRT(
     1(XX-XE)**2+YYL**2))-(2*XE-XX)/SQRT((XX-XE)**2+YYL**2
     1+(ZZL-ZQ)**2)-ZZL*(ZZL-ZQ)*(XX-XE)/(SQRT((XX-XE)**2+YYL**2
     1+(ZZL-ZQ)**2)*SQRT((XX-XE)**2+YYL**2))
      RETURN
      END
C
      FUNCTION CINT2R(XE)
C
      COMMON/ASD/XX,ZT,ZQ
      COMMON/ASFR/ZZR,YYR
      CINT2R=(2*XE-XX)/SQRT((XX-XE)**2+YYR**2+(ZZR-ZT)**2)-ZZR*(ZZR-
     1ZT)*(XX-XE)/(SQRT((XX-XE)**2+YYR**2+(ZZR-ZT)**2)*SQRT(
     1(XX-XE)**2+YYR**2))-(2*XE-XX)/SQRT((XX-XE)**2+YYR**2
     1+(ZZR-ZQ)**2)-ZZR*(ZZR-ZQ)*(XX-XE)/(SQRT((XX-XE)**2+YYR**2
     1+(ZZR-ZQ)**2)*SQRT((XX-XE)**2+YYR**2))
      RETURN
      END
C
      FUNCTION CINT3R(XE)
C
      COMMON/ASD/XX,ZT,ZQ
      COMMON/ASFR/ZZR,YYR
      CINT3R=-XE*(ZZR-ZT)*(XX-XE)/(SQRT((XX-XE)**2+YYR**2+(ZZR-ZT)**2)
     1*((XX-XE)**2+YYR**2))+XE*(XX-XE)*(ZZR-ZQ)/(((XX-XE)**2+YYR**
     12)*SQRT((XX-XE)**2+YYR**2+(ZZR-ZQ)**2))
      RETURN
      END
```

```
C
      FUNCTION CINT3L(XE)
C
      COMMON/ASD/XX,ZT,ZQ
      COMMON/ASFL/ZZL,YYL
      CINT3L=XE*(ZZL-ZT)*(XX-XE)/(SQRT((XX-XE)**2+YYL**2+(ZZL-ZT)**2)
     1*((XX-XE)**2+YYL**2))+XE*(XX-XE)*(ZZL-ZQ)/(((XX-XE)**2+YYL**
     12)*SQRT((XX-XE)**2+YYL**2+(ZZL-ZQ)**2))
      RETURN
      END
C
      FUNCTION CINT4L(XE)
C
      COMMON/ASD/XX,ZT,ZQ
      COMMON/ASFL/ZZL,YYL
      CINT4L=1./SQRT((XX-XE)**2+YYL**2+(ZZL-ZT)**2)
     1-1./SQRT((XX-XE)**2+YYL**2+(ZZL-ZQ)**2)
      RETURN
      END
      FUNCTION CINT4R(XE)
C
      COMMON/ASD/XX,ZT,ZQ
      COMMON/ASFR/ZZR,YYR
      CINT4R=1./SQRT((XX-XE)**2+YYR**2+(ZZR-ZT)**2)
     1-1./SQRT((XX-XE)**2+YYR**2+(ZZL-ZQ)**2)
      RETURN
      END
C
      FUNCTION CINT5R(XE)
C
      COMMON/ASD/XX,ZT,ZQ
      COMMON/ASFR/ZZR,YYR
      CINT5R=ZZR/SQRT((XX-XE)**2+YYR**2+(ZZR-ZT)**2)+ALOG
     1((SQRT((XX-XE)**2+YYR**2+(ZZR-ZT)**2)+(ZZR-ZT))/(XX
     1-XE)**2)-(ZZR-ZT)/SQRT((XX-XE)**2+YYR**2+(ZZR-ZT)**2)
     1-ZZR/SQRT((XX-XE)**2+YYR**2+(ZZR-ZQ)**2)-ALOG((SQRT
     1((XX-XE)**2+YYR**2+(ZZR-ZQ)**2)+(ZZR-ZQ))/(XX-XE)**2)
     1+(ZZR-ZQ)/SQRT((XX-XE)**2+YYR**2+(ZZR-ZQ)**2)
      RETURN
      END
C
      FUNCTION CINT5L(XE)
C
      COMMON/ASD/XX,ZT,ZQ
      COMMON/ASFL/ZZL,YYL
      CINT5L=ZZL/SQRT((XX-XE)**2+YYL**2+(ZZL-ZT)**2)+ALOG
     1((SQRT((XX-XE)**2+YYL**2+(ZZL-ZT)**2)+(ZZL-ZT))/(XX
     1-XE)**2)-(ZZL-ZT)/SQRT((XX-XE)**2+YYL**2+(ZZL-ZT)**2)
     1-ZZL/SQRT((XX-XE)**2+YYL**2+(ZZL-ZQ)**2)-ALOG((SQRT
     1((XX-XE)**2+YYL**2+(ZZL-ZQ)**2)+(ZZL-ZQ))/(XX-XE)**2)
     1+(ZZL-ZQ)/SQRT((XX-XE)**2+YYL**2+(ZZL-ZQ)**2)
      RETURN
      END
C
      FUNCTION WAKE(N,X11,X13,X12,Y11,Y13,Y12,Z11,Z13,Z12)
      DIMENSION X2(4),X3(4),XM(4),Y2(4),Y3(4),Y(4),Z2(4),Z3(4),ZM(4)
     1,XM(4)
      PAI=3.1417
      P=X12-X11
      Q=X12-X13
      R=Z12-Z11
      SS=Z12-Z13
      T=Y12-Y11
      U=Y12-Y13
      V=Z12+Z11
```

```
      A=ZJ2+ZJ3
      IF(TA.GE.2)P=P+2.0D0
      IF(TA.GE.2)Q=Q+2.0D0
      DDR=(P*U-Q*T)**2+(P*SS-Q*R)**2
      RQP=(WW*U-V*T)**2+(Q*U-P*T)**2+(Q*V-P*WW)**2
      DIM=1/(4.*PAI)
      UVW=((U-T)*P+(SS-R)*R+(U-T)*T)/SQRT(P*P+R*R+T*T)-((Q-P)*Q+
     1(SS-R)*SS+(U-T)*U)/SQRT(Q*Q+SS*SS+U*U))*DIM
      WVU=((P-Q)*Q+(V-WW)*WW+(U-T)*T)/SQRT(Q*Q+WW*WW+T*T)-((P-Q)*P
     1+(V-WW)*V+(U-T)*U)/SQRT(P*P+V*V+U*U))*DIM
      D1=SQRT(P*P+R*R+T*T)
      D2=SQRT(Q*Q+SS*SS+U*U)
C     CT2=((R*U-SS*T)/PQR)*UVW+((WW*U-V*T)/RQP)*WVU
C     CJ2=((Q*T-P*U)/PQR)*UVW+((P*T-Q*J)/RQP)*WVU+(T/(T*T+R*R))*
C     1(1.+P/D1)*DIM-(U/(U*U+SS*SS))*(1.+Q/D2)*DIM
      CK2=((P*SS-Q*R)/PQR)*UVW+((Q*V-P*WW)/RQP)*WVU-(R/(T*T-R*R))*
     1(1.+P/D1)*DIM+(SS/(U*U-SS*SS))*(1.+J/D2)*DIM
      WAKE=CK2
      RETURN
      END

C
      FUNCTION CINT6R(XE)
C
      COMMON/ASD/XX,ZT,ZQ
      COMMON/ASFR/ZZR,YYR
      CINT6R=(YYR*(ZZR-ZT)/SQRT((XX-XE)**2+YYR**2+(ZZR-ZT)**2)
     1-YYR*(ZZR-ZQ)/SQRT((XX-XE)**2+YYR**2+(ZZR-ZQ)**2)
     1)/SQRT((XX-XE)**2+YYR**2)
      RETURN
      END

C
      FUNCTION CINT6L(XE)
C
      COMMON/ASD/XX,ZT,ZQ
      COMMON/ASFL/ZZL,YYL
      CINT6L=(YYL*(ZZL-ZT)/SQRT((XX-XE)**2+YYL**2+(ZZL-ZT)**2)
     1-YYL*(ZZL-ZQ)/SQRT((XX-XE)**2+YYL**2+(ZZL-ZQ)**2)
     1)/SQRT((XX-XE)**2+YYL**2)
      RETURN
      END

C
      FUNCTION CINT7R(XE)
C
      COMMON/ASD/XX,ZT,ZQ
      COMMON/ASFR/ZZR,YYR
      CINT7R=(YYR*(ZZR*(ZZR-ZT)/SQRT((XX-XE)**2+YYR**2+(ZZR-ZT)**2)
     1+((XX-XE)**2+YYR**2)/SQRT((XX-XE)**2+YYR**2+(ZZR-ZT)**2)
     1-(ZZR)*(ZZR-ZQ)/SQRT((XX-XE)**2+YYR**2+(ZZR-ZQ)**2)
     1-((XX-XE)**2+(YYR)**2)/SQRT((XX-XE)**2+YYR**2+(ZZR-ZQ)**2))
     1)/SQRT((XX-XE)**2+YYR**2)
      RETURN
      END
      FUNCTION CINT7L(XE)

C
      COMMON/ASD/XX,ZT,ZQ
      COMMON/ASFL/ZZL,YYL
      CINT7L=(YYL*(ZZL*(ZZL-ZT)/SQRT((XX-XE)**2+YYL**2+(ZZL-ZT)**2)
     1+((XX-XE)**2+YYL**2)/SQRT((XX-XE)**2+YYL**2+(ZZL-ZT)**2)
     1-(ZZL)*(ZZL-ZQ)/SQRT((XX-XE)**2+YYL**2+(ZZL-ZQ)**2)
     1-((XX-XE)**2+(YYL)**2)/SQRT((XX-XE)**2+YYL**2+(ZZL-ZQ)**2))
     1)/SQRT((XX-XE)**2+YYL**2)
      RETURN
      END
      FUNCTION CINT8R(XE)
C
```

```
      COMMON/ASD/XX,ZT,ZQ
      COMMON/ASDR/ZZR,YYR
      CINTSR=(((ZZR-ZT)*XE/SQRT((XX-XE)**2+YYR**2+(ZZR-ZT)**2)
     1-(ZZR-ZQ)*XE/SQRT((XX-XE)**2+YYR**2+(ZZR-ZQ)**2))*YYR
     1)/SQRT((XX-XE)**2+YYR**2)
      RETURN
      END
      FUNCTION CINTSL(XE)
      COMMON/ASD/XX,ZT,ZQ
      COMMON/ASDL/ZZL,YYL
      CINTSL=(((ZZL-ZT)*XE/SQRT((XX-XE)**2+YYL**2+(ZZL-ZT)**2)
     1-(ZZL-ZQ)*XE/SQRT((XX-XE)**2+YYL**2+(ZZL-ZQ)**2))*YYL
     1)/SQRT((XX-XE)**2+YYL**2)
      RETURN
      END
C
      FUNCTION ZQ(XE)
      COMMON/ASF/XP,ZP
      ZQ=-XP*XE/ZP+XP
      RETURN
      END
C
      FUNCTION ZU(XE)
C
      COMMON/ASF/XP,ZP
      ZU=(-XP/ZP)*XE
      RETURN
      END
      SUBROUTINE GMQUAD(X1,X2,X3,X,Y1,Y2,Y3,Y,Z1,Z2,Z3,Z,NP)
C
      DIMENSION X1(NP),Y1(NP),X2(NP),Y2(NP),X3(NP),Y3(NP),XM(NP
     1),YM(NP),Z3(NP),F(NP),Z1(NP),Z2(NP),Z(NP)
      YA=0.0
      YB=0.5
      NX=4
      NY=10
      NZ=NY+1.
      BETA=0.0
      ZZ=90./FLOAT(NY)
      TAN=SIND(BETA)/COSD(BETA)
      F(1)=0.0
      X=1.33
      F(2)=X
      F(3)=X+X**2
      F(4)=X+X**2+X**4
      F(5)=X+X**2+X**4+X**8
      DO 10 I=1,NX
      DO 20 J=1,NZ
      ZQ=ZZ*(J-1)
      ZC=90-ZQ
      ZB=90-ZQ+ZZ
      X1(J)=(YB-YA)*COSD(ZC)
      X1(J)=(Y1(J)*TAN+F(I))/8.
      IF(J.EQ.1)GO TO 22
      Y2(J)=(YB-YA)*COSD(ZB)
      X2(J)=(Y2(J)*TAN+F(I+1))/8.
      GO TO 23
22    Y2(J)=-(YB-YA)*COSD(ZB)
      X2(J)=X2(J)*TAN+F(I)/8.
23    Y3(J)=(YB-YA)*COSD(ZC)
      X3(J)=(Y3(J)*TAN+F(I+1))/8.
      XM(J)=(X1(J)+X2(J)+X3(J))/3.
      YM(J)=(Y1(J)+Y2(J)+Y3(J))/3.
      IF(I.EQ.4)GO TO 97
      IF(I.EQ.3)GO TO 96
```

```
      IF(I.EQ.2) GO TO 95
      Z3(J)=-0.04
      Z1(J)=0.0
      GO TO 98
95    Z3(J)=-0.06
      Z1(J)=-0.04
      GO TO 98
96    Z3(J)=-0.08
      Z1(J)=-0.06
      GO TO 98
97    Z3(J)=-0.1
      Z1(J)=-.08
98    Z2(J)=Z3(J)
      Z(J)=(Z1(J)+Z2(J)+Z3(J))/3.
      WRITE(23,*)(X1(J),X2(J),X3(J),Y1(J),Y2(J),Y3(J),XM(I),YM(J),Z1
     1(J),Z2(J),Z3(J),Z(J))
20    CONTINUE
10    CONTINUE
      RETURN
      END
```

```
C       CIRCULATION DISTRIBUTION METHOD
C       -------------------------------
        DIMENSION X1(28),X2(28),X3(28),X(28),Y1(28),Y2(28),Y3(28)
        1,Y(28),Z1(28),Z2(28),Z3(28),Z(28),XB1(6),XB2(6),XB(6)
        1,YB1(6),YB2(6),YB(6),GM(6),WKSPCE(1000),UNIT(6,6),W
        1(6,12),C(6),VB(28),WB(28),VF(28),WF(28),VW(28),WW(28)
        1,UW(28),WU(28),TP(28),TW(28),IV(28),GN(6),TU(28)
        1,YN(28),ZN(28)
        COMMON/A1/XX,AA,BB,XP,E2,MM
        COMMON/A2/YYR,ZZR
        COMMON/A3/YYL,ZZL
        COMMON/A6/ALPHA,NX,NW
        COMMON/A7/NY
        EXTERNAL VELZ,VLINFZ,CINT1R,CINT1L,CINT2R,CINT2L,ZU,ZU
        1,VELY,VLINFY,WL,SIMSPN
        OPEN(UNIT=25,DEVICE='DSK')
        OPEN(UNIT=28,DEVICE='DSK')
        OPEN(UNIT=20,DEVICE='DSK')
        II=1
        NW=4
        NY=6
        NX=1
        NB=NX*NY
        NP=NY+1
        NF=NP*NW
        ALPHA=05
        XC=0.125000
        PAI=3.141592674
        WRITE(20,*)II
        CALL GEMTRY(X1,X2,X3,X,Y1,Y2,Y3,Y,NF)
        CALL CORD(XB,YB,XB1,YB1,XB2,YB2,C,NY)
        ITER=6
        DO 10 M=1,NB
        DO 10 N=1,NB
        W(M,N)=0.0
        DO 20 L=1,NW
        MO=(N-1)/NY
        NYLON=MO*NY
        NQ=N-NYLON
        LL=NQ+(L-1)*NP
        LO=NQ+(NW-1)*NP
        W(M,N)=W(M,N)+VELZ(X3(LL),X1(LL),XB(M),Y3(LL),Y1(LL),YB(M)
        1,Z3(LL),Z1(LL),0)+VELZ(X1(LL),X3(LL),XB(M),-Y1(LL),-Y3(LL)
        1,YB(M),Z1(LL),Z3(LL),0)+VELZ(X1(LL+1),X3(LL+1),XB(M)
        1,Y1(LL+1),Y3(LL+1),YB(M),Z1(LL+1),Z3(LL+1),0)+VELZ(X3(LL+1)
        1,X1(LL+1),XB(M),-Y3(LL+1),-Y1(LL+1),YB(M),Z3(LL+1),Z1(LL+1)
        1,0)
20      CONTINUE
        W(M,N)=W(M,N)+VELZ(XB1(N),XB2(N),XB(M),YB1(N),YB2(N),YB(M)
        1,0,0,0)+VELZ(X1(NQ),XB1(N),XB(M),Y1(NQ),YB1(N),YB(M),0,0,0)
        1+VELZ(XB2(N),X1(NQ+1),XB(M),YB2(N),Y1(NQ+1),YB(M),0,0,0)
        1+VELZ(XB1(N),X1(NQ),XB(M),-YB1(N),-Y1(NQ),YB(M),0,0,0)
        1+VELZ(X1(NQ+1),XB2(N),XB(M),-Y1(NQ+1),-YB2(N),YB(M),0,0,0)
        1+VELZ(XB2(N),XB1(N),XB(M),-YB2(N),-YB1(N),YB(M),0,0,0)
        1+VLINFZ(X3(LO),Y3(LO),Z3(LO),XB(M),YB(M),0)
        1-VLINFZ(X3(LO+1),Y3(LO+1),Z3(LO+1),XB(M),YB(M),0)
        1-VLINFZ(X3(LO),-Y3(LO),Z3(LO),XB(M),YB(M),0)
        1+VLINFZ(X3(LO+1),-Y3(LO+1),Z3(LO+1),XB(M),YB(M),0)
10      CONTINUE
        N=NB
        IA=NB
        IUNIT=NB
        IFAIL=0
C       CALL F01AAF(W,IA,N,UNIT,IUNIT,WKSPCE,IFAIL)
        CALL FINV(W,NY,UNIT,2*NY)
C       CALL FINVRS(W,NY,B,M,DETERM)
```

```
      DO 30 I=1,NB
      GN(I)=0.0
      DO 30 J=1,NB
      GN(I)=UNIT(I,J)*C(I)+GN(I)
30    CONTINUE
      WRITE(21,*)(GN(I),I=1,NB)
      DO 11 I=1,NY
      GM(I)=0.0
      DO 120 J=1,NX
      GM(I)=GM(I)+GN(I+(J-1)*NY)
120   CONTINUE
      WRITE(22,*)GM(I)
11    CONTINUE
      DO 28 IT=1,ITER
      WRITE(28,*)IT
      WRITE(20,*)IT
12    IF((IT.EQ.1).AND.(II.EQ.1))GO TO 83
C
CC-----------------CALCULATION FOR THE CONTRIBUTION OF BOUND VORTEX-----------------
C
      DO 14 M=1,NF
      VB(M)=0.0
      WB(M)=0.0
      DO 15 N=1,NB
      G=XB1(N)*SIND(ALPHA)
      H=XB2(N)*SIND(ALPHA)
      VB(M)=VB(M)+GN(N)*(VELY(XB1(N),XB2(N),X(M),YB1(N),YB2(N),Y(M)
     1,G,H,Z(M))+VELZ(X1(N),XB1(N),X(M),Y1(N),YB1(N),Y(M),0,G,Z(M))
     1+VELZ(XB2(N),X1(N+1),X(M),XB2(N),Y1(N+1),Y(M),H,0,Z(M))
     1+VELZ(XB1(N),X1(N),X(M),-YB1(N),-Y1(N),Y(M),G,0,Z(M))
     1+VELZ(X1(N+1),XB2(N),X(M),-Y1(N+1),-YB2(N),Y(M),0,H,Z(M))
     1+VELZ(XB2(N),XB1(N),X(M),-YB2(N),-YB1(N),Y(M),H,G,Z(M)))
15    CONTINUE
C     WRITE(20,*)VB(M),WB(M)
14    CONTINUE
CCC----------------CALCULATION FOR THE CONTRIBUTION OF FAR WAKE----------------
C
      DO 17 M=1,NF
      VF(M)=0.0
      WF(M)=0.0
      DO 18 N=1,NY
      LO=N+(NW-1)*NP
      VF(M)=VF(M)+GM(N)*(VLINFY(X3(LO),Y3(LO),Z3(LO),X(M),Y(M),Z(M)
     1)-VLINFZ(X3(LO+1),Y3(LO+1),Z3(LO+1),X(M),Y(M),Z(M))
     1-VLINFZ(X3(LO),-Y3(LO),Z3(LO),X(M),Y(M),Z(M))
     1+VLINFZ(X3(LO+1),-Y3(LO+1),Z3(LO+1),X(M),Y(M),Z(M)))
18    CONTINUE
C     WRITE(20,*)VF(M),WF(M)
17    CONTINUE
CCC----------------CALCULATION FOR THE CONTRIBUTION OF NEAR WAKE----------------
      DO 51 ND=1,NW
      DO 51 NC=1,NP
      I=(ND-1)*NP+NC
      LCG=II*NP
      MODI=(II-1)*NP
      IF((IT.EQ.1).AND.((I.GT.LCG).OR.(I.LE.MODI)))GO TO 83
      UW(I)=0.0
      VW(I)=0.0
      WW(I)=0.0
      DO 52 LU=1,NW
      DO 52 LC=1,NP
      J=(LU-1)*NP+LC
      DO 53 MM=1,2
```

```
      XP=X3(J)-X1(J)
      NAL=NP*(LU-1)+1
      LDH=NP*(ND-1)+1
      IF(J.EQ.NAL)JK=J-(MM-1)
      IF(J.NE.NAL)JK=J-(MM-2)
      IF(JK.EQ.NAL)E2=Y2(JK)-Y1(JK)
      IF(JK.GT.NAL)E2=Y3(JK)-Y2(JK)
      IF(MM.EQ.2)E2=-E2
      XX=X(I)-X1(J)
      YYR=Y(I)-Y1(J)
      YYL=-(Y(I)+Y1(J))
      ZZR=Z(I)-Z1(J)
      ZZL=-(Z(I)-Z1(J))
      IF((LC.EQ.1).AND.(MM.EQ.2))GO TO 53
      IF((LC.EQ.NP).AND.(MM.EQ.1))GO TO 53
      S13=SQRT((X3(J)-X1(J))**2+(Y3(J)-Y1(J))**2+(Z3(J)
     1-Z1(J))**2)
      F11=(X3(J)-X1(J))/S13
      F21=(Y3(J)-Y1(J))/S13
      F31=(Z3(J)-Z1(J))/S13
      Z7=(Z2(J)-Z1(J))*(Y3(J)-Y1(J))-(Y2(J)-Y1(J))*(Z3(J)-Z1(J))
      Z8=(X2(J)-X1(J))*(Z3(J)-Z1(J))-(Z2(J)-Z1(J))*(X3(J)-X1(J))
      Z9=(X3(J)-X1(J))*(Y2(J)-Y1(J))-(X2(J)-X1(J))*(Y3(J)-Y1(J))
      S12=SQRT(Z7*Z7+Z8*Z8+Z9*Z9)
      F13=Z7/S12
      F23=Z8/S12
      F33=Z9/S12
      IF(LC.EQ.1)GO TO 7
      K=J-1
      F23=Z5/S11
      F33=Z6/S11
7     F12=F23*F31-F33*F21
      F22=F33*F11-F13*F31
      F32=F13*F21-F11*F23
C     WRITE(23,92)F11,F12,F13,F21,F22,F23,F31,F32,F33,I,J
92    FORMAT(9F12.5,2I4)
      LO=LC
      IF(MM.EQ.1)LD=LC
      IF(MM.EQ.2)LD=LC-1
      JJ=LD+(LU-1)*NP
      IF(LD.EQ.1)WU(JJ)=2.*(GM(LD)-GM(LD+1))/(Y3(JJ+1)-Y2(JJ+1))
      IF(LD.GT.1)WU(JJ)=2.*(GM(LD)-GM(LD+1))/(Y3(JJ+1)-Y2(JJ+1))
     1-WU(JJ-1)
      IF(LD.GT.1)AA=WU(JJ-1)
      IF(LD.EQ.1)AA=0.0
      BB=(WU(JJ)-AA)/(Y3(JJ+1)-Y2(JJ+1))
      IF((I.EQ.J).AND.((MM.EQ.2).OR.(J.EQ.LDH)))GO TO 55
      VRY=SIMPSN(0,E2,8,CINT1R)
      VLY=SIMPSN(0,E2,8,CINT1L)
      VRZ=SIMPSN(0,E2,8,CINT2R)
      VLZ=SIMPSN(0,E2,8,CINT2L)
      GO TO 56
55    E3=E2/3.-E2/40.
      E4=E2/3.+E2/40.
      VRY=SIMPSN(0,E3,4,CINT1R)+SIMPSN(E4,E2,4,CINT1R)
C     VLY=SIMPSN(0,E3,4,CINT1L)+SIMPSN(E4,E2,4,CINT1L)
      VLY=SIMPSN(0,E2,8,CINT1L)
56    UW(I)=(VRY-VLY)*F12+(VRZ-VLZ)*F13+UW(I)
      VW(I)=(VRY-VLY)*F22+(VRZ-VLZ)*F23+VW(I)
      WW(I)=(VRY-VLY)*F32+(VRZ-VLZ)*F33+WW(I)
C     WRITE(23,*)VRY,VLY,VRZ,VLZ
53    CONTINUE
52    CONTINUE
      WRITE(20,*)VW(I),WW(I)
51    CONTINUE
```

```
83      IF(II.GT.1)GO TO 81
        WRITE(25,*)II
        DO 76 JJ=1,NP
        I=(II-1)*NP+JJ
        TU(I)=1.0+UW(I)
        TV(I)=VB(I)+VF(I)+VW(I)
        TW(I)=WB(I)+WF(I)+WW(I)
        TR(I)=SQRT(TU(I)**2+TV(I)**2+TW(I)**2)
        S13=SQRT((X3(I)-X1(I))**2+(Y3(I)-Y1(I))**2+(Z3(I)-Z1(I))**2)
        IF(II.EQ.1)Z3(I)=-S13*TAND(ALPHA)
        IF((II.EQ.1).AND.(JJ.NE.1))Z2(I)=Z3(I-1)
76      CONTINUE
        IF(II.EQ.1)GO TO 77
        DO 79 JJ=1,NP
        I=(II-1)*NP+JJ
        TU(I)=1.0+UW(I)
        TV(I)=VB(I)+VF(I)+VW(I)
        TW(I)=WB(I)+WF(I)+WW(I)
        TR(I)=SQRT(TU(I)**2+TV(I)**2+TW(I)**2)
        X1(I)=X3(I-NP)
        Y1(I)=Y3(I-NP)
        Z1(I)=Z3(I-NP)
        X3(I)=X1(I)+S13*TU(I)/TR(I)
        Y3(I)=Y1(I)+S13*TV(I)/TR(I)
        Z3(I)=Z1(I)+S13*TW(I)/TR(I)
        IF(JJ.NE.1)GO TO 78
        X2(I)=X3(I-NY)
        Y2(I)=Y3(I-NY)
        Z2(I)=Z3(I-NY)
        GO TO 79
78      X2(I)=X3(I-1)
        Y2(I)=Y3(I-1)
        Z2(I)=Z3(I-1)
79      CONTINUE
77      DO 71 IJ=1,NW
        DO 71 JJ=1,NP
        I=(IJ-1)*NP+JJ
        JQ=II*NP
        IF(I.GT.JQ)Z2(I)=Z3(I-NP)
        IF(I.GT.JQ)Z1(I)=Z2(I)
        IF(I.GT.JQ)Z3(I)=Z2(I)
        X(I)=(X1(I)+X2(I)+X3(I))/3.
        Y(I)=(Y1(I)+Y2(I)+Y3(I))/3.
        Z(I)=(Z1(I)+Z2(I)+Z3(I))/3.
        WRITE(25,*)((X1(I),X2(I),X3(I),X(I),Y1(I),Y2(I),Y3(I),Y(I)
       1,Z1(I),Z2(I),Z3(I),Z(I)))
71      CONTINUE
        IF(II.EQ.NW)GO TO 28
        II=II+1
        GO TO 12
81      DO 41 II=1,NW
        DO 42 JJ=1,NP
        I=(II-1)*NP+JJ
        S13=SQRT((X3(I)-X1(I))**2+(Y3(I)-Y1(I))**2+(Z3(I)-Z1(I))**2)
        TU(I)=1.0+UW(I)
        TV(I)=VB(I)+VF(I)+VW(I)
        TW(I)=WB(I)+WF(I)+WW(I)
        TR(I)=SQRT(TU(I)**2+TV(I)**2+TW(I)**2)
        IF(I.GT.NP) GO TO 107
108     X3(I)=X1(I)+S13*TU(I)/TR(I)
        Y3(I)=Y1(I)+S13*TV(I)/TR(I)
        Z3(I)=Z1(I)+S13*TW(I)/TR(I)
        GO TO 109
107     X1(I)=X3(I-NP)
        Y1(I)=Y3(I-NP)
```

```
      Z1(I)=Z3(I-NP)
      Z3(I)=Z1(I)+S13*TW(I)/IR(I)
109   IF(JJ.NE.1)GO TO 111
      IF(I.EQ.1)X2(I)=XC
      IF(I.EQ.1)Z2(I)=0.0
      IF(I.EQ.1)Y2(I)=Y2(I)
      IF((JJ.EQ.1).AND.(I.NE.1))X2(I)=X3(I-NP+1)
      IF((JJ.EQ.1).AND.(I.NE.1))Y2(I)=Y3(I-NP+1)
      IF((JJ.EQ.1).AND.(I.NE.1))Z2(I)=Z3(I-NP+1)
      GO TO 110
111   X2(I)=X3(I-1)
      Y2(I)=Y3(I-1)
      Z2(I)=Z3(I-1)
110   X(I)=(X1(I)+X2(I)+X3(I))/3.
      Y(I)=(Y1(I)+Y2(I)+Y3(I))/3.
      Z(I)=(Z1(I)+Z2(I)+Z3(I))/3.
      YN(I)=Y1(I)+(Y3(I)-Y1(I))*2./3.
      ZN(I)=Z1(I)+(Z3(I)-Z1(I))*2./3.
      WRITE(28,*)(X1(I),X2(I),X3(I),X(I),Y1(I),Y2(I)
     1,Y3(I),Y(I),Z1(I),Z2(I),Z3(I),Z(I),YN(I),ZN(I))
42    CONTINUE
41    CONTINUE
28    CONTINUE
      STOP
      END
C
      SUBROUTINE CORD(XM,YM,X1,Y1,X2,Y2,AN,NY)
C
C     PROGRAM FOR FINDING THE POINTS OVER WING SURFACE
      DIMENSION XM(NY),YM(NY),X1(NY),Y1(NY),X2(NY),Y2(NY),AN(NY)
     1,SLP(20),SLOP(20)
      COMMON/A6/ALPHA,NX,NW
      OPEN(UNIT=38,DEVICE='DSK',FILE='PLL.IN')
      OPEN(UNIT=25,DEVICE='DSK')
      READ(38,*) AR,SPAN,TPR,SWPLE
C     SWPLE=SWEEP AT L.E. IN DEGREES
C     TPR=CR/CT
      PAI=3.141592674
      XA=0.0
      YA=0.0
      AREA=((SPAN)**2)/AR
      YC=0.0
      YB=0.5
      YD=0.5
      CR=AREA*2.*TPR*COSD(SWPLE)/(SPAN*((TPR-1.)*COSD(SWPLE)+2))
      CT=CR/TPR
      XC=CR
      XB=YB*(SIND(SWPLE)/COSD(SWPLE))
      XD=CT+XB
      DO 10 N=1,NX
      SLP(N)=(XB+((N-1.)/NX)*(XD-XB)+(XD-XB)/(4.*NX)-(XA+((N-1.)/NX)
     1*(XC-XA)+(XC-XA)/(4.*NX)))/(YB-YA)
      SLOP(N)=(XB+((N-1.)/NX)*(XD-XB)+3.*(XD-XB)/(4.*NX)-(XA+((N-1.)
     1/NX)*(XC-XA)+3.*(XC-XA)/(4.*NX)))/(YB-YA)
C     TYPE *,SLP(N),SLOP(N)
      DO 20 I=1,NY
      J=(N-1)*NY+I
      ZZ=90*(I-1.)/FLOAT(NY)
      Y1(J)=0.5*SIND(ZZ)
      X1(J)=Y1(J)*SLP(N)+(XC-XA)/(4.*NX)+((XC-XA)*(N-1))/FLOAT(NX)
      YY=90.*I/FLOAT(NY)
      Y2(J)=0.5*SIND(YY)
      X2(J)=Y2(J)*SLP(N)+(XC-XA)/(4.*NX)+((XC-XA)*(N-1))/NX
      YM(J)=(Y1(J)+Y2(J))/2.
      XM(J)=YM(J)*SLOP(N)+(XC-XA)*3./(4.*NX)+((XC-XA)*(N-1.))/NX
```

```
29      CONTINUE
10      CONTINUE
        RETURN
        END
C
        FUNCTION VELZ(X3,X4,XN,Y3,Y4,YN,Z3,Z4,ZN)
C
        A=XN-X3
        B=XN-X4
        C=YN-Y3
        D=YN-Y4
        E=ZN-Z3
        F=ZN-Z4
        VELZ=-((A*D-B*C)/((C*F-D*E)**2+(A*F-B*E)**2+(A*D-B*C)**2)
        1)*(((B-A)*A+(D-C)*C+(F-E)*E)/SQRT(A*A+C*C+E*E)-((B-A)*B
        1+(D-C)*D+(F-E)*F)/SQRT(B*B+D*D+F*F))
        RETURN
        END
C
        FUNCTION VELY(X3,X4,XN,Y3,Y4,YN,Z3,Z4,ZN)
C
        A=XN-X3
        B=XN-X4
        C=YN-Y3
        D=YN-Y4
        E=ZN-Z3
        F=ZN-Z4
        VELY=((B*E-A*F)/((C*F-D*E)**2+(A*F-B*E)**2+(A*D-B*C)**2))
        1*(((B-A)*A+(D-C)*C+(F-E)*E)/SQRT(A*A+C*C+E*E)-((B-A)*B+
        1(D-C)*D+(F-E)*F)/SQRT(B*B+D*D+F*F))
        RETURN
        END
C
        FUNCTION TAND(BETA)
C
        TAND=SIND(BETA)/COSD(BETA)
        RETURN
        END
C
        FUNCTION SIMPSN(A,B,N,F)
C
        X=A
        H=(B-A)/N
        IP=4
        S=F(X)+F(X+N*H)
        I=1
2       IF (I.EQ.N)GO TO 3
        S=S+IP*F(X+I*H)
        I=I+1
        IP=6-IP
        GO TO 2
3       S=S*H/3
        SIMPSN=S
        RETURN
        END
C
        FUNCTION VLINFY(X5,Y5,Z5,XN,YN,ZN)
C
        A=XN-X5
        B=YN-Y5
        C=ZN-Z5
        VLINFY=(C/(B*B+C*C))*(1.0+A/SQRT(A*A+B*B+C*C))
        RETURN
        END
C
```

```
      FUNCTION VLINFZ(X5,Y5,Z5,XN,YN,ZN)
C
      A=XN-X5
      B=YN-Y5
      C=ZN-Z5
      VLINFZ=-(B/(B*B+C*C))*(1.0+A/SQRT(A*A+B*B+C*C))
      RETURN
      END
C
      FUNCTION CINT1R(XE)
C
      COMMON/A1/XX,AA,BB,XP,E2,MM
      COMMON/A2/YYR,ZZR
C     WRITE(23,92)XX,YYR,ZZR,AA,BB,XP,E2,CINT1R,XE,MM
92    FORMAT(12X,9F11.6,6X,I2)
      IF(MM.EQ.2)GO TO 101
      CMM=(AA+BB*XE)*ZZR/((YYR-XE)**2+ZZR**2)
      ZTE1=-XP*XE/E2+XP
      CINT1R=CMM*(SNZTE1-SNZLE1)
      RETURN
101   CMM=-(AA+BB*XE-BB*E2)*ZZR/((YYR-XE)**2+ZZR**2)
      ZLE2=XP*XE/E2
      SNZLE2=((XX-ZLE2)/SQRT((XX-ZLE2)**2+(YYR-XE)**2+ZZR**2))
      SNZTE2=((XX-XP)/SQRT((XX-XP)**2+(YYR-XE)**2+ZZR**2))
      CINT1R=CMM*(SNZTE2-SNZLE2)
      RETURN
      END
C
      FUNCTION CINT1L(XE)
C
      COMMON/A1/XX,AA,BB,XP,E2,MM
      COMMON/A3/YYL,ZZL
      IF(MM.EQ.2)GO TO 101
      CMM=(AA+BB*XE)*ZZL/((YYL-XE)**2+ZZL**2)
      ZTE1=-XP*XE/E2+XP
      SNZLE1=(XX/SQRT(XX**2+(YYL-XE)**2+ZZL**2))
      SNZTE1=((XX-ZTE1)/SQRT((XX-ZTE1)**2+(YYL-XE)**2+ZZL**2))
      CINT1L=CMM*(SNZTE1-SNZLE1)
C     WRITE(23,92)XX,YYL,ZZL,AA,BB,XP,E2,CINT1L,XE,MM
92    FORMAT(16X,9F11.6,6X,I2)
      RETURN
101   CMM=-(AA+BB*XE-BB*E2)*ZZL/((YYL-XE)**2+ZZL**2)
      ZLE2=XP*XE/E2
      SNZLE2=((XX-ZLE2)/SQRT((XX-ZLE2)**2+(YYL-XE)**2+ZZL**2))
      SNZTE2=((XX-XP)/SQRT((XX-XP)**2+(YYL-XE)**2+ZZL**2))
      CINT1L=CMM*(SNZTE2-SNZLE2)
      RETURN
      END
C
      FUNCTION CINT2R(XE)
C
      COMMON/A1/XX,AA,BB,XP,E2,MM
      COMMON/A2/YYR,ZZR
      IF(MM.EQ.2)GO TO 101
      CMM=-(AA+BB*XE)*(YYR-XE)/((YYR-XE)**2+ZZR**2)
      ZTE1=-XP*XE/E2+XP
      SNZLE1=(XX/SQRT(XX**2+(YYR-XE)**2+ZZR**2))
      SNZTE1=((XX-ZTE1)/SQRT((XX-ZTE1)**2+(YYR-XE)**2+ZZR**2))
      CINT2R=CMM*(SNZTE1-SNZLE1)
C     WRITE(23,92)XX,YYR,ZZR,AA,BB,XP,E2,CINT2R,XE,CMM,ZTE1,SNZLE1
C    1,SNZTE1,MM
92    FORMAT(13F9.4,I3)
      RETURN
101   CMM=(AA+BB*XE-BB*E2)*(YYR-XE)/((YYR-XE)**2+ZZR**2)
      ZLE2=XP*XE/E2
```

```
      SNZLE2=((XX-ZLE2)/SQRT((XX-ZLE2)**2+(YYR-XE)**2+ZZR**2))
      SNZTE2=((XX-XP)/SQRT((XX-XP)**2+(YYR-XE)**2+ZZR**2))
      CINT2R=CMM*(SNZTE2-SNZLE2)
C     WRITE(23,93)XX,YYR,ZZR,AA,BB,XP,E2,CINT2R,XE,CMM,ZLE2,SNZLE2
C     1,SNZTE2,MM
93    FORMAT(13F9.4,I3)
      RETURN
      END
C
      FUNCTION CINT2L(XE)
C
      COMMON/A1/XX,AA,BB,XP,E2,MM
      COMMON/A3/YYL,ZZL
      IF(MM.EQ.2)GO TO 101
      CMM=-(AA+BB*XE)*(YYL-XE)/((YYL-XE)**2+ZZL**2)
      ZTE1=-XP*XE/E2+XP
      SNZLE1=(XX/SQRT(XX**2+(YYL-XE)**2+ZZL**2))
      SNZTE1=((XX-ZTE1)/SQRT((XX-ZTE1)**2+(YYL-XE)**2+ZZL**2))
      CINT2L=CMM*(SNZTE1-SNZLE1)
C     WRITE(23,92)XX,YYL,ZZL,AA,BB,XP,E2,CINT2L,XE,CMM,ZTE1,SNZLE1
C     1,SNZTE1,MM
92    FORMAT(2X,13F9.4,I2)
      RETURN
101   CMM=(AA+BB*XE-BB*E2)*(YYL-XE)/((YYL-XE)**2+ZZL**2)
      ZLE2=XP*XE/E2
      SNZLE2=((XX-ZLE2)/SQRT((XX-ZLE2)**2+(YYL-XE)**2+ZZL**2))
      SNZTE2=((XX-XP)/SQRT((XX-XP)**2+(YYL-XE)**2+ZZL**2))
      CINT2L=CMM*(SNZTE2-SNZLE2)
C     WRITE(23,93)XX,YYL,ZZL,AA,BB,XP,E2,CINT2L,XE,CMM,ZLE2,SNZLE2
C     1,SNZTE2,MM
93    FORMAT(2X,13F9.4,I2)
      RETURN
      END
      SUBROUTINE GEMTRY(X1,X2,X3,XM,Y1,Y2,Y3,YM,NF)
C
      DIMENSION X1(NF),Y1(NF),X2(NF),Y2(NF),X3(NF),Y3(NF),XM(NF
      1),YM(NF)
      COMMON/A6/ALPHA,NX,NW
      COMMON/A7/NY
      YB=0.5
      NZ=NY+1
      BETA=0.0
      ZZ=90./FLOAT(NY)
      TAN=SIND(BETA)/COSD(BETA)
      DO 10 I=1,NW
      DO 20 J=1,NZ
      M=(I-1)*NZ+J
      ZO=ZZ*(J-1)
      ZC=90-ZO
      ZB=90-ZO+ZZ
      Y1(M)=(YB-YA)*COSD(ZC)
      IF(I.EQ.1)X1(M)=0.0
      IF(I.GT.1)X1(M)=0.09+0.6*(I-2)
      IF(J.EQ.1)GO TO 22
      Y2(M)=(YB-YA)*COSD(ZB)
      IF(I.EQ.1)X2(M)=0.09
      IF(I.GT.1)X2(M)=0.09+0.6*(I-1)
      GO TO 23
22    Y2(M)=-(YB-YA)*COSD(ZB)
      X2(M)=X1(M)
23    Y3(M)=(YB-YA)*COSD(ZC)
      IF(I.EQ.1)X3(M)=0.09
      IF(I.GT.1)X3(M)=0.09+0.6*(I-1)
      XM(M)=(X1(M)+X2(M)+X3(M))/3.
      YM(M)=(Y1(M)+Y2(M)+Y3(M))/3.
```

```
      X1(M)=X1(M)+0.125
      X2(M)=X2(M)+0.125
      X3(M)=X3(M)+0.125
      XM(M)=XM(M)+0.125
20    CONTINUE
10    CONTINUE
      RETURN
      END
C
      SUBROUTINE FINV(A,N,AI,M)
C
      DIMENSION A(N,M),AI(N,N)
      M2=N+1
      DO 34 LI=1,N
      DO 34 LJ=M2,M
34    A(LI,LJ)=0.0
      DO 85 K=1,N
      I2=K+N
85    A(K,I2)=1.0
      DO 99 LJ=1,N
      J2=LJ+1
      P=A(LJ,LJ)
      DO 95 I=1,M
95    A(LJ,I)=A(LJ,I)/P
      DO 99 LK=1,N
      DO 99 LI=J2,M
      IF(LK-LJ)20,99,20
20    A(LK,LI)=A(LK,LI)-A(LJ,LI)*A(LK,LJ)
99    CONTINUE
      DO 100 I=1,N
      DO 100 J=M2,M
      L3=J-N
100   AI(I,L3)=A(I,J)
      RETURN
      END
      SUBROUTINE FINVRS(A,N,B,M,DETERM)
      DIMENSION A(N,N),B(N,1),IPIVOT(350),INDEX(350,2),DT(350)
      EQUIVALENCE (IROW,JROW),(ICOLUM,JCOLUM),(AMAX,T,SWAP)
      DETERM=1.0
      do 20 J=1,N
20    IPIVOT(J)=0.0
      do 550 I=1,N
      AMAX=0.0
      do 105 J=1,N
      IF(IPIVOT(J)-1) 60,105,60
60    do 100 K=1,N
      IF(IPIVOT(K)-1) 80,100,740
80    IF(AMAX -ABS(A(J,K))) 85,100,100
85    IROW=J
      ICOLUM=K
      AMAX=ABS(A(J,K))
100   CONTINUE
105   CONTINUE

      IPIVOT(ICOLUM)=IPIVOT(ICOLUM)+1
      IF(IROW-ICOLUM) 140,260,140
140   DETERM=-DETERM
      do 200 L=1,N
      SWAP=A(IROW,L)
      A(IROW,L)=A(ICOLUM,L)
200   A(ICOLUM,L)=SWAP
      IF(M) 260,260,210
210    do 250 L=1,M
      SWAP=B(IROW,L)
      B(IROW,L)=B(ICOLUM,L)
```

```
250     B(ICOLUM,L)=SWAP
260     INDEX(I,1)=IROW
        INDEX(I,2)=ICOLUM
        PIVOT=A(ICOLUM,ICOLUM)
        DT(I)=PIVOT
        A(ICOLUM,ICOLUM)=1.0
        do 350 L=1,N
350     A(ICOLUM,L)=A(ICOLUM,L)/PIVOT
        IF(M) 380,380,360
360      do 370 L=1,M
370     B(ICOLUM,L)=B(ICOLUM,L)/PIVOT
380     do 550 L1=1,N
        IF(L1-ICOLUM) 400,550,400
400     T=A(L1,ICOLUM)
        A(L1,ICOLUM)=0.0
        do 450 L=1,N
 450     A(L1,L)=A(L1,L)-A(ICOLUM,L)*T
        IF(M) 550,550,460
460     do 500 L=1,M
500     B(L1,L)=B(L1,L)-B(ICOLUM,L)*T
550     CONTINUE
        do 710 I=1,N
        L=N+1-I
C--     DETERM=DETERM*DT(L)
        IF(INDEX(L,1)-INDEX(L,2)) 630,710,630
630     JROW=INDEX(L,1)
        JCOLUM=INDEX(L,2)
        do 705 K=1,N
        SWAP=A(K,JROW)
        A(K,JROW)=A(K,JCOLUM)
        A(K,JCOLUM)=SWAP
705     CONTINUE
710     CONTINUE
        do 11 K=1,N
        IF(IPIVOT(K).NE.1) GO TO 12
11      CONTINUE
        RETURN
12        WRITE(5,991)
991     FORMAT(10X,'MATRIX IS SINGULAR
740     RETURN
        END
```

```
      SUBROUTINE LSSQAR (A,B,M,NA,NB,IA,IB,IDGT,WKAREA,IER)
-LSSQAR---------S-------LIBRARY 2-----------------------------------------
   FUNCTION                - LEAST SQUARES SOLUTION OF OVERDETERMINED
                             SYSTEM OF LINEAR EQUATIONS
   USAGE                   - CALL LSSQAR(A,B,M,NA,NB,IA,IB,IDGT,WKAREA,IER)
   PARAMETERS    A         - THE COEFFICIENT MATRIX OF THE EQUATION
                             AX=B, WHERE A IS M X NA WITH M GREATER THAN
                             OR EQUAL TO NA. INPUT A IS REPLACED BY
                             THE PSEUDO-INVERSE OF A
                 B         - MATRIX OF THE RIGHT HAND SIDE OF THE EQUATION
                             AX=B, WHERE B IS M X NB. THE NA X NB
                             SOLUTION X OVERWRITES B.
                 M         - NUMBER OF ROWS IN A AND B.
                 NA        - NUMBER OF COLUMNS IN MATRIX A
                 NB        - NUMBER OF COLUMNS IN MATRIX B
                 IA        - ROW DIMENSION OF A IN THE CALLING
                             PROGRAM.
                 IB        - ROW DIMENSION OF B IN THE CALLING
                             PROGRAM.
                 IDGT      - THE ELEMENTS OF A ARE ASSUMED TO BE CORRECT
                             TO IDGT SIGNIFICANT  DIGITS. IDGT IS AN
                             INPUT PARAMETER.
                 WKAREA    - WORK AREA OF DIMENSION GREATER THAN OR EQUAL
                             TO NA(NA+4).
                 IER       - ERROR PARAMETER
                             TERMINAL ERROR = 128 + N
                               N = 1  INDICATES THAT INPUT A IS A ZERO
                                      MATRIX.
   PRECISION               - SINGLE
   REQ'D IMSL ROUTINES     - LPSOOR,LSVALR,UERTST,VSORTM
   LANGUAGE                - FORTRAN
-----------------------------------------------------------------------------
```

*UPTODATE F01AAF82NM
F01AAF - NAG FORTRAN ROUTINE SUMMARY
======

IMPORTANT: For a complete specification of the use of this routine see the NAG FORTRAN Library Manual. Terms marked // ... // may be implementation dependent.

A. Purpose
==========

//F01AAF// calculates the approximate inverse of a real matrix by Crout's method.

B. Specification
================

```
      SUBROUTINE //F01AAF// (A, IA, N, UNIT, IUNIT, WKSPCE,
     1    IFAIL)
C     INTEGER IA, N, IUNIT, IFAIL
C     //real// A(IA,N), UNIT(IUNIT,N), WKSPCE(N)
```

C. Parameters
=============

A - //real// array of DIMENSION (IA,p) where p.GE.N.

Before entry, A must contain the elements of the real matrix.

On successful exit, it contains the Crout factorisation with the unit diagonal of U understood.

IA - INTEGER.

On entry, IA must specify the first dimension of array A as declared in the calling (sub)program.
IA.GE.N.

Unchanged on exit.

N - INTEGER.

On entry, N must specify the order of matrix A.

Unchanged on exit.

UNIT - //real// array of DIMENSION (IUNIT,p) where p.GE.N.

On successful exit, UNIT contains the inverse of A.

IUNIT - INTEGER.

On entry, IUNIT must specify the first dimension of array UNIT as declared in the calling (sub)program.
IUNIT.GE.N.

Unchanged on exit.

WKSPCE - //real// array of DIMENSION at least (N).

Used as working space.

IFAIL - INTEGER.

Before entry, IFAIL must be assigned a value. For users not familiar with this parameter (described in Chapter P01 in the main NAG FORTRAN Library Manual) the recommended value is 0.

Unless the routine detects an error (see next section), IFAIL contains 0 on exit.

6. Error Indicators and Warnings

Errors detected by the routine:-

IFAIL = 1

The matrix A is singular or almost singular, possibly due to rounding errors.

END OF F01AAF FORTRAN SUMMARY - MARK 10
FEBRUARY 1983

** END OF F01AAFSUMM